The Hashemite Kingdom of Jordan Scientific Research Support Fund The Hashemite University

# JJEES

## Jordan Journal of Earth and Environmental Sciences

Volume (13) Number (2)

Cover photo © Prof. Khaled Al Tarawneh

JJEES is an International Peer-Reviewed Research Journal

ISSN 1995-6681 jjees.hu.edu.jo June 2022

# Jordan Journal of Earth and Environmental Sciences (JJEES)

JJEES is an International Peer-Reviewed Research Journal, Issued by Deanship of Scientific Research, The Hashemite University, in corporation with, the Jordanian Scientific Research Support Fund, the Ministry of Higher Education and Scientific Research.




## Submission address:

Manuscripts should be submitted electronically to the following e-mail:

**jjees@hu.edu.jo**

For more information and previous issues:

**www.jjees.hu.edu.jo**

Hashemite Kingdom of Jordan

Scientific Research Support Fund

Hashemite University

# Jordan Journal of Earth and Environmental Sciences

# JJEES

*An International Peer-Reviewed Scientific Journal*

*Financed by the Scientific Research Support Fund*

Volume 13 Number (2)

http:// jjees.hu.edu.jo/

ISSN 1995-6681

*Aritain volcanic center in Mafraq area.
Photographed by Prof. Khaled Al Tarawneh

JJEES

JJEES (2022) 13 (2): 74-81
ISSN 1995-6681

Jordan Journal of Earth and Environmental Sciences

# “Open Source GIS Solution: An Overview of the Architecture of Free Open Source Web GIS”.

Balqies Sadoun[1], Omar Al-Bayari[1] and Suhaib Al-Tawara

[1] *Department of Surveying Engineering and Geomatics Al-Balqa' Applied University, Al-Salt, Jordan*

*Received 3 June 2021; Accepted 31 August 2021*

**Abstract**

The advancement of modern Information and Communication Technologies (ICT) along with e-governments initiatives and the new digital world, during Covid-19, forced users to look for Free Open Source Software (FOSS) solutions, to serve different normal or specific needs, which is the real drawback of some Commercial software. The digital world is here and it needs modern management using advanced FOSS technology.

We will present an overview of the Architecture of the Free Open Source Web GIS platform to demonstrate its easiness, practicality, and ability to perform effectively and better than commercial GIS tools. The developed platform proposed will be explained based on the succession of published applications of a project which is a “Sewage Infrastructure Network”. A Web Map application for the project has been developed; starting from loading the software and data collection to publishing the results on the web. The Add-ons and other complementary software tools were used for full GIS creation and functions with database management, Applications, and an easy online updating of the published data. Applications, publishing, and easy online updating at low cost are major issues to future success and the OS is the solution.



**Keywords:** Free Open Source Software (FOSS), Geographic Information System (GIS), Web GIS, and Database Systems.

## 1. Introduction

Newly available solutions which are proposed (FOSS) need to be used to prove their capabilities to replace the expensive Commercial solutions. In previous research using an Open Source (OS) GIS, we created an Application (Water Pipes) for water and sewer complaints submission, using GIS Cloud (Al-Bayari, 2018). Using the app. was expensive to the public users (as they have to pay a fee to the Cloud), which reduced its efficiency. To improve the efficiency, we devised a new solution using the GIS Web app. (Al-Bayari et al., 2020) with little cost to the government we will be able to save expensive wasted resources using FOSS possibilities.

Web mapping is the right medium to circulate your GIS data through the web and publish it. The Creation of a web map is not the same as creating a GIS. To create a web map with GIS characters, you need web programmers and FOSS tools to convert the work in GIS to web maps. Web maps are important to publish maps for their ability to adapt and display in a web browser or a mobile phone. Web maps can be static or dynamic and dynamic maps may be active or interactive. We will present the creation of an interactive web map using QGIS & other Open Source applications for a real web GIS project for the infrastructure of a sewage network

Free Open Source refers to software in which its source code is publicly accessible and users can modify and share their modifications. It opens exchange, mutual participation, clearness, and community-oriented usage and development (Kevane and Gray, 1999). The source code of FOSS is open to all users to inspect, modify, and enhance for their general or specific needs. Its source code is available to all to use, copy, learn, teach, and modify. Computer users, while exporting checking their emails, web pages, or chatting, they use open-source software to route the data to the “local” devices (Tiemann and Initiative, 2009).

The Free Open Source GIS Software was developed as a Desktop GIS, like other GIS software such as Map window but lately, the most common Desk Top GIS solution used is the QGIS (Hugentobler, 2008). QGIS maintained by volunteer developers who continuously release updates, add-ons, and bug fixes. It is used by academics and professionals and translated into over 50 languages. The application of QGIS functions as GIS software allows analyzing and editing of spatial data and information and creating and exporting graphical maps. QGIS supports vector and raster layers, where vector data is stored as point, line, or polygon features. Various formats of raster images are supported in addition to the ability to georeference images. QGIS supports shapefiles, coverage, personal geodatabases, PostGIS, dxf, MapInfo, and other formats. Web services, including Web Map Service and Web Feature Service, are also supported to allow external sources of data usage. QGIS can integrate with other open-source GIS packages, including, GRASS GIS, PostGIS, and Map-Server to offer more functions (Kevane and Gray, 1999). Plug-ins are written in Python or C++ to increase the QGIS's capabilities and usage.

* Corresponding author e-mail: balqiessadoun@bau.edu.jo

## 2. Discussion and methodology

### *2.1 Open Source Web GIS Architecture:*

The WebGIS platform has different components and software to maneuver, analyze, store, broadcast, publish and envision spatial data. These components should be integrated as a dynamic system or platform using integration tools (Brovelli et al, 2017). The architecture of our proposed Free Open Source solution is presented in Figure 1, where all the main components and integration tools are defined based on the proposed application. The Desktop GIS software is the start point where GIS users can perform data cleaning, processing, structuring, and symbolizing work on their spatial data. In the working process, the spatial data should be stored properly to facilitate the communication between desktop GIS software and the middleware (server GIS software) and supports processing on the website as well (Minghini, 2014). Open-Source relational database systems with spatial extensions are the best to allow the publishing the spatial data. Then, GIS users need the middleware that connects the desktop to the web to publish the spatial data (or a subset of it) using SQL queries, as well as, needs to define the style description (Yao and Zou, 2008). The open-source middleware (server GIS software) provides web map services capability through different GIS standards to perform GIS services.

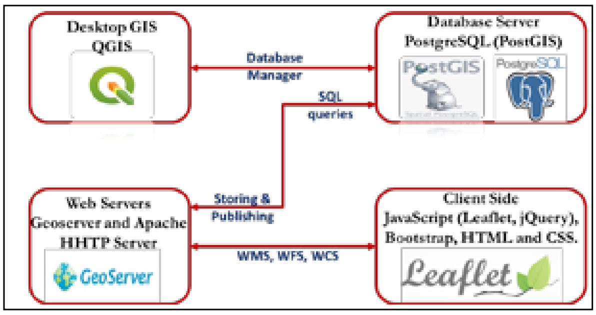


**Figure 1.** Platform Components and Integration Tools

There are many FOSS solutions to be used to build a WebGIS platform (Moreno-Sanchez, 2012). For demonstration and testing, we will present an easy solution to publish our spatial and non-spatial data using the WebGIS platform.

### *2.2 Desktop GIS (QGIS)*

QGIS is one of the best OS desktop GIS software tools that are globally used by GIS users (QGIS, 2021). It's integrated with different geospatial software like GRASS GIS and SAGA GIS to offer more capabilities and better options. QGIS users can download many plug-INS (available online), which were developed by different GIS users. QGIS is compatible with many operating systems like Windows, Linux, Mac OS, and Android, to be easily used on all devices, especially open-source operating systems. Figure 2, presents the main window of QGIS.

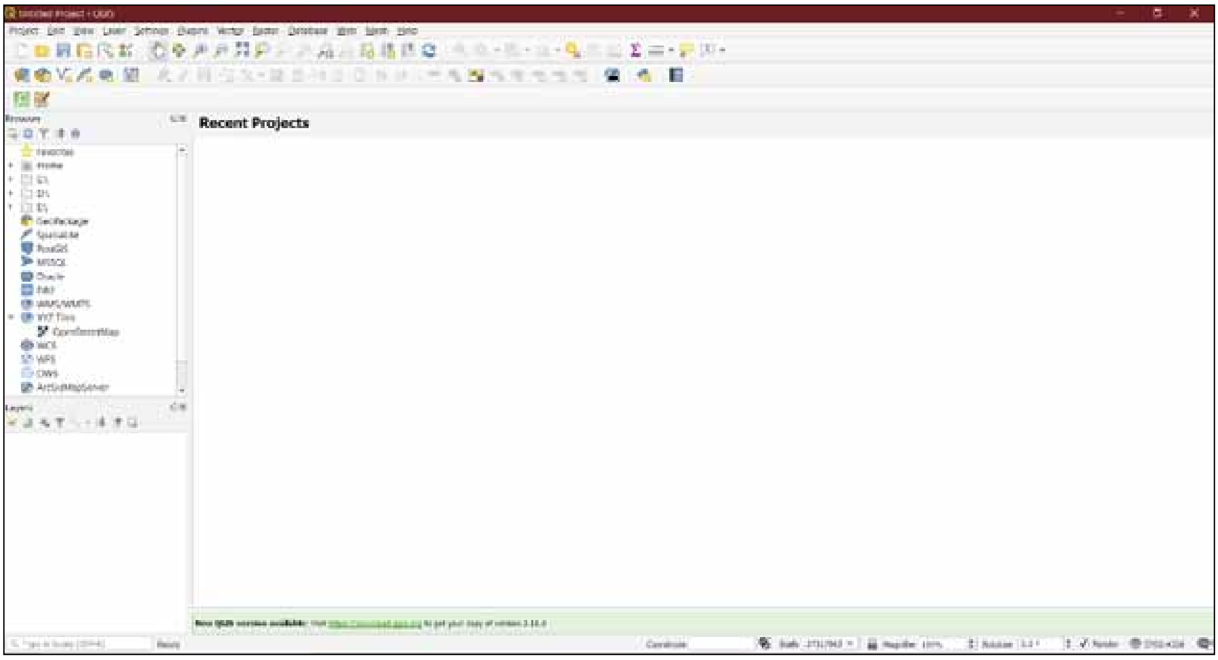


**Figure 2.** QGIS main Window

### *2.3 Database*

GIS users need a well-built system that can use different data types, as well as, spatial information. PostGIS is a spatial database extender for PostgreSQL object-relational database. It supports geographic objects to allow location queries to be run in SQL. PostgreSQL is an open-source object-relational database system that uses the SQL language combined with many features that safely store and scale the most complicated data workloads (Choi et al., 2015). PostgreSQL has a reputation for its good architecture, reliability, data integrity, strong feature set, and the devotion of the open-source community to deliver great and novel solutions. PostGIS supports different geometry types like points, multi-points, lines, multi-lines, polygons, and multi-polygons (Getman, 2015). Also, it is used to store raster data (PostGIS Raster).

QGIS connects to PostGIS databases, to allow GIS users to upload the spatial data on PostGIS to edit, update or remove spatial features that are uploaded or created on PostGIS. Using the DB manager in QGIS, the users can identify the connection parameters and start working on uploading, creating, and editing spatial data on PostGIS. Figure 3, displays the Database Manager in QGIS while importing the Shape file of our infrastructure project into PostGIS. Figure 4 displays how the PgAdmin uses the PostGIS extension to visualize, edit, analyze, update and remove spatial data using SQL language. In Figure 4, we can see a display of a part of the created Sewage Network.

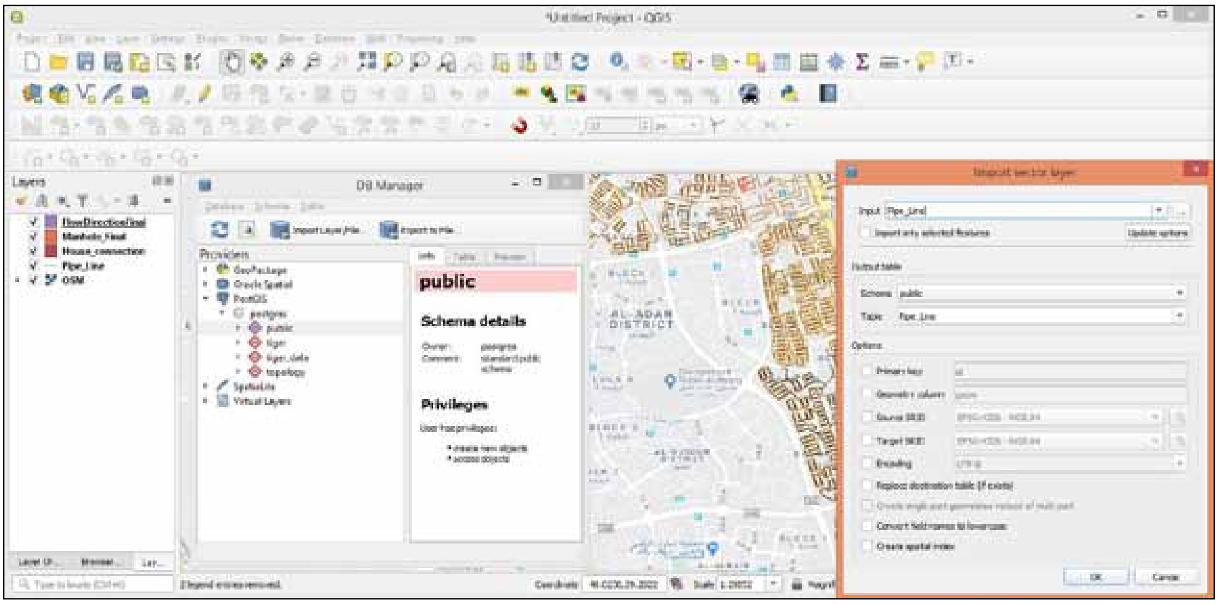


**Figure 3.** DB manager used to Import and Export spatial data to and from different types of spatial storage (DM Manager used to Import shape files to PostGIS).

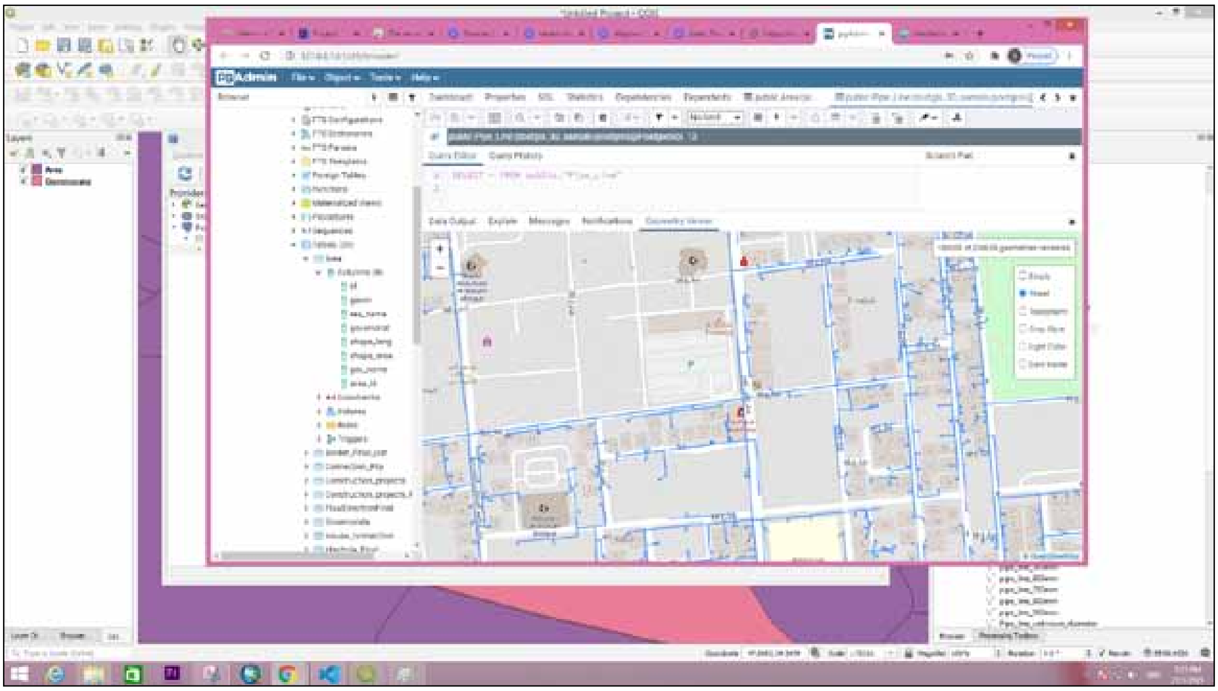

**Figure 4.** PgAdmin uses the PostGIS extension to visualize, edit, analyze updates, and remove spatial data using SQL language.

*2.4 GeoServer*

Storing spatial data in PostGIS makes the communication between desktop GIS and GIS servers easier and more efficient. OSGIS server can use PostGIS as a data source or store and can publish the spatial information on the Internet. GeoServer is an open-source server for sharing geospatial data (Yao and Zou, 2008; Garegnani, et al., 2015) It is a Java-based software server that allows users to view and edit geospatial data. GeoServer offers the facility of map creation and data sharing using open standards set out by the Open Geospatial Consortium (OGC), (Brovelli, et al., 2015). GeoServer along with Apache HTTP Server is used to publish spatial data in sync with the current HTTP standards. Apache HTTP Server is a collaborative software development effort for creating a strong, feature-full, free source code implementation of an HTTP (Web) server.

Figure 5, presents the publishing of our project in

GeoServer (GeoServer tools can publish the spatial data directly from PostGIS). Moreover, we will be able to publish updated layers or tables inside PostGIS. The Published data on GeoServer can be shared as WMS, WFS, WCS, and other standards (Steiniger and Hunter, 2012)., as shown in Figure 6, where the GeoServer presents the sewage pipelines as WMS (WMS can be linked with SLD to get a better presentation of the spatial data).

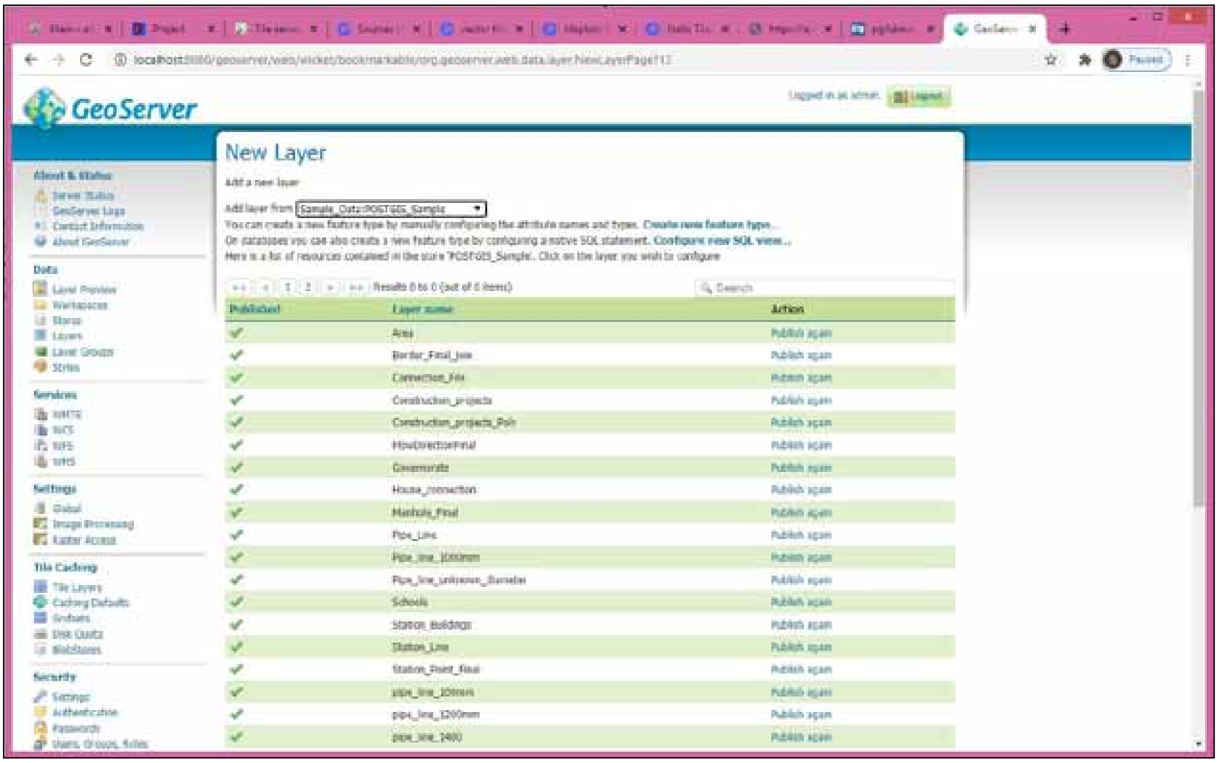


**Figure 5.** Geoserver can use PostGIS as a store of the spatial data and its tools to publish the spatial data directly from PostGIS or to publish any updated layer or table inside PostGIS.

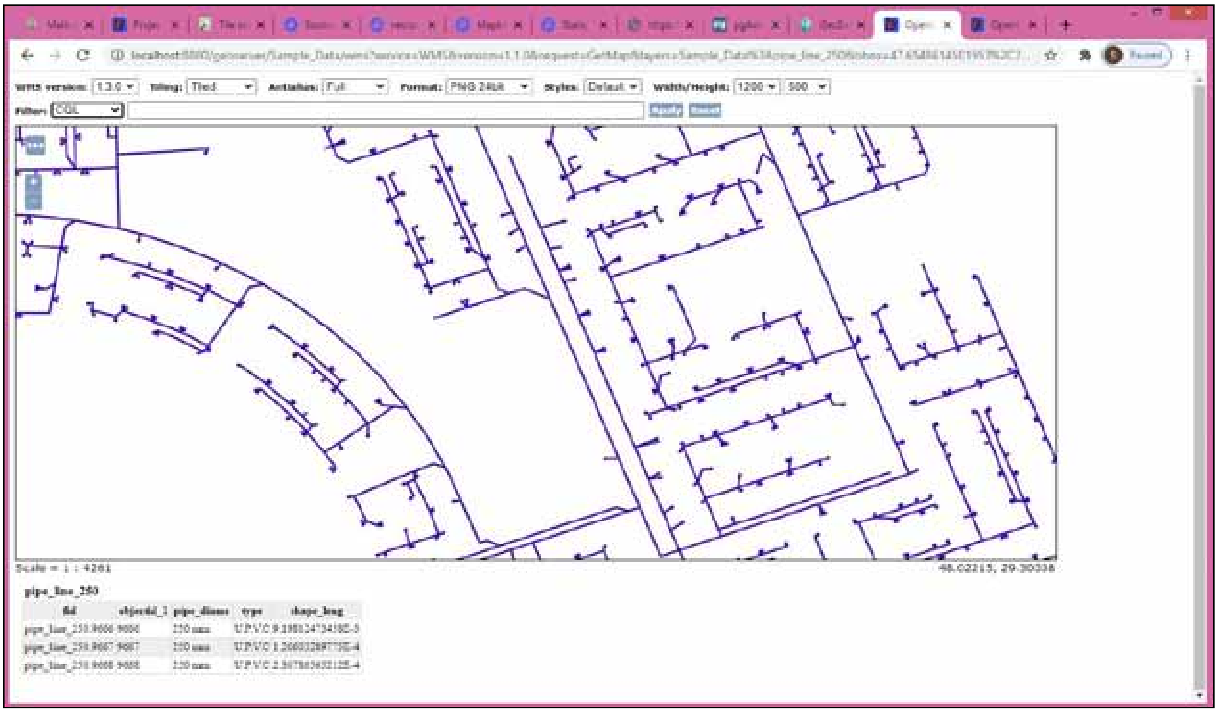

**Figure 6.** Published data on GeoServer can be shared as WMS, WFS, WCS, and other standards for specific purposes (WMS can be linked with SLD to have better spatial data visualization).

GeoServer serves spatial data using standard protocols established by the Open Geospatial Consortium (OGC) like WMS which supports requests for map images, WFS which supports requests for geographical feature data with vector geometry and attributes, and WCS which supports requests for coverage data (raster data). The Styled Layer Descriptor (SLD) Profile of the Web Map Service (WMS) Encoding Standard defines an encoding that extends the WMS standard to allow user-defined symbolization and coloring of geographic features and coverage data (Cannata, et al., 2015) SLD addresses the need for users and software to be able to control the visual portrayal of the geospatial data. The ability to define styling rules requires a styling language that the client and server can both understand. SLD can be generated using QGIS and uploaded easily on GeoServer. Published spatial data can be linked with SLD and WMS will show the data with its SLD by default.

### *2.5 JavaScript (Leaflet, jQuery)*

On the client side, JavaScript libraries (Leaflet, jQuery) as well as Bootstrap, HTML5, and CSS, are used to design the web app (client side). The leaflet is an open-source JavaScript library used to design friendly interactive maps. It has many mapping features and functions with simplicity in design. Leaflet facilitates editing, accessing, and communicating spatial data on the client side. Figure 7, presents a sample of a code developed by our team that uses JavaScript libraries, Bootstrap, HTML5, and CSS to design the client side of the GIS web application.

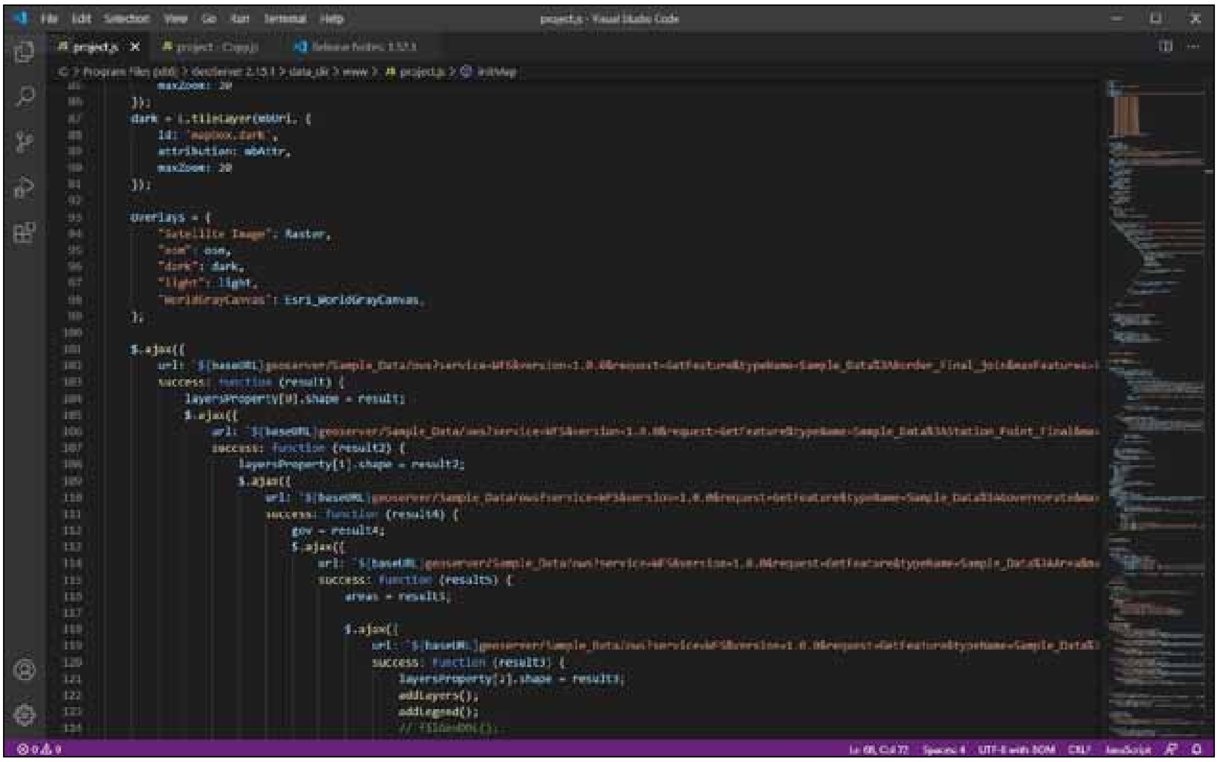

**Figure 7.** Sample of a code that uses JavaScript libraries, Bootstrap, HTML5, and CSS to design the client side of the GIS web application.

### *2.6 Web GIS Application Interface*

The application interface displays the different layers, satellite images, and non-spatial data, it consists of two frames, where the main components are the navigation tools (zoom in and zoom out), and search tools (load different layers and satellite images). Figure 8, presents the main viewer displaying some pipelines and manholes in our published project “Sewage Network”.

**Figure 8.** Sample of the final output – a web interactive map containing different services like WMS and WFS. WMS is symbolized and described by SLD attached with the spatial layers on GeoServer.

## 3. Sewer Network Description:

A Sewage network is composed of sewer lines that are connected at junction points, which are considered nodes. The sewer lines and nodes are treated as a geometric network. Geometric networks offer a way to model common networks water flow, manholes capacity, and pipes diameter can be modeled and analyzed using geometric networks (Najeeb, 2017). Many factors and data should be considered in the planning and design of sewage networks, such as the determination of population equivalent, peak flow, type and size of pipe, flow velocities, invert level, and outlet level, (Figure 9). Sewer Cad or excel sheet could be used to design the pressure flow and gravity flow through the pipelines and pumping stations.

The FOSS GIS platform is used to display and show old sewage networks, new networks, and designed infrastructure projects in the city, where the decision-maker can study and analyze the expansion of sewer networks based on GIS capabilities.

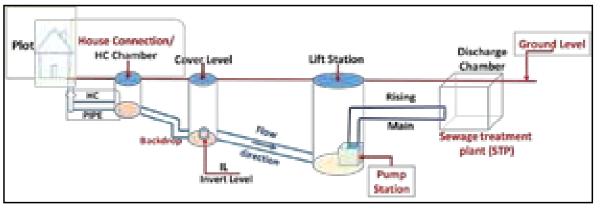


**Figure 9.** Sewage Network Components

## 4. Results and discussion

Researchers did many comparisons between commercial and OS software for different important technical points of view according to needs and functionality such as data type and data consumption, data processing, speed of processing, editing, and the type of results (Veenendaal, et al., 2017; Sandhya, 2017) to proof OS efficiency. We are presenting two new operational processes which were needed for the processing of our application, to test the effectiveness of our platform, and to set up a working process that will help future OS users follow to get the needed results for two specific tasks:

1- Data conversion, from Cad to GIS for sewer networks: the main feature of our WebGIS platform is to display the sewer networks on the WebGIS for planning and future applications purposes. It is well known that the design of Sewer Networks is done and stored in Cad design. It is not possible to upload these files into GIS without the data migration process from Cad to GIS format, for display and further analysis. Most commercial software such as ArcGIS well defined procedure for data conversion (based on the ArcGIS documentation or user manual). Commercial GIS software uses ETL tools to convert the Cad file into a GIS shapefile. Using OS software, such as QGIS the data conversion needs more time and a right well-defined setup for data conversion. Figure 10 presents the flowchart of the processing to convert the Cad files into QGIS. We get much better and correct results using the proposed process compared to when using the plug-in tools provided by QGIS (Particularly for Sewer Networks). The resulting conversion of Cad files is shown in Figure 11. As a result of our research, we set up a process (Figure 10) to convert Cad Files into GIS (Shapefile or PostGIS) using OS QGIS, for Cad files (Sewer Network data), which will better help the OS QGIS users.

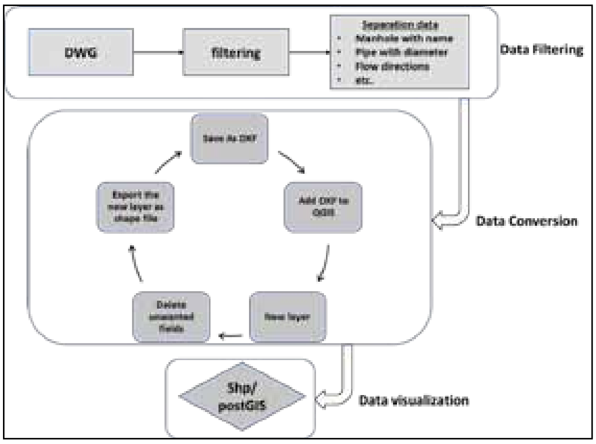


**Figure 10.** The flow chart of the proposed methodology of converting Cad to shapefiles using OS QGIS

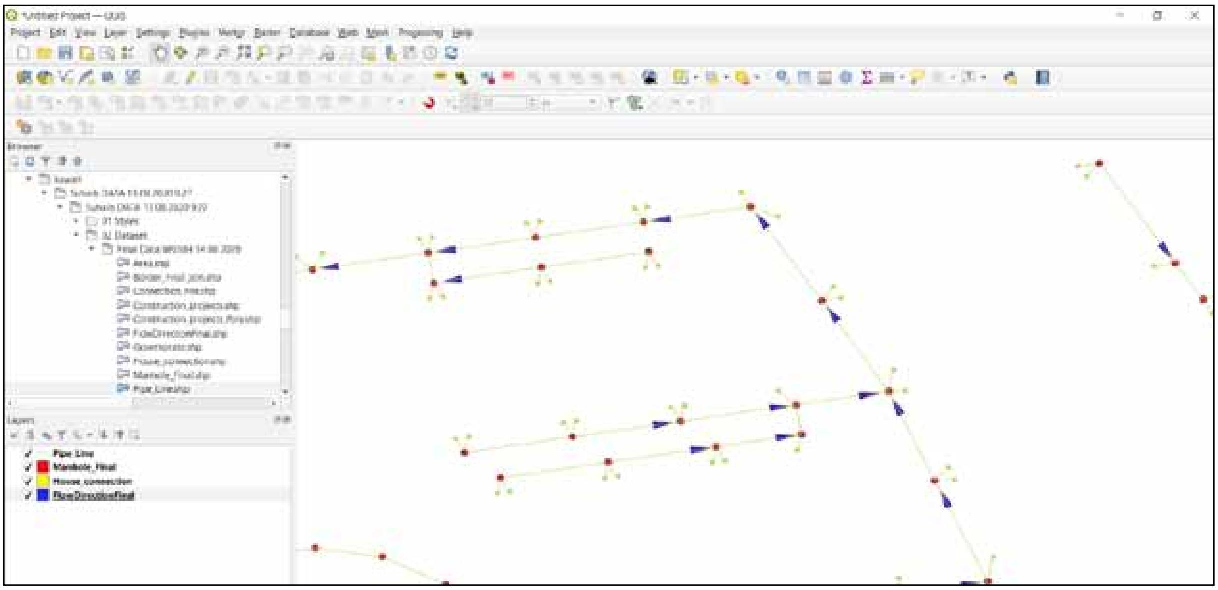

**Figure 11.** Sewer Network converted from CAD to GIS in QGIS

2- Dynamic update of published data on WebGIS using QGIS: Most Commercial software such as ArcGIS Enterprise can update the GIS database through direct connection with Desktop applications, the process of updating, and publishing data is very difficult and needs GIS experts. In our OS Application we set a much easier procedure to be followed by the GIS users, (Figure 12). OS offers the possibility to developers to master the GIS concepts and direct the functions to get the needed results from the Application. To update the GIS data, we edit the PostGIS spatial data in QGIS and then the data is published directly in Geoserver (Figure 13). Similar to the archiving process using ArcGIS enterprise tools, PostGIS can be used to track the edit history on the spatial tables using the trigger system, so it should be easy to see how has the data changed between two dates, who made the changes, and where did they occur?

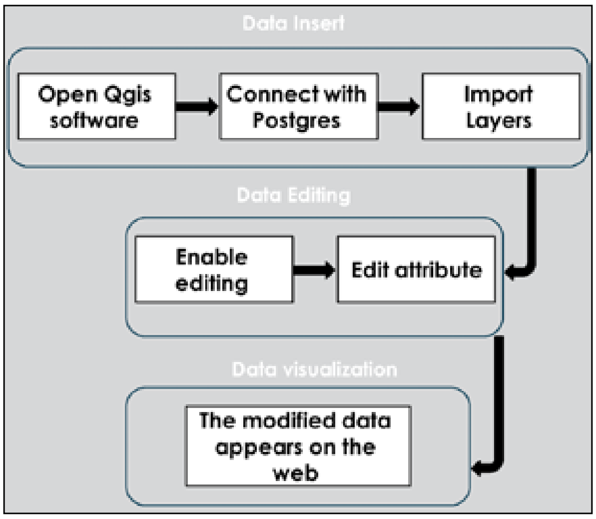


**Figure 12.** Flow chart process for updating data using OS Web GIS (Geoserver) and QGIS

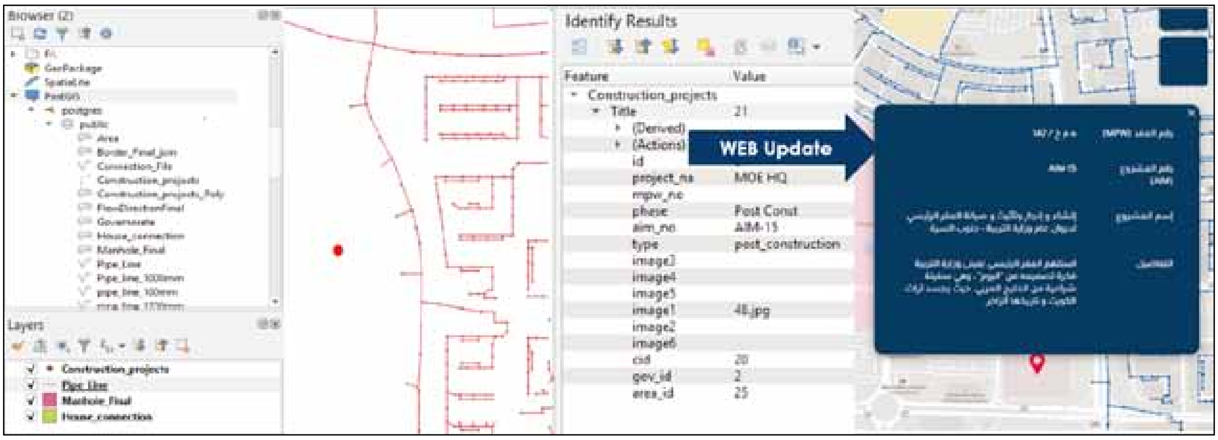


**Figure 13.** Example of update GIS Data on Geoserver using QGIS

## 4. Conclusions

We concluded with the following comments:

- OS software could be modified for general and specific needs, which is the real drawback of some expensive commercial software. It is constantly developing and under-verifying due to its open nature. OS solution offers the possibility-free of charge Applications.
- QGIS is an Open Source GIS that offers an easy-to-use solution at no cost and in no time. It is easy to install for MS Windows and Mac OS X. QGIS has an easy-to-use graphical user interface (GUI), providing common functions and features. It supports different raster and vector data formats and a new format is easily added using the plugins. QGIS is released under the GNU General Public License (GPL), so you can inspect and modify the source code, and guarantees that you have access to a GIS program as long as you need (stability).
- Publishing the data on the GeoServer allows for creating a Web Map Application. We can build the Code of the Web Map Application by Leaflet js. To allow the code to identify the linked data (from Geosphere) we had to alter the settings of the GeoServer by (Enable CORS). Enable CORS: The standalone distributions of GeoServer include the Jetty application server. Enable Cross-Origin Resource Sharing (CORS) allows JavaScript applications outside of your domain to use GeoServer.
- In this work we offered the methodology to follow using OS QGIS to acquire the following: a) An easiness and freedom in serving specific needs while using the available data (Cad files), b) more correct data conversion than using QGIS plug-ins, c) the creation of an efficient application and its web mapping processing, using QGIS OS, d) The ability and ease of the online updating of the published GIS without the need to a GIS expert contrary to the situation in case of using the QGIS plug-in tools, and finally e) we were able to do it all at a third of the cost when using Commercial software. We believe the future will be the use of the OS anywhere at any time.

**Acknowledgment**

This work has been carried out during the sabbatical leave granted to Prof. Balqies Sadoun from Al-Balqa' Applied University (BAU) during the academic year 2020-2021. Prof. Sadoun appreciates the support of BAU in supporting this research work.

**References**

Al-Bayari, O. (2018, July). GIS cloud computing methodology. In 2018 International Conference on Computer, Information and Telecommunication Systems (CITS) (pp. 1-5). IEEE.

Al-Bayari, O., Sadoun, B., & Shatnawi, N. (2020). An Internet and wireless networking-based water pipes web application for fault reporting. International Journal of Communication Systems, 33(8), e4363.

Brovelli, M. A., Minghini, M., & Zamboni, G. (2015). Public Participation GIS: a FOSS architecture enabling field-data collection. International Journal of Digital Earth, 8(5), 345-363.

Brovelli, M. A., Minghini, M., Moreno-Sanchez, R., & Oliveira, R. (2017). Free and open source software for geospatial applications (FOSS4G) to support Future Earth. International Journal of Digital Earth, 10(4), 386-404.

Cannata, M., Antonovic, M., Pozzoni, M., & Graf, A. (2015, April). Open Source and Open Standard based decision support system: the example of lake Verbano floods management. In EGU General Assembly Conference Abstracts (p. 11233). (accessed: 10 March 2021)

Choi, J., Kim, H., Ahn, J., & Kim, J. (2015). FOSS4G for rapidly urbanizing cities and UN sustainable development goals (SDGs); SDG 11 cities and human settlement. In Seoul, Korea: LH-OSGeo Joint Seminar: Open Source GIS for UN and Developing Countries.

Denver, September 24, 2015.

Garegnani, G., Geri, F., Zambelli, P., Grilli, G., Sacchelli, S., Paletto, A., Curetti, G. ,Ciolli, M., and D. Vettorato, (2015). "A new open source DSS for assessment and planning of renewable energy: r. green" Geomatics Workbooks, Vol. 12, pp. 39–49

Getman, Dan. 2015. "Visualization and Analysis of Spatiotemporal Data Using Free and Open

Hugentobler, M. (2008). Quantum GIS. In S. Shekar and H. Xiong (Eds.), Encyclopedia of GIS (pp. 935–939). New York: Springer.

Kevane, M., & Gray, L. C. (1999). A woman's field is made at night: Gendered land rights and norms in Burkina Faso. Feminist Economics, 5(3), 1-26.

Minghini, M. (2014). Multi-dimensional GeoWeb platforms for citizen science and civic engagement applications.

Moreno-Sanchez, R. (2012). Free and Open Source Software for Geospatial Applications (FOSS4G): A mature alternative in the geospatial technologies arena.

Najeeb, Z. (2017). Evaluation of Combined Sewer Network Design Using GIs and Multi-Criteria Decision Making (MCDM). Al-Nahrain Journal for Engineering Sciences, 20(5), 1143-1153.

QGIS, (2021), https://qgis.org/en/site/ (10 March 2021)

Sandhya, M. C. (2017). Exploring opportunities with open source GIS.

Sandinska, Y. (2016, June). Technological Principles and Mapping Applications of Web GIS. In 6th INTERNATIONAL CONFERENCE ON CARTOGRAPHY AND GIS (p. 287).

Source Software at the National Renewable Energy Laboratory." Presented at GIS on the Rockies,

Steiniger, S., & Hunter, A. J. (2012). Free and open source GIS software for building a spatial data infrastructure. In Geospatial free and open source software in the 21st century (pp. 247-261). Springer, Berlin, Heidelberg.

Tiemann, M., & Initiative, P. O. S. (2009). How open source software can save the ICT industry one trillion dollars per year. retrieved July 3, 2009.

Veenendaal, B., Brovelli, M. A., & Li, S. (2017). Review of web mapping: Eras, trends, and directions. ISPRS International Journal of Geo-Information, 6(10), 317.

Yao, X., & Zou, L. (2008). Interoperable internet mapping—an open source approach. Cartography and Geographic Information Science, 35(4), 279-293.

JJEES

Jordan Journal of Earth and Environmental Sciences

JJEES (2022) 13 (2): 82-88
ISSN 1995-6681

# Geoelectrical Study of Groundwater Potential at Waziri Umaru Federal Polytechnic's Gesse Campus BirninKebbi, Kebbi State, Nigeria

Ibrahim Mohammed[1] and Suleiman Taufiq[2]

*1Department of Preliminary Studies, Waziri Umaru Federal Polytechnic, Birnin Kebbi, Nigeria.*
*2Department of Science Education, Waziri Umaru Federal Polytechnic, Birnin Kebbi, Nigeria.*

*Received 7 August 2021; Accepted 2 September 2021*

**Abstract**

Vertical Electrical Soundings (VES) are utilised in geophysical exploration to provide quick and cost-effective measurements. VES was utilised to explore groundwater at Waziri Umaru Federal Polytechnic's permanent campus in Birnin Kebbi. Eighteen (18) Vertical Electrical Soundings (Schlumberger array, maximum AB/2 spacing 100 m) were conducted, with data collected using an ABEM terameter (SAS 300c) to determine the geoelectric units in the subsurface strata and to delineate groundwater potential in the area. The acquired field data was evaluated using (IPI2win), which provides the interpretation of apparent resistivity in an ohm.meter. The resistivity and thickness of subsurface layers were used to analyse the data. Three to five (3-5) unique strata were identified in the research region, including topsoil, which is mostly sand, clayey sand/lose sand, sandy clay/fine sand, and clay unit. Water bearing aquifer exists at layer three in some identified VES locations, such as VES 3, VES5, VES13, and VES14, with thickness and associated resistivity values of 40.5 m, 37.5 m, 45.8 m, 60 m, and 173 ohm.m, 148 ohm.m, 222 ohm.m, and 432 ohm.m, respectively. As a result of the electrical resistivity data, acceptable accurate results may be obtained that can be used to comprehend stratigraphy.



**Keywords:** Free Open Source Software (FOSS), Geographic Information System (GIS), Web GIS, and Database Systems.

## 1. Introduction

Freshwater is highly a valuable resource often on which life depends, and its availability is critical to any community's long-term viability (Adagunodo *et al.,* 2018; Omosuyi *et al.,* 2021). There are different sources of water, such as streams, rivers, and ponds; none are as sanitary as groundwater, which is of great purity as well as appropriate chemical quality for numerous applications (Ventaka *et al*., 2014). Groundwater is found in diverse rock types and at various depths in variable proportions. Geophysical techniques are applied in the exploration of this portable freshwater source, which is a unique experience (Anomohanran *et al.,* 2020; Maxwell *et al.,* 2015). Among several methods used in groundwater exploration, the resistivity method is the most effective for locating productive wells, and VES provides information on the vertical variation in the ground's resistivity with depth (Al-Garni *et al.,* 2002). The resistivity method in geophysical exploration for groundwater in a sedimentary environment has proven reliable among other geophysical methods (Dahab, 2012). However, among different electrode arrays used for resistivity measurement, VES is the most popular (Abdulrazzaq *et al.,* 2020; Ekwok *et al.,* 2020; Raji & Abdulkadir, 2020) and is used to forecast the thickness and depth of aquifers (Rahajoeningroem & Indrajana, 2020).

This approach is reliable in finding layers with low resistivity values that may be a sign of saturated strata in a variety of geophysical terrains. The quality and quantity of groundwater resources are influenced by the climate and geology of an area. The climate maintains a consistent supply or recharge of groundwater resources through rainfall and surface water resources in a complicated hydrological cycle. The geology of the area determines the aquifer zones where exploitable groundwater may occur, as well as the geochemical features of the groundwater; human activities influence the geochemical aspects of the groundwater, among other things (Olasehinde *et al.,* 2015; Raji & Abdulkadir, 2020). In the sedimentary terrain, permeable and porous rock masks such as sandstone and lose sands, etc. are good indicators of the aquifer (Kola *et al*., 2013).

Due to the continual evacuation of students and staff from the temporary to the permanent campus of the institution, available water resources are threatened by an expanding population trend. However, it appears that groundwater research in Kebbi State is not keeping up with the state's high demand due to population increase, which is a major problem for the state's future groundwater development. The demand for groundwater has increased dramatically in recent years due to population growth, urbanisation, industrialisation, and intensive agricultural activities in the State in particular and Nigeria in general. However, surface water in Nigeria can easily be contaminated due to the failure of regulatory bodies to address water-related issues (Joel *et al*., 2020). This study aimed at using the electrical resistivity method to determine the groundwater potential at the permanent site of Waziri Umaru Federal Polytechnic, Birnin Kebbi with the following objectives: (i) determine the resistivity at earth's layers (ii) obtain the thickness of the earth's layers (iii) present the resistivity patterns at earth's layer (contour maps) and (iv) the depth to the confined aquifer. A thorough understanding of the geology of the area is required for

* Corresponding author e-mail: ibrahimmohd628@yahoo.com

successful groundwater investigation in sedimentary terrain. The exploration of groundwater has been easier in the study area because it is a sedimentary landscape (Abbey & Onyebueke, 2020).

## 2. Location, meteorology, and geology of the area

The area under study is within the sedimentary region of northern Nigeria between latitudes 12°27.454'N to 12°28.239'N and longitudes 004°13.624'E to 004°14.874'E in Birnin Kebbi metropolis of Kebbi State in north-western Nigeria (Figure 1).

Kebbi State belongs to the savanna climate where the rainy season and the dry season are clear. From May to October is the rainy season whereas from November to April is the dry season. Between December and March, it hardly rains with mean monthly precipitation of almost 0mm, though the annual mean precipitation is 835mm. The annual average minimum temperature is 22.2$^{o}$C, and the annual average maximum temperature is 34.7$^{o}$C (JICA, 2011).

Two formations dominate the study region Kebbi State: Prec. Gneiss is found in huge areas across the Basement Complex, while schist and granite are found in smaller areas. In the Cretaceous, argillaceous strata with intercalated sandstone layers predominate in the lower portion of the Cretaceous, whereas sandstone strata thicken in the upper section. The argillaceous strata predominate in the Tertiary's lower section, whereas sandstone layers are intercalated in the Tertiary's higher part. The Quaternary alluvial deposit is distributed over the lowlands along big rivers such as River Niger and Sokoto River, with a small thickness of the deposit (Figure 2). It is presumed that the aquifer consists of (i) the weathered and fractured part of the Basement Complex, (ii) the sandstone and the fractured part of the Cretaceous, and (iii) the sandstone layers of Tertiary (JICA, 2011).

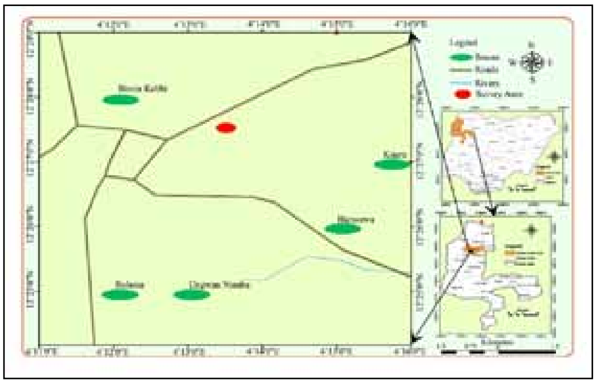


**Figure 1.** Location Map of Study Area


**Figure 2.** Geological Map of Nigeria showing Kebbi State

## 3. Materials and Method

Materials used include Global Positioning System (GPS), ABEM Terrameter (SAS 300c), connecting cables, four electrodes (steel rods), measuring tapes, and hammers. The IP2Win software (version 12.0) was used for analyzing geo-electrical data. 18 VES were conducted at different points using Schlumberger configuration with electrode spread at maximum AB/2 = 100m (Figure 3). Current electrodes (A and B) of equal distance on the opposite sides of the VES station and potential electrodes (M and N) were derived into the ground for proper contact to be made with the ground (Figure 4). With MN/2 fixed at its initial distance and AB/2 symmetrically expanded, the measurements were repeated and recorded. MN/2 was proportionately increased whenever the measured resistance became low. These pairs of electrodes were connected to the Terrameter through points AB and MN, which is referred to as the Schlumberger configuration.

**Figure 3.** VES Points in the Area under Study (Google Earth).

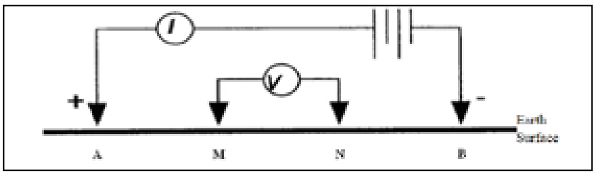

**Figure 4.** Schlumberger Array followed in this study.

## 4. Results and Discussion

The true resistivity model is determined by variations in the characteristics of subsurface materials (Hasan *et al.,* 2018). The results of the geoelectrical survey were presented in Tables 1, 2, and 3. Resistivity and thickness obtained from the analysis of the data (Figure 5) were used to adjudge the aquifer or non-aquifer layers and expected geologic formations (Bersi & Saibi, 2020; MO *et al*., 2020). The real resistivity-depth curve takes the shape of a sounding curve, with increasing electrode spacing, the perceived resistivity's rise (or drop) as the true resistivity's rise (or drop). This is especially true for layers whose thickness increases in direct proportion to their depth (Zohdy, 1989). Resistivity variations exist across lithologic interfaces or geo-electric boundaries in the subsurface. The interpreted result revealed 3 to 5 layers in which the top layer shows the diversity of resistivity and thickness ranging from (383 - 2089 ohm.m and 0.3 - 2.7 m). Resistivity values of layer 2 range between 1141 to 29558 ohm.m, thickness between 0.5 m to 13.4m and are interpreted as clayey sand/lose sand formation. Layer 3 with resistivity range of 60 to 1441 ohm.m and thickness varies from 7.9 to 67 m which was interpreted as sandy clay/ fine sand. Layer 4 resistivity ranges between 1.23 ohm.m to 13389 ohm.m, thickness, from 2.1 to 39.7 m, and is interpreted as clay formation. The fifth layer exists in VES 1, 6, 8, 11, 12, 17, and 18 with unknown thickness, which indicates medium grain sand and sandstone formation. The fourth and fifth layers have very low resistivity values in some parts of the area which attribute to the saturated clay (Olasehinde *et al.,* 2015). Due to the decrease in resistivity values in layer 3 compared to layer 2 in some parts of the area, shows that layer 3 delineates a probable water saturation zone (Kola *et al*., 2013). The depth of the aquifer layer ranged between 9.7 m to 69 m in VES 17 and VES 14 respectively (Figure 6). These values are comparable to those of (JICA, 2011) and (Usman, 2020) and the result was also correlated with borehole log data obtained from drilled boreholes close to the study area (Figure 7). According to Omosuyi *et al.* 2007, high groundwater prospect zones are defined as those where the aquifer thickness exceeds 18 m, while medium and low groundwater prospective zones are defined as those where the aquifer thickness is between 10 and 18 m and below 10 m, respectively. The research area's relatively high aquifer thickness value makes it productive and desirable (Eugene-Okorie *et al*., 2020). Five separate subsurface layers were identified based on the quantitative interpretation and lithology of the locations, with their geoelectric curves denoted as K, KH, KQ, QQ, and HKH. It was observed that KQ is the dominant curve type in the study area (38.9%) followed by HKH (33.3%), KH (16.7%), and then K and QQ (5.5%) each (Figure 8).

The iso-resistivity analysis provides a qualitative assessment of the differences in resistivity at a certain depth, as well as the overall lateral changes in electrical characteristics in the surrounding area. The iso-resistivity and iso-depth contour maps of the aquifer layer are shown in Figures 9 and 10. Due to the significant values of thickness, the depth contour maps support the hypothesis that certain places may have a substantial groundwater yield. Figures 8 and 9 show that VES 3, VES 5, VES 13, and VES 14 are the ideal locations for groundwater exploration based.

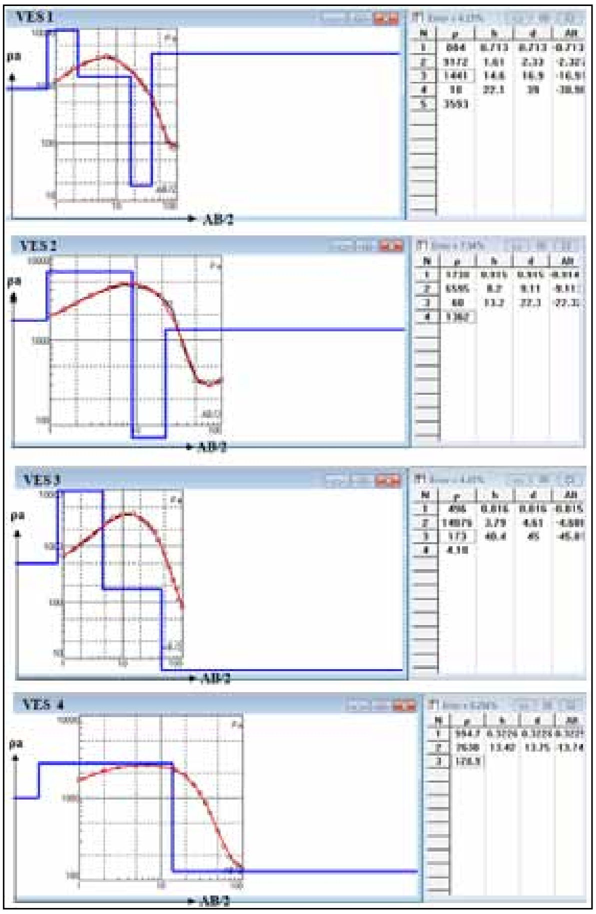

**Figure 5.** Model Curves and analysis.

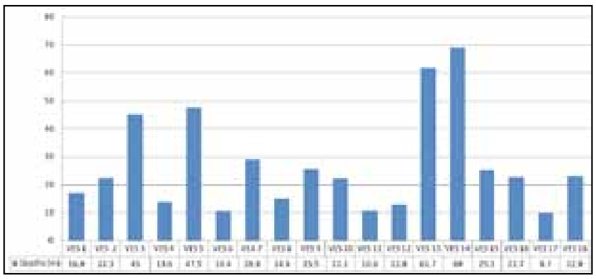
**Figure 6.** VES Depths of aquifer layer.

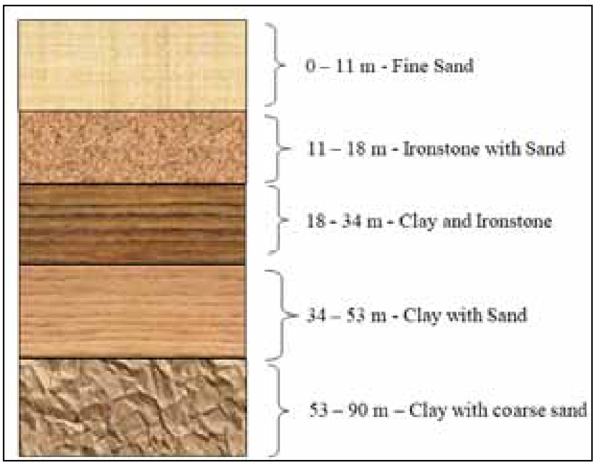


**Figure 7.** Borehole log close to the study area (SARDA, 1988).

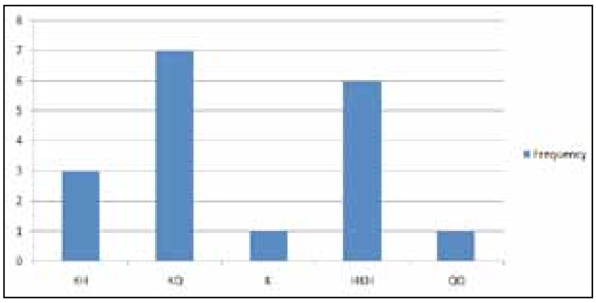

**Figure 8.** Frequency distribution of VES Curves.

**Table 1**. Geoelectric parameters of VES 1 to VES 6.

| Coordinates | VES No. | Layer No. | Resistivity (ohm.m) | Thickness (m) | Depth (m) | Curve Types |
|---|---|---|---|---|---|---|
| 12º27.904'N 004º14.392'E Elevation:744 | 1 | 1 | 884 | 0.7 | 0.7 | KH |
| | | 2 | 9172 | 1.6 | 2.3 | |
| | | 3 | 1441 | 14.6 | 16.9 | |
| | | 4 | 18 | 22.1 | 39 | |
| | | 5 | 3593 | … | … | |
| 12º27.952'N 004º14.365'E Elevation:734 | 2 | 1 | 1738 | 0.9 | 0.9 | KH |
| | | 2 | 6595 | 8.2 | 9.1 | |
| | | 3 | 60 | 13.2 | 22.3 | |
| | | 4 | 1362 | … | … | |
| 12º28.005'N 004º14.351'E Elevation: 734 | 3 | 1 | 496 | 0.8 | 0.8 | KQ |
| | | 2 | 14876 | 3.7 | 4.6 | |
| | | 3 | 173 | 40.4 | 45 | |
| | | 4 | 4.18 | … | … | |
| 12º28.058'N 004º14.351'E Elevation: 726 | 4 | 1 | 994.7 | 0.3 | 0.3 | K |
| | | 2 | 2638 | 13.4 | 13.8 | |
| | | 3 | 128.9 | … | … | |
| 12º28.112'N 004º14.335'E Elevation: 704 | 5 | 1 | 782 | 0.5 | 0.5 | KH |
| | | 2 | 2868 | 9.5 | 10 | |
| | | 3 | 148 | 37.5 | 47.5 | |
| | | 4 | 13389 | … | … | |
| 12º28.167'N 004º14.337'E Elevation: 716 | 6 | 1 | 412 | 0.4 | 0.4 | HKH |
| | | 2 | 9867 | 0.5 | 0.9 | |
| | | 3 | 1247 | 9.6 | 10.4 | |
| | | 4 | 289 | 31.7 | 42.2 | |
| | | 5 | 0.69 | … | … | |

**Table 2.** Geoelectric parameters of VES 7 to VES 12.

| Coordinates | VES No. | Layer No. | Resistivity (ohm.m) | Thickness (m) | Depth (m) | Curve types |
|---|---|---|---|---|---|---|
| $12^{0}$27.920'N<br>$004^{0}$14.445'E<br>Elevation:726 | 7 | 1 | 513 | 0.7 | 0.7 | KQ |
| | | 2 | 8505 | 1.1 | 1.8 | |
| | | 3 | 950 | 27.1 | 28.8 | |
| | | 4 | 1.23 | | | |
| $12^{0}$27.971'N<br>$004^{0}$14.428'E<br>Elevation: 731 | 8 | 1 | 884.7 | 0.5 | O.5 | HKH |
| | | 2 | 12292 | 0.6 | 1.1 | |
| | | 3 | 1296 | 13.7 | 14.9 | |
| | | 4 | 351.9 | 25.9 | 40.8 | |
| | | 5 | 1.31 | | | |
| $12^{0}$28.024'N<br>$004^{0}$14.409'E<br>Elevation: 730 | 9 | 1 | 382 | 0.5 | 0.5 | KQ |
| | | 2 | 1781 | 5.4 | 5.9 | |
| | | 3 | 962 | 19.6 | 25.5 | |
| | | 4 | 13 | | | |
| $12^{0}$28.075'N<br>$004^{0}$14.396'E<br>Elevation: 727 | 10 | 1 | 445 | 0.5 | 0.5 | KQ |
| | | 2 | 2725 | 2.9 | 3.4 | |
| | | 3 | 1194 | 18.7 | 22.1 | |
| | | 4 | 33.3 | | | |
| $12^{0}$28.132'N<br>$004^{0}$14.392'E<br>Elevation: 720 | 11 | 1 | 775 | 1.1 | 1.1 | HKH |
| | | 2 | 8312 | 1.5 | 2.5 | |
| | | 3 | 1080 | 8.0 | 10.6 | |
| | | 4 | 308 | 37.9 | 48.4 | |
| | | 5 | 1.99 | | | |
| $12^{0}$28.186'N<br>$004^{0}$14.389'E<br>Elevation: 670 | 12 | 1 | 1307 | 1.0 | 1.0 | HKH |
| | | 2 | 5633 | 0.5 | 1.4 | |
| | | 3 | 1269 | 11.4 | 12.8 | |
| | | 4 | 265 | 38.1 | 50.9 | |
| | | 5 | 0.78 | | | |

**Table 3.** Geoelectric parameters of VES 13 to VES 18.

| Coordinates | VES no | Layer | Resistivity (ohm.m) | Thickness (m) | Depth (m) | Curves |
|---|---|---|---|---|---|---|
| $12^{0}$28.188'N<br>$004^{0}$14.446'E<br>Elevation: 718 | 13 | 1 | 2089 | 2.7 | 2.7 | QQ |
| | | 2 | 1141 | 13.3 | 16 | |
| | | 3 | 222 | 45.8 | 61.7 | |
| | | 4 | 2.1 | | | |
| $12^{0}$28.135'N<br>$004^{0}$14.457'E<br>Elevation: 719 | 14 | 1 | 951 | 1.2 | 1.2 | KQ |
| | | 2 | 7544 | 0.9 | 2.0 | |
| | | 3 | 432 | 67 | 69 | |
| | | 4 | 4.81 | | | |
| $12^{0}$28.086'N<br>$004^{0}$14.457'E<br>Elevation: 719 | 15 | 1 | 616 | 0.7 | 0.7 | KQ |
| | | 2 | 6504 | 1.8 | 2.5 | |
| | | 3 | 907 | 22.6 | 25.1 | |
| | | 4 | 20.3 | | | |
| $12^{0}$28.033'N<br>$004^{0}$14.468'E<br>Elevation: 723 | 16 | 1 | 866 | 0.4 | 0.4 | KQ |
| | | 2 | 29558 | 0.7 | 1.1 | |
| | | 3 | 756 | 21.6 | 22.7 | |
| | | 4 | 60.9 | | | |
| $12^{0}$27.979'N<br>$004^{0}$14.474'E<br>Elevation: 722 | 17 | 1 | 555 | 0.8 | 0.8 | HKH |
| | | 2 | 3583 | 1.1 | 1.8 | |
| | | 3 | 1006 | 7.9 | 9.7 | |
| | | 4 | 411 | 24.4 | 34.2 | |
| | | 5 | 0.849 | | | |
| $12^{0}$27.926'N<br>$004^{0}$14.492'E<br>Elevation: 738 | 18 | 1 | 970.4 | 1.0 | 1.0 | HKH |
| | | 2 | 2578 | 3.4 | 4.4 | |
| | | 3 | 637.9 | 18.5 | 22.9 | |
| | | 4 | 114.4 | 39.7 | 62.5 | |
| | | 5 | 2.76 | | | |

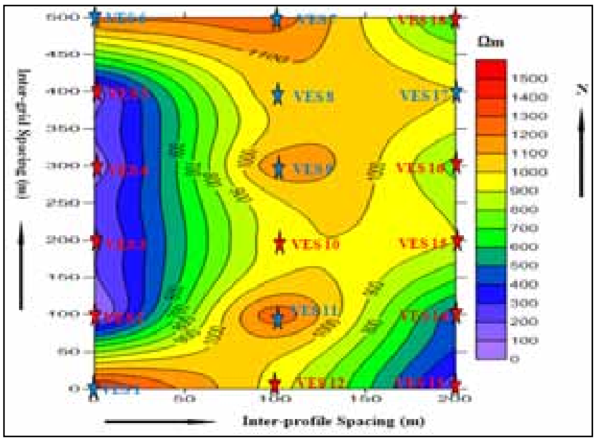


**Figure 9.** Resistivity Contour Map (Layer 3).

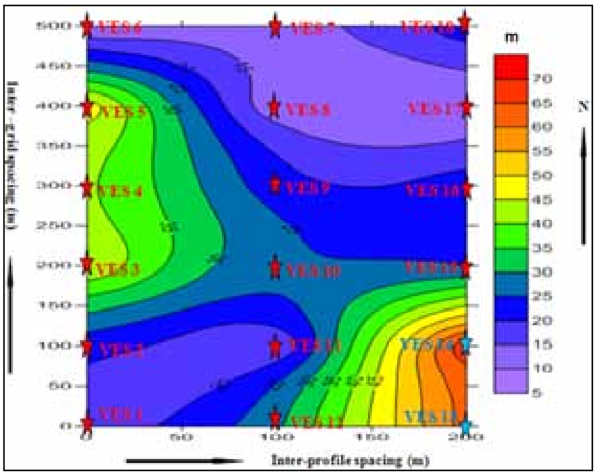


**Figure 10.** Depth Contour Map (Layer 3)

## 5. Conclusion

VES for groundwater exploration at the study area delineates a network of probable features, suspected to be groundwater occurrence. Different metrics, such as resistivity and the thickness of subsurface layers and their lithologic boundaries, were determined, and it was discovered that groundwater potential levels varied from one portion of the research region to the next. Within the research region, where the depth to bedrock is relatively deep and has a low resistivity value, there are good prospects for groundwater potential, whereas those with shallow depth to bedrock and a high resistivity value have a lesser potential for groundwater. The VES results for the entire area revealed a range of depths to strike the top of the water-bearing zones of 9.1 to 69 m. Using iso-resistivity and iso-depth contour maps of the aquifer layer it was observed that the optimum locations for groundwater investigation are within the soundings, VES 3, 5, 13, and 14. The geological formation in the study area consists of sand, clayey sand/lose sand, sandy clay/fine sand, and clay unit. Furthermore, the results obtained from the survey indicate the efficiency of VES techniques for the study of groundwater potential in the sedimentary region.

## Acknowledgment

This research was supported by the Tertiary Education Trust Fund of Nigeria (TETFund).

## References

Adagunodo, T. A., Akinloye, M. K., Sunmonu, L. A., Aizebeokhai, A. P., Oyeyemi, K. D., & Abodunrin, F. O., 2018. Groundwater exploration in aaba residential area of Akure, Nigeria. Frontiers in Earth Science, Pp. 1–12.

Abbey, M. E., & Onyebueke, D. E., 2020. Geoelectric evaluation of groundwater potential: a case study at Omuma local government area, Rivers State, Nigeria. Journal of Petroleum Exploration and Production Technology, 10(8), Pp. 3255–3261.

Abdulrazzaq, Z. T., Al-Ansari, N., Aziz, N. A., Agbasi, O. E., & Etuk, S. E., 2020. Estimation of main aquifer parameters using geoelectric measurements to select the suitable wells locations in Bahr Al-Najaf depression, Iraq. Groundwater for Sustainable Development, 11, 100437.

Al-Garni, M. A., Alisiobi, A. R., Ako, B. D., Andersen, K. R., Wan, L., Grombacher, D., Lin, T., Auken, E., Arefayne Shishaye, H., Abdi, S., Awad Sultan Araffa, S., Sabet, H. S., Dabour, A., Balasubramanian, A., Buursink, M. L., Jr, J. W. L., Survey, U. S. G., Clement, W. P., Knoll, M. D., Yaramanci, U., 2002. Groundwater Investigation Using Combined Geophysical Methods *. Journal of Applied Geophysics, 50(1–2), Pp. 1–8.

Anomohanran, O., Oseme, J. I., Iserhien-Emekeme, R. E., & Ofomola, M. O., 2020. Determination of groundwater potential and aquifer hydraulic characteristics in Agbor, Nigeria using geo-electric, geophysical well logging and pumping test techniques. Modeling Earth Systems and Environment, 0123456789.

Bersi, M., & Saibi, H., 2020. Groundwater potential zones identification using geoelectrical sounding and remote sensing in Wadi Touil plain, Northwestern Algeria. In Journal of African Earth Sciences (Vol. 172). Elsevier Ltd.

Dahab, M. A. H., Abbas, M. Y, and Abdelhakam, E. M, 2012. Geoelectric investigation of groundwater potential in Khor Abu Habil drainage basin. Journal of Science and Technology 13(2).

Ekwok, S. E., Akpan, A. E., Kudamnya, E. A., & Ebong, E. D., 2020. Assessment of groundwater potential using geophysical data: a case study in parts of Cross River State, south-eastern Nigeria. Applied Water Science, 10(6), Pp. 1–17.

Eugene-Okorie, J. O., Obiora, D. N., Ibuot, J. C., & Ugbor, D. O., 2020. Geoelectrical investigation of groundwater potential and vulnerability of Oraifite, Anambra State, Nigeria. Applied Water Science, 10(10), Pp. 1–14.

Hasan, M., Shang, Y., Akhter, G., & Jin, W., 2018. Geophysical Assessment of Groundwater Potential: A Case Study from Mian Channu Area, Pakistan. Groundwater, 56(5), Pp. 783–796.

Japan International Cooperation Agency (JICA), 2011, preparatory survey on the project for inprovement of rural water supply in the federal republic of nigeria. final report. Pp 11 - 046.

Joel, E. S., Olasehinde, P. I., Adagunodo, T. A., Omeje, M., Oha, I., Akinyemi, M. L., & Olawole, O. C., 2020. Geo-investigation on groundwater control in some parts of Ogun state using data from Shuttle Radar Topography Mission and vertical electrical soundings. Heliyon, 6(1).

Kola, O. R., Akinyem, L. P., Akinsegun, O., & Ijeoma, G. C., 2013. Application of Vertical Electrical Method in Groundwater Exploration at Remo North Local Government in Ogun State of Nigeria Corresponding Author : Akinyem L . P. 4(4), Pp. 672–678.

Maxwell, O., Ejike, E. J., & Ugwuoke, P. E., 2015. Geophysical Analysis of Basement Terrain Groundwater Using Vertical Electrical Sounding : A Case Study of Parts of Abuja North Central Nigeria. 2(4), Pp. 92–97.

MO, E., C, O., & AOI, S., 2020. Geoelectrical Parameters for the Estimation of Groundwater Potential in Fracture Aquifer at Sub-Urban Area of Abakaliki, SE Nigeria. International

Journal of Earth Science and Geophysics, 6(1).

Olasehinde, A., Sulaiman, A., Bute, S. I., & Hamza, Y. S., 2015. Hydro Geophysical Investigation of Kushi and its Environs , Northeastern , Nigeria. International Journal of Research in Geography 1(1), Pp. 13–21.

Omosuyi, G.O., Adeyemo, A., & Adegoke, A. O., 2007. Investigation of groundwater prospect using electromagnetic and geoelectric sounding at afunbiowo, near Akure, Southwestern Nigeria. Pacific J. Sci. Technol, 8(2), Pp. 172–182.

Omosuyi, Gregory Oluwole, Oshodi, D. R., Sanusi, S. O., & Adeyemo, I. A., 2021. Groundwater potential evaluation using geoelectrical and analytical hierarchy process modeling techniques in Akure-Owode, southwestern Nigeria. Modeling Earth Systems and Environment, 7(1), Pp.

Rahajoeningroem, T., & Indrajana, B., 2020. Groundwater Potential Investigation Using Geoelectric Method with Schlumberger Electrode Configuration in Catur Rahayu Village, Dendang District, Tanjung Jabung Timur Regency, Jambi Province. IOP Conference Series: Materials Science and Engineering, 879(1).

Raji, W. O., & Abdulkadir, K. A., 2020. Evaluation of groundwater potential of bedrock aquifers in Geological Sheet 223 Ilorin, Nigeria, using geo-electric sounding. Applied Water Science, 10(10), Pp.1–12.

Sokoto Agricultural and Rural Development Authority (SARDA), 1988. Sokoto Fadama Shallow Groundwater Study. Field Report Vol. II Ministry of Agriculture, Sokoto. Pp. 59 – 61.

Usman, Z. M., 2020. Geoelectric Survey For Groundwater Exploration At Birnin-Kebbi, Kebbi State, Nigeria, FUDMA Journal of Science, 3(1), Pp. 168-178.

Ventaka, R. G., 2014. Groundwater Investigation Using Geophysical Methods- a Case Study of Pydibhimavaram Industrial Area. International Journal of Research in Engineering and Technology, 03(28), Pp. 13–17.

Zohdy, A. A. R., 1989. A new method for the automatic interpretation of Schlumberger and Wenner sounding curves. Geophysics, 54(2), Pp.245–253.

JJEES

JJEES (2022) 13 (2): 89-96
ISSN 1995-6681

Jordan Journal of Earth and Environmental Sciences

# Kinematic and Q-slope Application for Stability Assessment of the Rock Slopes Along Goshan_Qupy Qaradagh Road, Sulaimaniyah, NE-Iraq

Ghafor Ameen Hamasur

*Department of Geology, College of Science, University of Sulaimani, Sulaimaniyah, Iraq*

*Received 5 July 2021; Accepted 4 September 2021*

**Abstract**

In the mountainous areas of Iraqi Kurdistan, road and highway networks play a significant role in far-away transportation and social activities. Any slope failure may lead to traffic disruption, and loss of lives. The undesigned excavations of rock slopes for construction or expanding purposes may weaken the slope stability.

In this study, eight (8) cut-rock slope stations have been chosen along Goshan–Qupy Qaradagh tourist road at Sulaimani, NE-Iraq, and these are for evaluating the stability of cut-rock slopes by various techniques. The choice of slope stations was based on variation in the discontinuities pattern, slope morphology, and type of failure. The field data were analyzed for their possible degree of stability by slope kinematic analysis, using DIPS v6.008 software, and to examine the stability condition, the Q-slope system, which is a practical way for rock slope engineering classification, was also used.

Slope kinematic analysis revealed three types of failures, i.e., Planar sliding, wedge sliding, and direct toppling failure. Planar sliding may occur in rock slopes of stations 1, 2, 4, and 8, wedge sliding in rock slopes of stations 3, 4, and 6, direct toppling in rock slope of station 7, and no failures may occur in the rock slope of station 5.

The results of Q-slope revealed that the rock slopes in stations 1, 2, 3, 4, 6, 7, and 8 are in unstable condition, whereas the rock slope in station 5 is in stable condition.



**Keywords:** *Slope stability, Kinematic analysis, Q-slope system, High-folded zone, Western Zagros, Northeast Iraq.*

## 1. Introduction

Many researchers such as Basahel and Mitri (2017), Sarannathan and Kannan (2017), Sharma et al., (2019), studied the rock slope stability along with road cuts that are joining far-away areas in the valleys-plains and mountain slopes. Also, there are many engineering geological studies about "rock slope stability" in Iraq such as those that used the kinematic method (Mamlesi, 2010), other study used the landslide possibility index (LPI) method (Hamasur, 2013), also several studies were used kinematic method and slope mass rating (SMR) system (Hussien et al., 2020; Hamasur & Qadir, 2020),

There are many engineering classification systems, some have been developed for specific purposes like slope engineering design and some have been developed for general assessments (Azarafza et al., 2017). The engineering classification systems were developed practically by determining the essential parameters, yielding each parameter a digital value and a rating factor. This is made, via empirical formulae, to determine the final value for a rock mass. The final value has a relation to the underground excavation stability, which is used for the evolution of the engineering classification system (Hack et al., 2003).

There is no stability evaluation of the rock slopes by the Q-slope system in Iraq and the Iraqi Kurdistan region, so this study is the first one that is done with the mentioned system.

In this study, slope kinematic analysis and the Q-slope system are utilized to assess the stability of cut-rock slopes along Goshan – Qupy Qaradagh road.

The study area is located about 36 km (aerial distance) to the southwest of Sulaimaniyah, city-NE Iraq, and along Goshan – Qupy Qaradagh road, between latitudes 35° 15′ 58″ N - 35° 16′ 50″ N and longitudes 45° 21′ 09″ E - 45° 22′ 53″ E, (Figure 1).

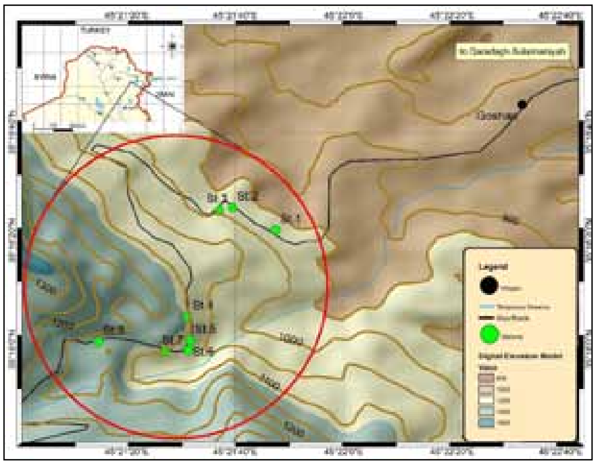


**Figure 1.** Topographic map showing the location of the study area

* Corresponding author e-mail: ghafor.hamasur@univsul.edu.iq

## 2. Geological setting

From the tectonic point of view, the area is located in the western Zagros fold-thrust belt's high-folded zone. Structurally, the area shows a homoclinal structure that dips towards the northeast at an intermediate - high dip angle, whereas a homocline is a structure where the sequence layers of rock strata, dip uniformly in one direction, that has approximately the same inclination (Jackson et al., 2005; Huggett, 2011). A homocline can be combined with limbs of a dissected fold (Bloom, 1998; Gerrard, 1998), in the area of study, the homoclines that are existed in Fat'ha (Lower Fars), Pilaspi, and Sinjar Formations run with the NE-limb of Sagrma anticline.

Geomorphological landforms in the study area are depositional, erosional, and structural landforms.

The most conspicuous landforms in the selected slope stations for stability study represent homoclinal ridges. Homoclinal ridges are the expression of dipping strata, typically sedimentary strata, that consist of alternating beds of hard and weak strata (Twidale and Campbell, 1993), in the study area, the detrital limestone of Fat'ha (Lower Fars) Formation, limestone of Pilaspi and Sinjar Formations represent the hard resistant strata, the red claystone and siltstone of Fat'ha Formation, marl of Pilaspi Formation and marl with shale of Sinjar Formation represent the weak non-resistant strata.

Stratigraphically the study area was composed from old to young of Sinjar, Gercus, Pilaspi, and Fat'ha Formations (Figure 2) (Abdullah and Qayim, 2016). Sinjar Formation consists of intermediate-massive beds of detrital and fossiliferous limestone that are intercalated with marl beds. Gercus Formation consists of a red clastic sequence of pinkish red to purple siltstone and claystone alternating with gray to reddish-brown coarse-grained sandstone, and occasionally the conglomerate bed may exist at the bottom of sandstone beds. Pila Spi Formation consists of well-bedded, highly fractured limestone, dolomitic limestone, dolomite, chalky limestone, and Fat'ha Formation alternating sedimentary cycles of yellowish-gray fossiliferous limestone, green marlstone, claystone, siltstone, and sandstone.

The cut-rock slopes are composed of thin-intermediate beds of detrital (stations 1and 2), detrital limestone with a succession of marl and intercalation of sandstone beds (station 3), thick conglomerate beds in the upper part, and claystone in the lower part (station 4), thin-thick beds of limestone and dolomitic limestone (stations 5, 6 and 7) and intermediate-massive beds of detrital and fossiliferous limestone that are intercalated with marl beds (station 8). The cut-rock slopes have steep to very steep dip angles with a developed discontinuities system (Table 1).

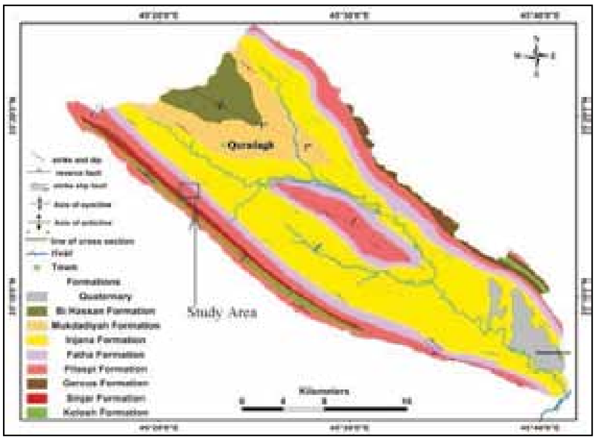


**Figure 2.** Regional geological map showing the location of the study area (Abdullah and Qayim, 2016)

**Table 1**. Dip direction /Dip angle of slope face, bedding, and joint sets at the stations (rock slopes) of the area under study.

| Station No. (Slope site) | Geologic Formation | Slope (Direction / Angle) | Bedding plane Dip direction / Dip | Join set (J1) Dip direction / Dip | Joint set (J2) Dip direction / Dip | Joint set (J3) Dip direction / Dip | Joint friction Angle (ϕ) |
|---|---|---|---|---|---|---|---|
| 1 | Fat'ha (Lower Fars) | 035°/60° | 048°/41° | 324°/88° | 223°/60° | -------- | 21° |
| 2 | | 045°/80° | 052°/42° | 321°/88° | 235°/47° | -------- | 21° |
| 3 | | 255°/80° | 049°/44° | 322°/70° | 234°/50° | -------- | 36° |
| 4 | Contact of Fat'ha / Pilaspi | 070°/70° | 052°/50° | 170°/72° | 265°/40° | 307°/71° | 36° |
| 5 | Pilaspi | 122°/80° | 050°/60° | 320°/86° | 230°/28° | -------- | 36° |
| 6 | | 130°/80° | 050°/60° | 140°/75° | 231°/35° | ------- | 36° |
| 7 | | 212°/70° | 050°/62° | 310°/67° | 225°/30° | ------- | 36° |
| 8 | Sinjar | 165°/65° | 050°/60° | 148°/57° | 315°/70° | ------- | 36° |

## 3. Methodology

### 3.1. General Methodology

In tunneling and underground mining, the following empirical engineering systems are used to give appropriate support and reinforcement for specific excavation spans:

* Q-system (Barton et al., 1974)

* Rock mass rating (RMR) (Bieniawski, 1976; Bieniawski, 1989).

For rock slope stability, engineering systems are less used, and either easy kinematics or numerical modeling may be chosen. The following empirical engineering systems were developed to predict the support, reinforcement, and performance of excavated slopes (Bar and Barton, 2017).

* SMR: slope mass rating (Romana, 1985).

* Global slope performance index (Sullivan, 2013).

None of the mentioned previous rock engineering systems supply guidance concerning appropriate, long-term stable slope angles in which rock reinforcement and support are absent (Bar and Barton, 2017).

***3.2. Methods in the study area***

Detailed engineering geological survey was carried out at eight (8) cut-rock slope stations, three (3) of them (stations No. 1, 2 & 3) are in Ft'ha Formation, station No.4 is at the contact of Fat'ha / Pila Spi Formations, Stations No.5, 6 & 7 are in Pila Spi Formation, and station No.8 is in Sinjar Formation. All field attitude measurements of discontinuities (bedding planes and joints) and results are in the dip direction/dip amount manner.

The assessment of rock slopes hints at qualitative and quantitative assessments for different rock mass components. This study concentrates on the stability evaluation of the cut-rock slopes by kinematic analysis and the Q-slope system.

Slope kinematic analysis is the easy failure analysis in terms of joint sets, bedding plane, slope, and sliding friction angle, it is only practical for preliminary design (Hoek and Bray, 1981). The kinematic analysis is a way of determining the probable failure types (plane, wedge & toppling) in jointed rock mass from the relation between discontinuities and slope surface (Hoek and Bray, 1981). Markland test (Markland, 1972) is a method designated to evaluate the probability of wedge sliding. In contrast, the wedge-shaped mass slides along the intersection line of two geological planes, the planar sliding may occur when a discontinuity dips in the same direction (within 20°) as the slope face, at an angle less than the angle of the slope but larger than the friction angle along the sliding surface. A satisfactory improvement to Markland's test has been made as Hocking (1976), and the flexural toppling failure may occur when a sharply dipping discontinuity is parallel or subparallel to the slope face (within 30°) and dips into it (Goodman, 1989), Block toppling (direct and oblique toppling) requires the converging of two discontinuities to create detached blocks. Furthermore, the presence of the basal plane facilitates the occurrence of block toppling. The field data were analyzed stereographically using DIPS v6.008 software (Rocscience, 2015). Friction angles of potential failure planes were calculated by the tilting method (Bruce et al., 1989).

Q-slope is a practical engineering system that allows the quick assessment of the stability of natural cut, artificially cut-rock slopes, roads, and cuttings of the railway in the field, during or after excavation. This system is based on the perception and utilized as a first assessment in the field stage (Barton and Bar, 2015).

Q-slope is modified from the Q-system, which has been used for the rock exposure characterization, core, and tunnels (Barton et al., 1974; Barton and Grimstad, 2014).

During excavation, the Q-slope use reduces the support requirements or bench-width needs (in larger slope profiles) of slopes that permit geotechnical engineers to evaluate in-situ excavated rock slope stability and make slope angle adjustments as the condition of the rock mass evident during construction. In 2015, tests on several engineering projects worldwide have revealed a straightforward correlation between Q-slope values and unsupported stable slope angles for a long time (Barton and bar, 2015).

Barton and Bar (2015) recommend that it can be used for all types of rock slope failures such as planar, wedge, toppling, and local debris failures.

Q-slope uses the same six parameters RQD, Jn, Jr, Ja, Jw, and SRF of standard Q-system. The Q parameters (RQD, Jn, Jr, and Ja) remain unaltered in the Q-slope system, and a new way for estimating Jr/Ja ratios for the two sides of probable wedges may be utilized along with applying orientation factors. Jw, who is now termed $J_{wice}$, considers a broader range of environmental conditions agree with rock slopes, which acted for a long time. These conditions include severe erosive rainfall and ice effects, as may seasonally occur at opposite ends of the rock type. There are also slope-relevant SRF ($SRF_a$, $SRF_b$, and $SRF_c$) categories (Barton and Bar, 2015; Bar and Barton, 2016; Bar and Barton, 2017). Q-slope is determined using the expression after (Barton and Bar, 2015):

$$\text{Q-slope} = (RQD / J_n) \cdot (J_r / J_a)_o \cdot (J_{wice} / SRF_{slope}) \quad \text{............} \quad (1)$$

Where: RQD= Rock Quality Designation.

$J_n$ = Joint set number.

$J_r$ = Joint roughness number.

$J_a$ = Joint alteration number.

O =Orientation factor.

$J_{wice}$ = Condition Number of environment and geology.

$SRF_{slope}$ = Strength Reduction-Factor related to the slope.

$SRF_a$ = SRF is related to Physical condition.

$SRF_b$ = SRF is related to stress.

$SRF_c$ = SRF is related to major discontinuity.

Barton and Bar (2015) proposed a simple formula for the steepest slope angle (β) not needing reinforcement or support for slope heights less than 30 m. This formula is now extended to all slope heights (Bar and Barton, 2017):

$$\beta = 20 \log_{10} \text{Q-slope} + 65^{\circ} \quad \text{..............................................} \quad (2)$$

Equation 2 matches the slopes ranged between 35° and 85°.

## 4. Results and Discussion

The cut-rock slopes create the best places for determining the lithological variations, weathering conditions, and the outcrops' structural geological behaviors to record discontinuity patterns. This study comprised an investigation of slopes at eight (8) stations (cut-rock slope sites) with different geotechnical characteristics.

The cut-rock slopes have steep to very steep dip angles with a developed discontinuities system, as in Table 1.

Kinematic analysis of cut-rock slopes was achieved for failure controlled by structure, utilizing DIPS v6.008 software (Rocscience, 2015). The kinematic analysis results reveal the probability of planar sliding in stations 1, 2, 4, and 8 (Figures 3, 4, 6, and 10). The probability of wedge sliding in stations 3, 4, and 6 (Figures 5, 6, and 8). Only station No.7 shows the probability of direct toppling (Figure 9). Also, kinematic analysis reveals that the slope in station 5 is stable (Figure 7).

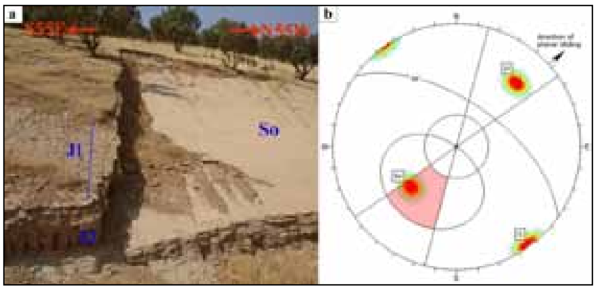


**Figure 3.** a-Field view for station No.1 with marked discontinuity sets. b-Kinematic analysis for station No.1 shows planar sliding on the bedding plane (So). Where: SF=slope face; J1= joint set No.1; J2= joint set No.2, the pink color is a possible failure zone

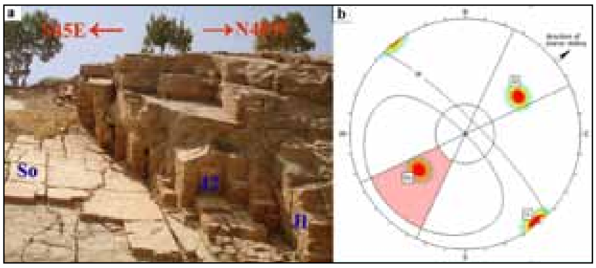


**Figure 4.** a-Field view for station No.2 with marked discontinuity sets. b-Kinematic analysis for station No.2 shows planar sliding on the bedding plane (So)

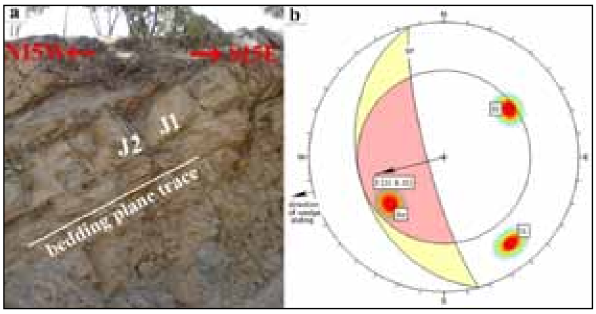


**Figure 5.** a-Field view for station No.3 with marked discontinuity sets. b-Kinematic analysis for station No.3 shows wedge sliding on J1 and J2. Where: I=intersection between two discontinuity sets

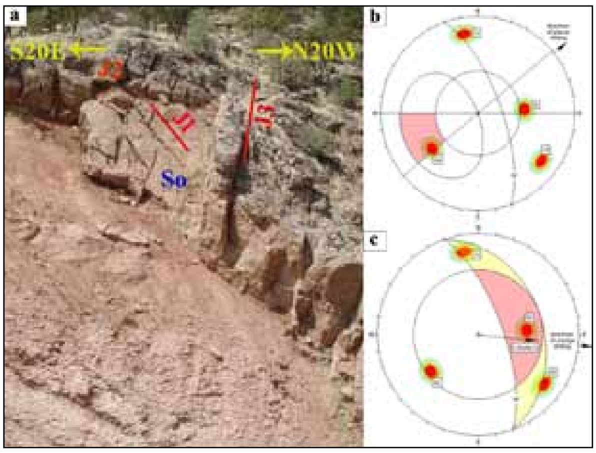


**Figure 6.** a-Field view for station No.4 with marked discontinuity sets. b-Kinematic analysis for station No.4 shows planar sliding on the bedding plane (So). c-Wedge sliding on So and J1

All cut-rock slope stations are sites that already failed (Figures 2(a), 4(a), 5(a), 6(a), 7(a), 8(a), 9(a) and 10(a)). The results of kinematic analysis in all stations are listed in Table 2.

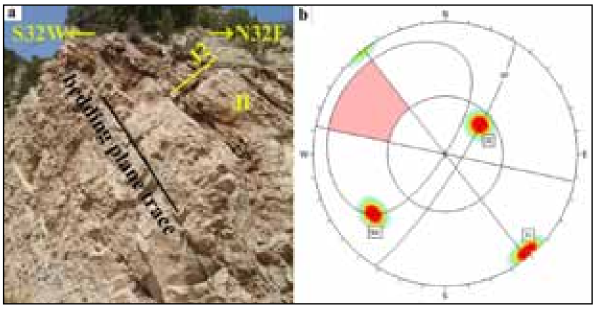


**Figure 7.** a-Field view for station No.5 with marked discontinuity sets. b-Kinematic analysis for station No.5 shows that the slope is stable

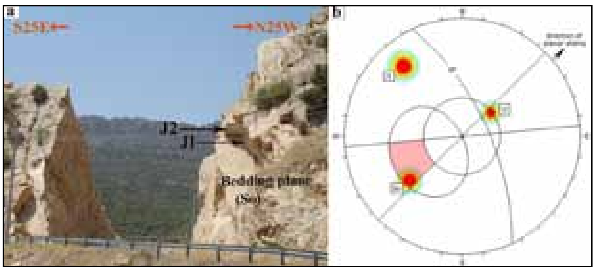


**Figure 8.** a-Field view for station No.6 with marked discontinuity sets. b-Kinematic analysis for station No.6 shows planar sliding on the bedding plane (So)

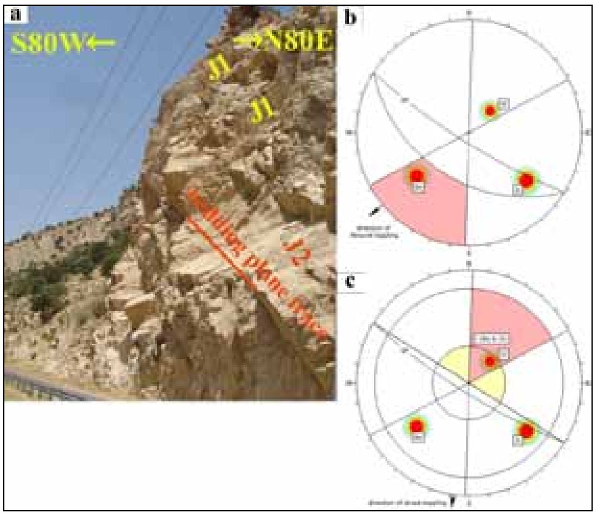


**Figure 9.** a-Field view for station No.7 with marked discontinuity sets. b-Kinematic analysis for station No.7 shows flexural toppling about So. c- Direct toppling via release intersected planes (So & J1)

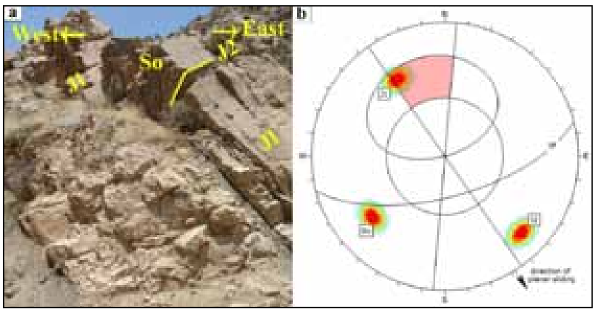


**Figure 10.** a-Field view for station No.8 with marked discontinuity sets. b-Kinematic analysis for station No.8 shows planar sliding on the J1

**Table 2.** Results of kinematic analysis in all slope stations, using DIPS-Software.

| Station No. (Slope site) | Planar sliding & its direction | Wedge sliding & its direction | Flexural toppling & its direction | Direct toppling & its direction |
|---|---|---|---|---|
| 1 | √ (048°) | -------- | -------- | -------- |
| 2 | √ (052°) | -------- | -------- | -------- |
| 3 | -------- | √ (255°) | -------- | -------- |
| 4 | √ (052°) | √ (096°) | -------- | -------- |
| 5 | -------- | ------- | -------- | -------- |
| 6 | √ (050°) | -------- | -------- | -------- |
| 7 | -------- | -------- | √ (230°) | √ (187°) |
| 8 | √ (148°) | -------- | -------- | -------- |

The six mentioned parameters calculated Q-slope values for the eight cut-rock slopes. Palmstrom-way was utilized in the estimation of the average spacing and frequency of discontinuities sets, also estimating the volumetric joint count, and then calculating RQD-value from the relation of RQD with joint counting in a unit volume (Jv) (RQD = 110 -2.5 Jv) (Palmstrom, 2005), as shown in Tables 3 and 4.

**Table 3.** Joints count in a unit volume (Jv), Rock-Quality Designation (RQD), and average spacing of all discontinuities observed in the detrital limestone of Fatʾha (Lower Fars) Formation at station No.1.

| Discontinuities (Bedding plane and Joints) | Set spacing and frequency | | | | Average spacing(m) | Average frequency* |
|---|---|---|---|---|---|---|
| | Spacing (m) | | Max. frequency | Min. frequency | | |
| | Min. | Max. | | | | |
| Bedding plane ($S_o$) | 0.10 | 0.40 | 10 | 2.5 | 0.25 | 4 |
| Joint set 1 ($J_1$) | 0.30 | 4 | 3.333 | 0.25 | 2.15 | 0.465 |
| Joint set 2 ($J_2$) | 0.2 | 3 | 5 | 0.333 | 1.60 | 0.625 |
| 2Random joint ** | | | | | | |
| Volumetric joint count Jv=∑Frequencies (joints/m³) | | | | | | 5.09 |
| RQD = 110 – 2.5 Jv……………. (RQD=100 for Jv ≤ 4) | | | | | 97 | |

**Table 4.** Joints count in a unit volume (Jv), Rock-Quality Designation (RQD), and average spacing of all discontinuities observed in all stations.

| Geologic Formation | Lithology | Station No. | Jv (joints /m³) | RQD |
|---|---|---|---|---|
| Fatʾha (Lower Fars) | Detrital Limestone | 1 | 5.09 | 97 |
| | Detrital Limestone | 2 | 5.803 | 95 |
| | Detrital Limestone | 3 | 5.261 | 96 |
| Contact of Fatʾha/Pilaspi | Basal Conglomerate | 4 | 3.479 | 100 |
| Pilaspi | Limestone | 5 | 4.395 | 99 |
| | Limestone | 6 | 2.483 | 100 |
| | Limestone | 7 | 2.483 | 100 |
| Sinjar | Limestone | 8 | 4.741 | 98 |

Uniaxial compressive strength (UCS) of intact rock was estimated indirectly from the point load test, utilizing the procedure of ISRM (1985), with an index-to-strength conversion factor equal to 21 (k=21), this value seems to be working well for a variety of rock types (Rusnak and Mark, 2000). The results of the mentioned test have appeared in Table 5; UCS-value in conjunction with maximum principal stress (σ1) is necessary for estimating the $SRF_b$ - stress. The climatic condition of the study area is semi-arid (six months are very rainy and cold, whereas the other six months are dry and semi-hot to hot), and because most landslides have occurred during rainy seasons, so the environmental condition is considered as a a wet environment for $J_{wice}$. The summary of the rock mass's characterization for the Q-slope parameters in the mentioned cut-rock slope stations has appeared in Table 6. After determining the rock mass characteristics in each rock slope station, the required Q-slope parameters were rated from a comparison of parameters characteristic (Table 6) with standard Q-slope Tables of Barton and Bar (2015).

**Table 5.** Results of the Point-load test and value of uniaxial compressive strength (UCS) of the intact rock in the rock slopes of stations 1, 2, 3, 4, 5, 6, 7 & 8.

| Station. No | 1 | 2 | 3 | 4 | 5 | 6 | 7 | 8 |
|---|---|---|---|---|---|---|---|---|
| Geologic Formation | Fat'ha (Lower Fars) | | | Contact Fat./Pila. | Pila Spi | | | Sinjar |
| D (mm) | 45 | 40 | 45 | 42 | 40 | 45 | 50 | 40 |
| W (mm) | 50 | 52 | 46 | 60 | 50 | 45 | 55 | 60 |
| F (KN) | 5.1 | 6.86 | 5.6 | 6.84 | 12.2 | 12 | 15 | 13.1 |
| F (MN) | 0.0051 | 0.00686 | 0.0056 | 0.00684 | 0.0122 | 0.012 | 0.015 | 0.0131 |
| A ($mm^2$) | 2250 | 2080 | 2070 | 2520 | 2000 | 2025 | 2750 | 2400 |
| $D_e^2=(4A/\pi)$ $m^2$ | 0.00286 | 0.00264 | 0.00263 | 0.0032 | 0.00254 | 0.00257 | 0.00349 | 0.00305 |
| $Is=F/D_e^2$ (MPa) | 1.78321 | 2.59848 | 2.12927 | 2.1375 | 4.80314 | 4.66926 | 4.29799 | 4.29508 |
| $f=(D/50)^{0.45}$ | 0.95369 | 0.90446 | 0.95369 | 0.92453 | 0.90446 | 0.95369 | 1 | 0.90446 |
| $Is_{(50)}=Is*f$ | 1.70062 | 2.35022 | 2.03066 | 1.97618 | 4.34424 | 4.45302 | 4.29799 | 3.88472 |
| $UCS=21*Is_{(50)}$ (MPa) | 35.713 | 49.354 | 42.643 | 41.5 | 91.229 | 93.513 | 90.257 | 81.579 |
| UCS (MPa) | 36 | 49 | 43 | 42 | 91 | 94 | 90 | 82 |

Where: D=Diameter (distance between the two loaded points), W=Width of the specimen
A=W*D((Area of idealized failure plane), F=Force at failure,Is=Point load strength index
$f$ =(size correction factor), UCS=uniaxial compressive strength.

**Table 6.** Characterization of the rock mass for the Q-slope parameters in all slope stations.

| Formation | Fatha (Lower Fars) | | | Contact Fat./Pila. | Pila Spi | | | Sinjar | Remarks |
|---|---|---|---|---|---|---|---|---|---|
| Slope Station | 1 | 2 | 3 | 4 | 5 | 6 | 7 | 8 | |
| Slope Height(m) | 16 | 10 | 10 | 10 | 10 | 20 | 70 | 10 | From field |
| $б_1$ (MPa) | ≈ 0.4 | ≈ 0.25 | ≈ 0.25 | ≈ 0.25 | ≈ 0.25 | ≈ 0.5 | ≈ 1.75 | ≈ 0.25 | $б_1$=Ɣ. h |
| UCS (=бc) (Mpa) | 36 | 49 | 43 | 42 | 91 | 94 | 90 | 82 | Table 5 |
| бc / б1 | 90 | 196 | 172 | 168 | 364 | 188 | 51 | 328 | |
| Failure Mode | Planar<br>sliding | Planar<br>sliding | Wedge<br>sliding | * PS<br>*WS | Stable<br>slope | Planar<br>sliding | Direct<br>toppling | Planar<br>sliding | Table 2 |
| RQD | 97 | 95 | 96 | 100 | 99 | 100 | 100 | 98 | Table 4 |
| Jn | F | F | F | G | F | F | G | H | |
| Jr | C | C | C | C | C | F | F | C | |
| Ja | OPR | OPR | E | E | C | B | B | E | |
| O-Factor | A- Causing<br>failure if<br>unsupported. | A- Causing<br>failure if<br>unsupported | A-VUnfa<br>B- VUnfa | *PS:VUnfa.<br>*WS:VUnfa<br>B-Fav. | A- Very<br>favorably<br>oriented | A-Very<br>Unfa. | A- Causing<br>failure if<br>unsupported | A- Causing<br>failure if<br>unsupported | |
| J wice | Un-Com<br>WE | Un-Com<br>WE | Un-Com<br>DE+WE | Un-Com<br>WE | St-Com<br>WE | Un-Com<br>WE | Un-Com<br>WE | Un-Com<br>WE | |
| $SRF_a$ | B | B | B | B | A | A | B | B | |
| $SRF_b$ | F | F | F | F | F | F | F | F | |
| $SRF_c$ | L (very<br>unfav.) | L (very<br>unfav.) | L (very<br>unfav.) | L(PS:Vunf<br>WS: Unfa. | L (fav.) | L (fav.) | L (unfav) | L (very<br>unfav) | |

Where: б1=Maximum principal stress (Ɣ-rock ≈ 0.025MN/$m^3$), Fat.=Fatha, Pila.=Pila SpiUCS (бc)=Uniaxial compressive strength,PS=Planar sliding, WS=Wedge sliding,
(For Jn: F=Three joint sets, G=Three joint sets plus random joints, H=Four or more joint sets)
(For Jr: C=Smooth, undulating; F=Smooth, planar)
(For Ja: OPR=Thick, continuous zones or bands of clay; B=Unaltered joint walls, surface staining only; C=Slightly altered joint walls. Non-softening mineral coatings, sandy particles, clay-free disintegrated rock, etc; E=Softening or low friction clay mineral coatings, i.e., kaolinite or mica. Also chlorite, talc, gypsum, graphite, etc., and small quantities of swelling clays)
(For $SRF_a$: A=Slight loosening due to surface location; B=Loose blocks, signs of tension cracks and joint shearing, susceptibility to weathering)
(For $SRF_b$: F= Moderate stress-strength range ($\sigma_c/\sigma_1$: 50-200 or greater))
VUnfa.=Very Unfavorable,Fav.=Favorable, Unfa.=Unfavorable,
Un-Com=Unstable structure-Competent rock, St-Com=Stable structure-Competent rock,
WE=Wet Environment, L=Major discontinuity with little or no clay

Finally, the Q-slope values were determined for rock slopes in each station, as shown in Table 7.

**Table 7.** Rating of the Q-slope parameters, Q-slope value, slope angle and stable slope angle.

| Formation | Lower Fars (Fatha) | | | | Pila Spi | | | Sinjar | Remarks |
|---|---|---|---|---|---|---|---|---|---|
| Slope Station | 1 | 2 | 3 | 4 | 5 | 6 | 7 | 8 | |
| RQD | 97 | 95 | 96 | 100 | 99 | 100 | 100 | 98 | Table 4 |
| Jn | 9 | 9 | 9 | 12 | 9 | 9 | 12 | 15 | From Comparison of Table 6 with standard Q-slope Tables |
| Jr | 2 | 2 | 2 | 2 | 2 | 1 | 1 | 2 | |
| Ja | 10 | 10 | 4 | 4 | 2 | 1 | 1 | 4 | |
| O-Factor | 0.25 | 0.25 | A=0.5<br>B=0.8 | PS: 0.5<br>WS:A-0.5<br>B-0.9 | 2 | 0.5 | 0.25 | 0.25 | |
| J wice | 0.6 | 0.6 | 0.6 | 0.6 | 0.7 | 0.6 | 0.6 | 0.6 | |
| $SRF_a$ | 5 | 5 | 5 | 5 | 2.5 | 2.5 | 5 | 5 | |
| $SRF_b$ | 2.0 | 1.5 | 1.5 | 1.5 | 1 | 1.5 | 2.0 | 1 | |
| $SRF_c$ | 8 | 8 | 8 | PS: 4<br>WS: 2 | 1 | 1.5 | 8 | 8 | |
| Max. SRF | 8 | 8 | 8 | PS: 5<br>WS: 5 | 2.5 | 2.5 | 8 | 8 | |
| Qslpoe-value | 0.0404 | 0.0395 | 0.08 | PS;0.25<br>WS:0.1125 | 6.16 | 1.33 | 0.1562 | 0.0612 | |
| Slope angle | 60 | 80 | 80 | 70 | 80 | 80 | 90 | 65 | Table 1 |
| Stability condition of slope | Unsta-ble | Unsta-ble | Unsta-ble | Unsta-ble | Stable | Unsta-ble | Unsta-ble | Unsta-ble | Fig. 11 |
| Stable slope angle without support | ≈ 37 | ≈ 37 | ≈ 43 | PS: ≈ 53<br>WS: ≈ 46 | ≈ 81 | ≈ 68 | ≈ 49 | ≈ 41 | Equation No. 2 |
| Where: PS=Planar sliding, WS=Wedge sliding | | | | | | | | | |

To determine the stability condition of cut-rock slopes in each station, the Q-slope value and slope dip angle in each station were projected on the Q-slope chart. The location of this projection on the chart defines the slope stability condition (Figure 11). Figure 11 reveals that the cut-rock slopes are unstable in stations 1, 2, 3, 4, 6, 7, and 8, and the cut-rock slope is stable in station 5. Also, the sharper slope angle (β) not needing support or reinforcement was determined from formula number 2 (Table 7).

Q-slope system reveals that the slopes with the same slope angle are more stable with increasing Q-slope value, this relation is obvious from a comparison among slope stations 2, 3, 6 and 5. whereas the slope with the same Q-slope value are more stable with decreasing the slope angle and they are stable in the same slope angle, this relation is obvious from the comparison between slope stations 1 and 2 (Figure 11).

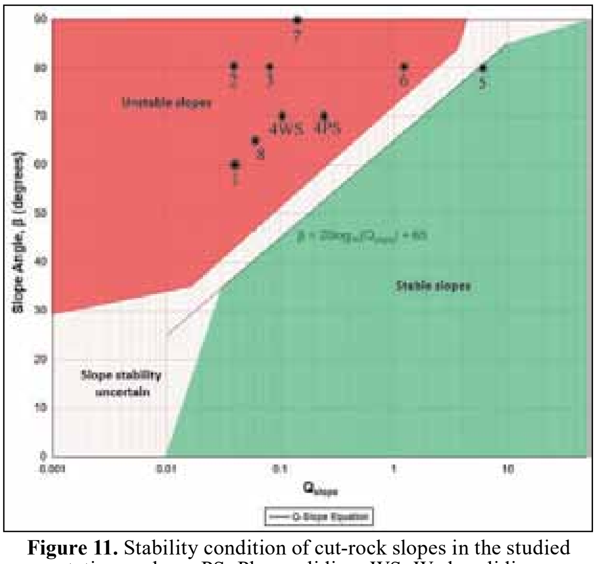


**Figure 11.** Stability condition of cut-rock slopes in the studied stations, where: PS=Planar sliding; WS=Wedge sliding

## 5. Conclusions

The Slope kinematic analysis revealed four types of failures, i.e., Planar sliding, wedge sliding, flexural toppling, and direct toppling failures.

The Q-slope results revealed that the rock slopes in seven stations are unstable, whereas the rock slope in one station (station 5) is stable.

## Acknowledgment

I would like to thank Dr. Erfan Omer Mossa for his assisting during the point load test performance. I also appreciate the assistance of Mr. Fahmy Osman Mohammed for supporting in drawing the location map by Arc-GIS software.

## References

Abdullah, L. H. and Al-Qayim, B., 2016. GIS-based morphometric analysis of the Dewana basin, Sulaimani, Kurdistan, Iraq. JZS Journal, Special Issue, GeoKurdistan II Conference (163-187).

Azarafza M.; Asghari-Kaljahi E. and Akgün H., 2017. Assessment of discontinuous rock slope stability with block theory and numerical modeling: a case study for the South Pars Gas Complex, Assalouyeh, Iran. Environmental Earth Sciences, 76(11): 397.

Bar, N. and Barton, N., 2016. Empirical slope design for hard and soft rocks using Q-slope. In: Proceedings of the 50th US rock mechanics/ geomechanics symposium, ARMA 2016, Houston, 26–29 June 2016. ARMA 16-384.

Bar, N. and Barton, N., 2017. The Q-Slope Method for Rock Slope Engineering. Rock Mechanics and Rock Engineering, DOI: 10.1007/s00603-017-1305-0.

Barton, N.R.; Lien, R. and Lunde, J., 1974. Engineering classification of rock masses for the design of tunnel support. Rock Mechanics. Volume 6, pp. 189-236. Springer-Verlag.

Barton, N. R. and Bar, N., 2015. Introducing the Q-slope method and its intended use within civil and mining engineering projects. In: Proceedings of the ISRM Regional Symposium (Eurock 2015) and 64th Geomechaics Colloquium, Salzburg, Oct.

Barton, N.R. and Grimstad, E., 2014. An illustrated guide to the Q-system following 40 years use in tunnelling. In-house publisher: Oslo. Retrieved March 12, 2015 from www.nickbarton.com.

Bloom, A. L., 1998. Geomorphology – A systematic analysis of Late Cenozoic landforms (3rd edition). Prentice- Hall of India Private Limited, New Delhi, 482p.

Basahel, H. and Mitri, H., 2017. Application of rock mass classification systems to rock slope stability assessment: A case study. Journal of Rock Mechanics and Geotechnical Engineering, 9 (6): 993- 1009.

Bieniawski, Z.T., 1976. Rock mass classification in rock engineenig. In Exploration for rock engineering, Proc. of the Symp.,(ed. Z.T. Bieniawski). Vol.1, pp.97-106. Cape Town: Balkema.

Bieniawski, Z.T., 1989. Engineering rock mass classification. John Wiley, New York.

Bruce, I. G.; Cruden, D. M. and Eaton, T. M., 1989. Use of a tilting table to determine the basic friction angle of hard rock samples. Can. Geotech. J. 26, 274-279.

Gerrard, J., 1998. Rocks and landforms. Allen & Unwin Inc. Winchester, Mass. 319 pp.

Goodman, R. E., 1989. Introducion to rock mechanics 2nd edn., Wiley, New York, 562pp.

Hack, R.; Price, D. and Rengers, N., 2003. A new approach to rock slope stability–a probability classification (SSPC). Bull. Eng. Geol. Environ. 62, 167–184. https://doi.org/ 10.1007/s10064-002-0155-4.

Hamasur, G. A., 2013. Slope Stability Assessment Within and Around the Reservoir of the Proposed Basara Dam, Sulaimani, NE-Iraq. Iraqi Bulletin of Geology and Miming, Vol. 9, No. 3, pp: 51-66.

Hamasur, G. A. and Qadir, N. M., 2020. Slope Stability Assessment along Qalachwalan-Suraqalat Main Road, Sulaimani, NE-Iraq. Tikrit Journal of Pure Science, Vol. 25 (3).

Hocking, G., 1976. A method for distinguishing between single and double plane sliding of tetrahedral wedges. Int. J. Rock Mech. Min. Sci. Geomech. Abstr. 13, pp.225- 226.

Hoek, E. and Bray, J.W., 1981. Rock Slope Engineering. 3rd Edition, The Institution of Mining and Metallurgy, London, UK.

Huggett, J. R., 2011. Fundamentals of Geomorphology, 3rd ed., Routledge, New York. 516 pp.

Hussien, S. A.; Al-Kubaisi, M. Sh. and Hamasur, G. A., 2020. Impact of Geological Structures on Rock Slope Stability in The NW Nose (Plunge ) of Surdash Anticline, Sulaimaniya/ NE Iraq. Iraqi Journal of Science, Vol. 61, No. 3, pp: 550-566.

ISRM, P.L.T., 1985. Suggested method for determining point load strength. Int J Rock Mech Min Sci Geomech Abstr, 22: 51–70.

Jackson, J. A.; Mehl, J. and Neuendorf, K., 2005. Glossary of Geology. American Geological Institute, Alexandria, Virginia. 800 pp.

Mamlesi, F. O., 2010. Engineering geological study of rock slope stability along Dokan-Khalakan road, Kurdistan region, NE-Iraq. Unpublished MSc thesis, University of Sulaimani, Iraq. 150 pp.

Markland, J.T., 1972. A useful technique for estimating the stability of rock slopes when the rigid wedge sliding type of failure is expected. Imp. Coll. Rock Mech. Res. Rep. 19, pp.10-26.

Palmstrom, A., 2005. Measurements of and correlations between block size and rock quality designation (RQD). Journal of Tunneling and Underground Space Technology, Vol.20 (4), pp.362–377.

Romana, M., 1985. New adjustment ratings for application of Bieniawski classification to slopes, in: Proceedings of the International Symposium on the Role of Rock Mechanics in Excavations for Mining and Civil Works. International Society of Rock Mechanics, Zacatecas, pp.49-53.

Rocscience: Inc. Dip v. 6.008, 2015. Graphical and statistical analysis of orientation data. Toronto, Canada.

Rusnak, J. and Mark, C., 2000. Using the point load test to determine the uniaxial compressive strength of coal measure rock. In: Proceedings of 19th international conference on ground control in mining, Morgantown, WV, pp.362–371.

Saranaathan, S. E. and Kannan, M., 2017. SMR and kinematic analysis for slope instability along Bodi-Bodimettu Ghat section, Tamil Nadu. Journal Geological Society of India, 89 (5): 589-599.

Sharma, M.; Sharma, S., Kumar, M. and Singh, S. K., 2019. Analysis of slope stability of road cut slopes of Srinagar, Uttakhand, India. International Journal of Applied Engineering Research ISSN 0973- 4562, 14 (3): 609-615.

Sullivan, T.D., 2013. Global slope performance index. Proceedings of Slope Stability, 55–80.

Twidale, C. R. and E.M. Campbell, E. M., 1993. Australian Landforms: Structure, Process and Time. Gleneagles Publishing, Adelaide, South Australia, Australia. 568 pp.

JJEES

Jordan Journal of Earth and Environmental Sciences

JJEES (2022) 13 (2): 97-104
ISSN 1995-6681

# Integrating 'The Triangle of Geography, Geology, and Geophysics' into Sustainable Development

Iain S. Stewart

*Royal Scientific Society, 70 Ahmad Al Tarawneh St, Al Jubaiha, Amman, Jordan*

*Received 11 August 2021; Accepted 22 September 2021*

**Abstract**

In the context of tackling climate change in the eastern Mediterranean and the Middle East, HRH Prince El-Hassan bin Talal has called for an integrated approach to human and natural resources management that takes account of "the triangle of geography, geology, and geophysics". The lack of application of geoscientific knowledge to sustainable development issues is surprising given that advancing human progress lies at the roots of modern geoscience and aligns with the intellectual mindsets and technical skills that geoscientists are trained in. Applying this Earth Science toolkit to the challenges of long-term sustainability will require the global geoscience community to repurpose its principles and practices. In particular: (1) better communicating what geoscientists know and do, and how that is socially useful; (2) reaching out to other disciplines more engaged in sustainability issues; and (3) re-designing Earth science education and training programs to place sustainability and human wellbeing at the heart of a 21st-century geoscientist's professional purpose.



**Keywords:** Geoscience; Sustainability; Sustainable Development Goals; Human wellbeing

## 1. Introduction

In his opening address to 2020: "Climate Change in the Eastern Mediterranean and the Middle East" Symposium organized by the Jordanian Atomic Energy Commission. HRH Prince El-Hassan bin Talal called for a strengthening of scientific and technological cooperation in the Middle East and the eastern Mediterranean basin to face the climate change challenge. As part of that strategic planning, Prince El Hassan stressed the importance of an integrated approach to human and natural resources management, considering the triangle of geography, geology, and geophysics.

It is welcome but rare to hear a global public figure highlight the critical role of geoscience in sustainable development. As acknowledged in Prince El Hassan's remarks, the '3Gs' of (physical) geography, geology and geophysics remain underrepresented concerning other disciplines in contributing knowledge and expertise to regional and global concerns over planetary health and human wellbeing (Mora 2013, Stewart & Gill 2017). This 'invisibility' of geoscience in sustainable development discourse is surprising because the social mission of human advancement exists deep in the historical roots of contemporary geoscience. Two centuries ago, distilled by socially progressive Enlightenment thinking, James Hutton (Hutton 1788) placed the 'physiology' of the planet at the heart of a new integrated and holistic Earth Science amid the technological birth of Britain's industrial revolution. His seminal 1788 opus 'Theory of the Earth' opened with the remark: 'This globe of the earth is a habitable world, and on its fitness for this purpose, our sense of wisdom in its formation must depend' (Hutton 1788). The subsequent refinement of modern Earth Science has only served to reinforce its intellectual credentials as a science that 'looks forwards backward' to advance human progress (Lucchesi 2017, Rajendran 2019).


**Figure 1.** The 2015-2030 United Nations Sustainable Development Goals

This article sets out the contextual background to Prince El Hassan's provocation and examines the contributions that geoscience and geoscientists might bring to the principles and practices of sustainable development. In doing that, it advances several key challenges that the geoscience community will need to address on the global sustainability agenda.

* Corresponding author e-mail: ehrcs@rss.jo

## 2. The Challenges Ahead

Our planet, or more specifically those living on it, will face a gathering storm of 'grand challenges in the 21st century. Those challenges arise from global socio-economic drivers of international trade, industrialization, and urbanization, as a growing human population consumes its natural resource base at an ever-accelerating pace and tackles a consequent climatic and ecological crisis that imperils humanity's ultimate survival. Geoscience - the study of our planet's 4.5-billion-year-old history, how it works, and what it means for those living on it – potentially offers important knowledge, experience, and guidance on how to confront many of these critical challenges (Schlosser & Pfirman 2012, Gill 2017, Stewart & Gill 2017) (Figure 1). Despite its traditional focus on looking backward into 'deep time', geological input now seems essential for forward-looking sustainable stewardship of the planet (Beer et al. 2018). Geoscientific expertise is needed for ensuring the material supply for the 'energy transition' to renewable technologies and supporting the wider 'clean, green economy' that major countries are moving towards. In addition, geoscientists can contribute important knowledge for responding to increasing water and food insecurity crises in regions suffering the effects of climate change, tackling the ecological ravages of habitat destruction and biodiversity loss, and reducing the risk of disasters in the world's swelling urban centers (Figure 2).


**Figure 2.** A promotional poster from the Geological Society of London, available in multiple languages, highlighting the diversity of contributions that geoscientists can make to society.

The urgent imperative for Earth Science to help address society's growing unsustainability gains deeper motivation from the perversity that humans themselves have become a dominant geological force, now sufficient in intensity to warrant our bespoke era: The Anthropocene (Steffen et al. 2011, Crutzen 2016, Zalasiewicz et al. 2019). Although the conceptual space for creating the modern Anthropocene was carved during the nineteenth-century foundation of geology (Davis 2011), geoscientific methods designed to unravel 'deep time' now track the environmental and ecological fallout from present-day human actions. The Huttonian science in which 'the present is the key to the past' now looks forwards to guiding planetary boundaries, earth system tipping points, and a safe operating space for humanity' (Rockstrom et al. 2009). The fact that some of the cumulative impacts of our anthropogenic changes are now significant enough to be able to be compared with natural analogs in the geological past (Burke et al. 2018) means that now, more than ever before, the central tenets of 'palaeoscience' bear directly on future society (Mills & Jones 2021.

Entering this new 'human age', geoscience's direction of travel seems clear. Although 'discovery science' about our planet's distant geological past will continue, '…Earth Sciences research needs to be more focused on problem-solving rather than refining our knowledge of the problems that face the Earth system' (Ludden 2020, p.69). Traditional applied geological and geophysical fields (economic geology, petroleum geology, engineering geology, hydrogeology, and geohazards) will assume even greater importance, alongside the more geographical facets of climate science, land management, and disaster risk reduction. Increasingly, society will look to the geosciences not only for sustainably providing its resource demands (Lambert 2001) but for also resolving the impact of developmental projects on the environment, the severity of natural hazards, and human health. Even very basic geological and environmental knowledge can help transform resource-poor communities and tackle development barriers in many regions (Gill et al. 2019), and economic livelihoods can be improved directly through geo-heritage and geo-tourism, such as UNESCO Geo-parks (Catana & Brilha 2020).

In countless ways, sustainable stewardship of the planet will benefit from a more explicit acknowledgment of the critical importance of the natural world's underpinning 'geodiversity' (Schrodt et al. 2019). So, with that mission in mind, what are the specific key skillsets and mindsets that geoscientists can bring to the global sustainability agenda?

## 3. The Sustainable Geoscience Toolkit

Geoscientists are Earth Scientists, meaning that their core concern is the fundamental working of the planet. They do that through a multidisciplinary science that integrates physics, chemistry, and biology, draws from engineering, computing, and mathematics, and spills over into the geographical and environmental sciences (Figure 3).

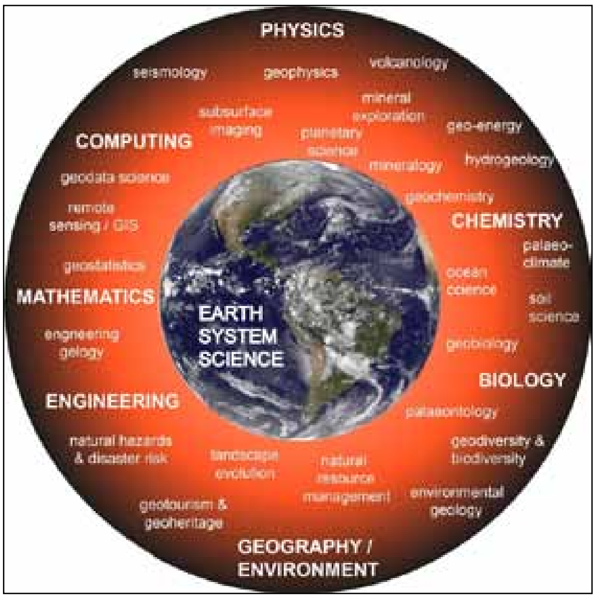


**Figure 3.** The multidisciplinary nature of geoscience, integrating physics, chemistry, and biology and drawing from engineering, mathematics, and geography

Blending and balancing these disparate disciplines develops high-level competency across a broad portfolio of technical specialists, notably:

- Geophysics – deploys a wide array of techniques that image inside the planet's depths and monitor the action of earthquakes (seismology) and volcanoes (volcanology).
- Geochemistry – where the tools and principles of chemistry are used to forensically characterize the materials, minerals, and rocks that make up our physical world (mineralogy and petrology).
- Geobiology - reveals the intimate relations between environments and ecosystems, past and present, and charts the evolution of life as preserved in the rock record (paleontology).
- Engineering geology - uses our understanding of soil and rock properties to solve practical problems for infrastructure and the built environment whilst hydrogeology examines the flow of groundwater in the subsurface.
- Geodata science uses probability and statistics to measure Earth variables over time and space, and high-level mathematical modeling and computation tools alongside Artificial Intelligence and Machine Learning to solve and visualize complex planetary problems.

In combining these disparate disciplines into a coherent model of planetary inquiry, geoscience manages to balance and blend a suite of complementary methodological mindsets (Frodeman 1995, Clelland 2001, Baker 2014). These are:

- Geoscience as an interpretative science: indirect, ambiguous, enigmatic, and subjective clues in the rock record or the deep subsurface need to be deciphered to shed light on Earth processes (Curtis 2012)
- Geoscience is an observational science: observations play a central role in geoscientists' reasoning and testing of new ideas and theories (Rogers 1989, Kastens et al. 2009)
- Geoscience is a historical science: observations of present-day phenomena and environments are used to infer conditions in the past (Frodeman 1995, Dodick & Orion 2003)
- Geoscience as a 'big data science: vast volumes of data have informed geological inquiry but the 'digital revolution' promises a new era of data-driven geoscientific discovery (Pennington et al. 2020, Stephenson et al. 2020, Wang et al 2020)
- Geoscience as systems science: recognizing the dynamic interconnections that maintain a habitable planet (Clark et al. 2004, Stillings 2006)

Geoscientists understand that the Earth is a system integrating the solid earth (lithosphere) and the other 'spheres' (atmos, hydro, cryo, and bio) and that feedback between these constituent parts is critical for sustainability (Clark et al. 2004). Earth systems are "complex" in the technical sense: exhibiting nonlinear interactions, multiple stable states, fractal and chaotic behavior, self-organized criticality, and non-Gaussian distributions of outputs. However, they are also "complicated" in the ordinary sense of the word; multiple processes (mechanical, chemical, biological, and anthropogenic) may operate and interact at the same time and place. Although geoscientists are not the only scientists who work with complicated, complex systems, their ability and propensity to apply a systems approach to understanding the Earth across multiple scales is an important expertise that geoscientists offer society. As Gosselin et al. (2013) note, 'As a historical and interpretative science, geology can inform society about interactions in coupled human-environmental systems because our skills and proficiencies allow us to recognize the varying manifestations of phenomena at different spatial and temporal scales.

These intellectual and technical competencies are well known and accepted within the geoscience community (though much less so beyond), but arguably it is our lesser appreciated conceptual and creative thinking skills that may be the most valuable to sustainable development. As the pioneering petroleum geologist, Wallace Pratt pointed out decades ago "Where oil is first found, in the final analysis, is in the minds of men" (Pratt, 1952). The human mind is arguably the geoscientist's most important tool (Rajendran 2019). It is the geoscience mind that '…converts colors and textures of dirt, or blotches on a satellite image, or wiggles on a seismogram, into explanatory narratives about the formation and migration of oil, the rise, and fall of mountain ranges, the opening and closing of oceans' (Kastens et al. 2009, p.265).

Geoscientists also take a long view of time, appreciating the relative brevity of human history within the vastness of the age of the Earth (Orion 2006). This perspective is unusual: short time frames, of the order of days to years, drive most decisions in business, politics, and media news cycles. If widely adopted, geoscientists' more attenuated view of time might provide a crucial counterweight, and support decision making with a time horizon of decades to centuries. What's more, in their guise as time travelers, geoscientists can envision Earth in states drastically different from the planet that currently exists, a perceptive skill that in turn draws on other key conceptual skillsets (Manduca & Mowk 2006, Kastens 2009, and Kastens & Manduca 2012):

- Interdisciplinary problem-solving geoscientists solve problems in the context of an open and dynamic system of interacting parts and processes
- Managing uncertainty: geoscientists revel in incomplete data and subjectivity, probability and uncertainty are integral to all geoscience interpretations
- 3D & 4D thinking being able to visualize and solve problems in three dimensions and across time requires geoscientists to have considerable intellectual flexibility, imagination, and creativity (Reynolds 2012)
- Multi-scalar levels of inquiry: geoscientists span from the nanoscale to the planetary scale to understand how the Earthworks
- Geoscience reasoning and synthesis: geoscientists apply a very particular form of scientific reasoning,

recognizing that most geological problems have no clear, unambiguous answers and working by analogy and inference to make predictions with limited data (Frodeman 1995, 2014, Clelland 2001, Baker 2014)
- Working in the real-world 'laboratory': field-based learning helps geoscientists develop a feel for Earth processes and a sense of scale, and strengthens their ability to integrate messy, fragmentary information, reason spatially and temporally, and comment on the quality of observational data.

Although much modern geoscientific analysis is undertaken in the laboratory or imaged from space, 21st-century geoscience remains at its traditional core a field-based science. In undertaking reconnaissance geological mapping and geophysical exploration, geoscientists are often the first 'boots on the ground'. They are, therefore, generally the initial interface between their organizations and local neighborhoods and communities, and with securing the 'social license to operate a critical part of the publically contested infrastructure, minerals, and energy development projects, communication is an implicit geoscience skill (Stewart & Lewis 2017). Although generally a 'soft skill' in which they are rarely formally trained, geoscientists find themselves daily explaining their science to other technical specialists and other professionals, translating partial and obscure data and observations into coherent narratives that link past, present and future. In that regard, geoscientists are natural storytellers, routinely developing compelling narratives to explain our often-abstract ideas about the deep Earth or ancient worlds (Stewart & Nield 2013).

None of these technical, conceptual, and social skills, taken individually, is unique to geoscience. Nor does every individual geoscientist have every one of these skills or apply them in their work. Nevertheless, taken collectively, this combination of attributes provides a powerful toolkit for addressing the uncertain and untested problems of sustainable development. With that recognition, many national geological surveys are already reformulating their strategies around sustainable geosciences principles and practices (Smelror 2020, Ludden 2021). At the same time, the key professional sectors that geoscience serves are also rapidly adjusting, with the construction, minerals extraction, and energy sectors increasingly projecting themselves, their practices, and their people through the lens of sustainability and the Sustainable Development Goals framework (Capella et al. 2017, Calas et al. 2017, Mudd 2021) (Figure 4).

Whether geoscientists like it or not, a brave new world is rapidly coming. Yet, despite the signs that a new Earth sciences revolution is underway, the academic geoscience community in universities and research institutes around the world still appears to remain wedded to traditional 20th-century Earth science pedagogies and practices. So, what needs to change?


**Figure 4.** The Geophysics Sustainability Wheel (Capella et al. 2017)

## 4. Looking Forward Backwards

The challenge from Prince El Hassan about how the triangle of geography, geology, and geophysics can be integrated effectively into national and regional sustainability agendas presents a critical question for modern geoscience. Currently, too few geoscientists have direct involvement in the growing societal shift towards achieving the 2030 UN Sustainable Development Goals (Schlosser & Pfirman 2012, Mora et al. 2013, and Stewart 2016). 'Sustainability' and 'sustainable development' are rarely featured in many universities' geoscience courses or professional geoscientific training, and the topic is largely absent from Earth science research in specialist journals or academic conferences (Stewart & Gill 2017). At the individual level, many geoscientists can (and do) make more contributions that are directly relevant to sustainable development. However, at the strategic level of the global geoscience community, three 'missions' seem paramount:

1. Geoscience needs to better communicate what it knows, what it does, and why it is useful.
2. Geoscience needs to reach out to other disciplines more engaged in sustainability issues
3. Geoscience needs to re-design its education and training programs to place sustainability and human wellbeing at the core of its professional purpose.

### *4.1 The Communication Challenge*

Outside of long-suffering wives, husbands, and partners, few non-geologists know what geoscience is. There is a general sense that geology is rocks ('stones') and fossils ('dinosaurs'), but the harsh reality is that beyond that ordinary people pay little attention to and have no interest in the wider Earth sciences realm (Stewart & Nield 2013). Therefore, if the average person in the street has little or no grasp of what a geologist is or does, then why should a local government official, business executive, or policy maker have any better idea?

Traditionally, there has been an academic disinterest and an institutional lack of incentive to encourage scientists to translate their technical science for non-technical audiences (Stewart & Lewis 2017). That, however, is no longer the case. More and more, national governments, through their funding agencies, are demanding public accountability for research funds, and the response has been a dramatic increase in university support for science communication training and academics taking part in associated public engagement and educational outreach activity. As part of that sector-wide academic mind-shift, geoscientists around the world are being expected not just to undertake geological investigations but to justify why their work is important and tell end-users what it means for them. It is a change that geoscientists should embrace because, as highlighted above, most are natural storytellers, and the subject of the Earth, its extraordinary history, and its present-day impact on those living on it provide a rich diet for popular science consumption (Stewart & Nield 2013). But 'selling planet earth' to the public and policymakers will require more than just strengthening our geoscience outreach activity, but rather will require the systemic embedding of the science (and art) of science communication into our graduate, postgraduate, and early-career training programs (Stewart & Hurth 2021).

### *4.2 The Interdisciplinary Challenge*

Addressing complex and contested sustainability issues demands integrated solutions from multiple disciplines. Although geoscience is already a multidisciplinary field of inquiry (Figure 5) wider cross-disciplinary collaborations are required. In the first comprehensive overview of geology for sustainable development, the Geological Survey of India stressed the need for geologists, geochemists, geophysicists, geomorphologists, and the like to work together in integrated projects with engineers and planners (GSI 2010). Such collaborations are now fairly commonplace, and there are encouraging signs of research partnerships with allied disciplines such as biology, zoology, ecology, agronomy, and environmental science, such as in the emerging interdisciplinary field of 'critical zone science' (Anderson et al. 2010, Banwart et al. 2013, and Brantley et al. 2016). However, if the geoscience community is to meaningfully address global sustainability issues. Then even more ambitious and challenging collaborations will be needed, extending to the social sciences and humanities - human geography, anthropology, psychology, sociology, political science, and law - which are concerned with the human dimensions and societal institutions whose values underlie our currently unsustainable ways of living (Stewart 2016, Stewart & Gill 20217).


**Figure 5.** Each of the main technical specialisms within geoscience has applications to help tackle the challenges of sustainable development.

### *4.3 The Education Challenge*

Geoscience's emboldened interdisciplinary inquiry will need to be rooted in teaching and learning that emphasizes the interactions of geological, biological, chemical, and physical processes and environments, in combination with their social, economic, political, and cultural dimensions – the realm of 'sustainability science' (Gosselin et al. 2020). By more directly addressing the formidable challenges of global unsustainability, traditional geoscience has the potential to be revitalized, at a time when recruitment to university geology and earth science courses around the world is struggling. The promise is of a refreshed discipline – 'human geoscience' (Himiyama et al. 2020) – that is a better fit for purpose in managing the pressing social and environmental concerns of sustainable development (Gill & Smith 2021).

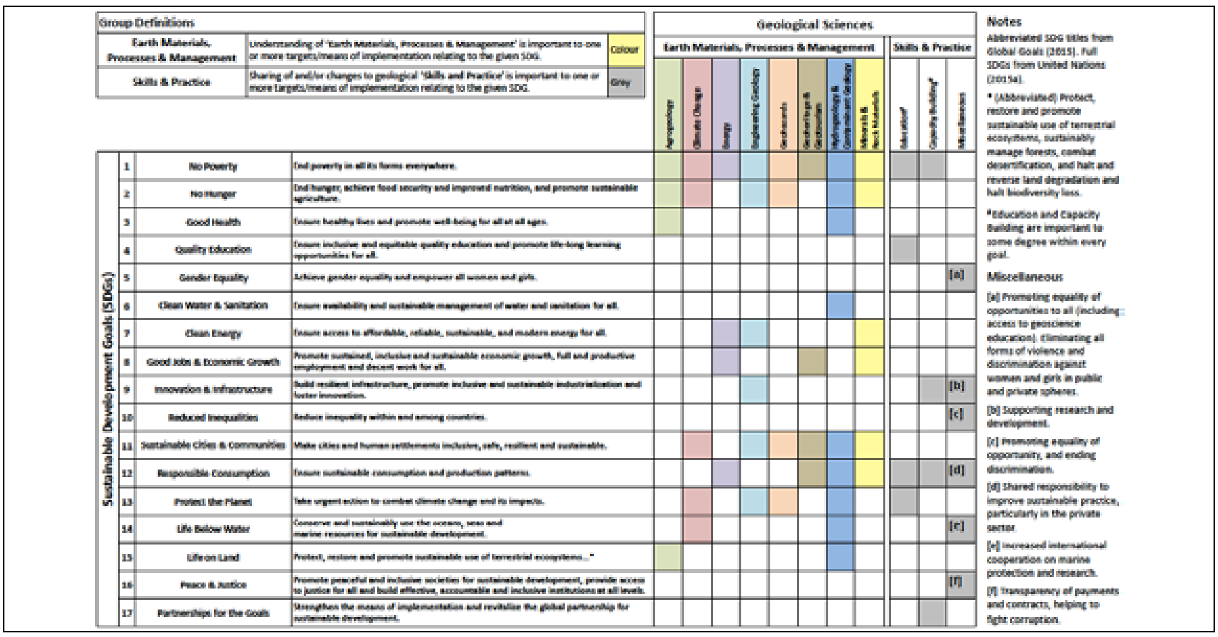


**Figure 6.** A matrix to visualize the role of geologists in helping to achieve the internationally agreed Sustainable Development Goals (from Gill 2017)

Quite how this new pedagogic model of ‘sustainable geoscience’ can best be embedded into or grafted onto university geoscience courses and programs will vary from country to country. In the USA, there is a long tradition in which ‘sustainability is promoted as a strong organizing principle for modern liberal arts and technical education programs, requiring systems thinking, synthesis, and contributions from all disciplines - geoscientists, natural/ physical scientists, social scientists, human and behavioral scientists, and engineers’ (Gosselin et al. 2013). Here and elsewhere, geoscience courses are being restructured around the framework of the UN Sustainable Development Goals, the traditional emphasis on fossil fuel extraction rebadged as geo-energy or energy transition science, and, in the UK, the first chair in Sustainable Geoscience has been appointed. In many universities, an introductory undergraduate course on ‘Geology and Society’ is a simple and obvious first step in helping students appreciate the relevance of their geoscientific training in the broad arena of sustainable development (Figure 6). At a more advanced level, and whilst maintaining the technical rigor and academic integrity of conventional geoscience training, applied courses on economic geology, petroleum geology, and engineering geology can be reframed through a sustainability lens (e.g., natural resource management, geo-energy, urban geoscience). However, arguably the most transformative way for geoscience to integrate into sustainability science will be in developing bespoke postgraduate courses in sustainable geoscience that take advantage of interdisciplinary alliances within universities to establish Masters and Ph.D. level training in a new holistic 21st century Earth science thinking.

There are broader win-wins to building sustainability into geology curricula and professional development training. It promises to develop a new generation of geo-professionals well versed in understanding and addressing sustainability issues (Mora 2013) and more able to effectively work with other scientists, businesspeople, and politicians to develop viable solutions to current and future environmental and resource challenges. Graduate employability prospects will be further improved by stronger academic engagement on local environmental issues with external community-based stakeholders and the wider public. Finally, engaging with socially contested issues means dealing with ethical dimensions of sustainability (Metzger & Curren 2017), which provides much needed ways to introduce geoscience students to the growing awareness of the principles and practices of gothics, which are increasingly regarded as a vital component of professional geoscience practice (Peppoloni & Di Capua 2016, 2021, Wyss & Peppoloni 2014, Bohle & Marone 2021).

## 5. Concluding Remarks

Reframing geoscience – and university geoscience education - around the grand challenges of the 21$^{st}$ century would appear to be essential if Prince El Hassan’s ‘3G’ triangle of geography, geology, and geophysics is to help guide the wise stewardship of the planet.

For geoscientists, sustainable geoscience has the potential to revitalize Earth science and re-connect it with its distant Huttonian roots. That wider re-enchantment could help reverse the current decline in geoscience student numbers at many universities around the world, and perhaps ameliorate the damaging association that the subject has with those vocational sectors that are now publically rejected as environmentally destructive, notably the fossil fuel and mineral extraction industries.

The inclusion of socially relevant modules or content in university courses could make geoscience more relevant to students who are fascinated by the planet but who do not pursue it, possibly because they see it as less salient, prestigious, or scientific than other disciplines, viewing it simply as ‘the study of rocks’ (Mora 2013).

Whether this re-purposing is for young students or senior decision-makers, redefining James Hutton’s social mission for the modern age will help society deliver its ambitious, enduring and motivating over-arching goal of long-term wellbeing for all (Stewart & Hurth 2021), and in doing so show that 21$^{st}$ century geoscience is more than simply the study of old stones.

## Acknowledgments

This article began as a presentation in a ‘Looking Forwards Backwards’ seminar for British Institute in Amman’s Council for British Research in the Levant (CBRL), and I appreciate the support and feedback of Carol Palmer, Nizar Abu Jaber, and Matthew Jones. It has also benefitted from a range of activities relating to my new post as El Hassan Research Chair in Sustainability at the Royal Scientific Society, and conversations with RSS President HRH Princess Sumaya and with RSS Chairman HRH Prince El Hassan. Comments by Nizar Abu Jaber and two anonymous reviewers greatly improved the final manuscript. It is a contribution to UNESCO IGCP Project 685 on ‘Geology and Sustainable Development’ and part of the author’s ongoing work as a UNESCO Chair in Geoscience and Society.

## References

Anderson, S.P., Bales, R.C., and Duffy, C.J., 2008, Critical Zone Observatories: Building a network to advance the interdisciplinary study of Earth surface processes. Mineralogical Magazine, v. 72, 7–10.

Baker, V.R., 2014. Uniformitarianism, earth system science, and geology. Anthropocene, 5, pp.76-79.

Banwart, S.A., Chorover, J., Gaillardet, J., Sparks, D.,White,T., Anderson, S., Aufdenkampe,A., Bernasconi, S., Brantley, S.L, Chadwick, O., Dietrich, W.E., Duffy, C., Goldhaber, M., Lehnert, K., Nikolaidis, N.P, and Ragnarsdottir, K.V., 2013, Sustaining Earth's Critical Zone - Basic Science and Interdisciplinary Solutions for Global Challenges. The University of Sheffield, United Kingdom, 47p., ISBN: 978-0-9576890-0-8.

Bartos, P.J., Boland, M.A. and Freeman, L.W., 2006. The Human Face of Economic Geology: Education, Careers, and Innovation. Society of Economic Geologists Special Publication, 12, 171-19.

Brantley, S.A., DiBiase, R.A., Russo Tess, A., Shi, Y., Lin, H., Davis, K.J., Kaye, M., Hill, L., Kaye, J., Eissenstat, D.M., Hoagland, B., Dere, A.L., Neal, A.L., Brubaker, K.M., and Arthur, D.K., 2016, Designing a suite of measurements to understand the critical zone. Earth Surface Dynamics, v. 4, pp. 211–235, https://doi.org/10.5194/esurf-4-211-2016.

Beer, T., Li, J. and Alverson, K. eds., 2018. Global Change and Future Earth: The Geoscience Perspective (Vol. 3). Cambridge University Press.

Bohle, M. and Marone, E., 2021. Geoethics, a Branding for Sustainable Practices. Sustainability, 13(2), p.895.

Burke, K.D., Williams, J.W., Chandler, M.A., Haywood, A.M., Lunt, D.J. and Otto-Bliesner, B.L., 2018. Pliocene and Eocene provide best analogs for near-future climates. Proceedings of the National Academy of Sciences, 115(52), pp.13288-13293.

Calas, G., 2017. Mineral resources and sustainable development. Elements: An International Magazine of Mineralogy, Geochemistry, and Petrology, 13(5), pp.301-306.

Capello, M.A., Shaughnessy, A. and Caslin, E., 2021. The Geophysical Sustainability Atlas: Mapping geophysics to the UN sustainable development goals. The Leading Edge, 40(1), pp.10-24.

Catana, M.M. and Brilha, J.B., 2020. The role of UNESCO global geoparks in promoting geosciences education for sustainability. Geoheritage, 12(1), pp.1-10.

Clark, W.C., Crutzen, P.J. and Schellnhuber, H.J., 2004. Science for global sustainability. Earth system analysis for sustainability. MIT, Cambridge, pp.1-28.

Cleland, C.E., 2001. Historical science, experimental science, and the scientific method. Geology, 29(11), pp.987-990.

Crutzen, P.J., 2016. Geology of mankind. In Paul J. Crutzen: A Pioneer on Atmospheric Chemistry and Climate Change in the Anthropocene (pp. 211-215). Springer, Cham.

Curtis, A., 2012. The science of subjectivity. Geology, 40(1), pp.95-96.

Davis, R., 2011. Inventing the present: historical roots of the Anthropocene. Earth Sciences History, 30(1), pp.63-84.

Dodick, J. and Orion, N., 2003. Geology as an historical science: Its perception within science and the education system. Science & Education, 12(2), pp.197-211

Frodeman, R., 1995. Geological reasoning: Geology as an interpretive and historical science. Geological Society of America Bulletin, 107(8), pp.960-968.

Frodeman, R., 2014. Hermeneutics in the field: The philosophy of geology. In: The multidimensionality of hermeneutic phenomenology (pp. 69-79). Springer, Cham.

Gilbert, L., Teasdale, R. and Manduca, C., 2020. A New Vision of Sustainability in Earth Science Education. Eos, 101.

Gill, J.C., 2017. Geology and the sustainable development goals. Episodes, 40(1), pp.70-76.

Gill, J.C. and Bullough, F., 2017. Geoscience engagement in global development frameworks. Annals of geophysics, 60.

Gill, J.C., Mankelow, J. and Mills, K., 2019. The role of Earth and environmental science in addressing sustainable development priorities in Eastern Africa. Environmental Development, 30, pp.3-20.

Gill, J C. & Smith, M. (Eds.) 2021. Geosciences and the Sustainable Development Goals. Springer.

Gosselin, D., Manduca, C., Bralower, T., Mogk, D. 2013. Transforming the Teaching of Geoscience and Sustainability. Eos, Vol. 94, No. 25, 221–222.

Gosselin, D.C., Egger, A.E. and Taber, J.J. eds., 2019. Interdisciplinary teaching about Earth and the environment for a sustainable future. Springer.

Himiyama, Y., Satake, K. and Oki, T. eds., 2020. Human geoscience. Springer.

Lambert, I.B. 2001. Mining and sustainable development: considerations for minerals supply. Natural Resources Forum, Vol 25, No. 4, 275–284.

Lucchesi, S., 2017. Geosciences at the service of society: the path traced by Antonio Stoppani. Annals of Geophysics, 60.

Ludden, J., 2020. Where is geoscience going? Geological Society, London, Special Publications, 499(1), pp.69-77.

Kastens, K., C.A. Manduca, C. Cervato, R. Frodeman, C. Goodwin, L.S. Liben, D.W. Mogk, T.C. Spangler, N.A. Stillings, and S. Titus (2009), How Geoscientists Think and Learn, Eos Trans. AGU, 90(31), 265.

Kastens, K.A. and Manduca, C.A. eds., 2012. Earth and mind II: A synthesis of research on thinking and learning in the geosciences (Vol. 486). Geological Society of America

Kastens, K.A., Agrawal, S. and Liben, L.S., 2009. How students and field geologists reason in integrating spatial observations from outcrops to visualize a 3-D geological structure. International Journal of Science Education, 31(3), pp.365-393.

Manduca, C.A. and Mogk, D.W. eds., 2006. Earth and mind: How geologists think and learn about the earth (Vol. 413). Geological Society of America.

Metzger, E.P. and Curren, R.R., 2017. Sustainability: Why the language and ethics of sustainability matter in the geoscience classroom. Journal of Geoscience Education, 65(2), pp.93-100.

Mills, K. and Jones, M., 2021. Paleoscience and the UN sustainability goals. Past Global Changes Horizons, 1, pp.4-5.

Mora, G., 2013. The need for geologists in sustainable development. GSA Today, 23(12), pp.33-37.

Mudd, G.M., 2021. Sustainable/responsible mining and ethical issues related to the Sustainable Development Goals. Geological Society, London, Special Publications, 508(1), pp.187-199.

Peppoloni, S. and Di Capua, G., 2016. Geoethics: Ethical, social, and cultural values in geosciences research, practice, and education. Geological Society of America Special Papers, 520, pp.SPE520-03.

Peppoloni, S. and Di Capua, G., 2021. Geoethics as global ethics to face grand challenges for humanity. Geological Society, London, Special Publications, 508(1), pp.13-29.

Orion, N., 2006. Building an understanding of geological time: A cognitive synthesis of the "macro" and "micro" scales of time. Earth and Mind: How geologists think and learn about the Earth, 413, p.77.

Pennington, D., Ebert-Uphoff, I., Freed, N., Martin, J. and Pierce, S.A., 2020. Bridging sustainability science, earth science, and data science through interdisciplinary education. Sustainability Science, 15(2), pp.647-661.

Pratt, W., 1952, Towards a philosophy of oil finding: Bulletin of the American Association of Petroleum Geologists, v. 36, No. 12, p. 2231-2236.

Rajendran, C.P., 2019. Shifting Paradigms: Why History Matters in Geological Sciences. Current Science, 117(6), pp.927-931.

Reynolds, S.J., 2012. Some important aspects of spatial cognition in field geology. Earth & Mind II: Synthesis of research on thinking and learning in the geosciences. Geological Society of America Special Publication, 486, pp.75-78.

Rockström, J., Steffen, W., Noone, K., Persson, Å., Chapin, F.S., Lambin, E.F., Lenton, T.M., Scheffer, M., Folke, C., Schellnhuber, H.J. and Nykvist, B., 2009. A safe operating space for humanity. Nature, 461(7263), pp.472-475.

Rogers, R.D., 1989. Use of observational patterns in geology. Geology, 17(2), pp.131-134.

Rogers, S.L., Egan, S.S. and Stimpson, I.G., 2018. Tracking Sustainability Concepts in Geology and Earth Science Teaching and Learning, Keele University, UK. The Journal of Academic

Development and Education, (10).

Schlosser, P. and Pfirman, S., 2012. Earth science for sustainability. Nature Geoscience, 5(9), pp.587-588.

Schrodt, F., Bailey, J.J., Kissling, W.D., Rijsdijk, K.F., Seijmonsbergen, A.C., Van Ree, D., Hjort, J., Lawley, R.S., Williams, C.N., Anderson, M.G. Beier, P. et al. 2019. Opinion: To advance sustainable stewardship, we must document not only biodiversity but geodiversity. Proceedings of the National Academy of Sciences, 116(33), 16155-16158.

Smelror, M. 2020. Geology for society in 2058: some down-to-earth perspectives Geological Society, London, Special Publications, 499, https://doi.org/10.1144/SP499-2019-40

Steffen, W., Persson, Å., Deutsch, L., Zalasiewicz, J., Williams, M., Richardson, K., Crumley, C., Crutzen, P., Folke, C., Gordon, L. and Molina, M., 2011. The Anthropocene: From global change to planetary stewardship. Ambio, 40(7), 739-761.

Stewart, I., 2016. Sustainable geoscience. Nature Geoscience, 9(4), pp.262-262.

Stewart, I., 2020. Geology for society: Earth science for sustainable development. Humanistic futures of learning, p.39.

Stewart, I.S. & Gill, J.C., 2017. Social geology—integrating sustainability concepts into Earth sciences. Proceedings of the Geologists' Association, 128(2), 165-172.

Stewart, I.S. & Lewis, D., 2017. Communicating contested geoscience to the public: Moving from 'matters of fact 'to 'matters of concern'. Earth-Science Reviews, 174, 122-133.

Stewart, I.S. & Nield, T. 2013. Earth stories: context and narrative in the communication of popular geoscience. Proceedings of the Geologists' Association, 699-712. doi.org/10.1016/j.pgeola.2012.08.008.

Stewart, I.S. and Hurth, V., 2021. Selling Planet Earth: re-purposing geoscience communications. Geological Society, London, Special Publications, 508(1), pp.265-283.

Stephenson, M.H., Cheng, Q., Wang, C., Fan, J. and Oberhänsli, R., 2020. Progress towards the establishment of the IUGS Deep-time Digital Earth (DDE) programme. Episodes, 43(4), pp.1057-1062.

Stillings, N., 2012. Complex systems in the geosciences and in geoscience learning. Geological Society of America Special Papers, 486, pp.97-111.

Wang, C., Hazen, R.M., Cheng, Q., Stephenson, M.H., Zhou, C., Fox, P., Shen, S.Z., Oberhänsli, R., Hou, Z., Ma, X. and Feng, Z., 2020. The Deep-time Digital Earth program: data-driven discovery in geosciences. National Science Review.

Wyss, M. and Peppoloni, S. eds., 2014. Geoethics: Ethical challenges and case studies in earth sciences. Elsevier.

Zalasiewicz, J., Waters, C.N., Williams, M. and Summerhayes, C.P. eds., 2019. The Anthropocene as a geological time unit: A guide to the scientific evidence and current debate. Cambridge University Press.

JJEES

JJEES (2022) 13 (2): 105-113
ISSN 1995-6681

Jordan Journal of Earth and Environmental Sciences

# Morpho-physiological Effects of Drought on Medicinal Plants and the Potential Use of Remote Sensing - A Review

Tewfik Al-hamed[1*], Safwan M. Shiyab[2], and Jawad Al-Bakri[3]

[1]Department of Horticulture and Crop Science, Faculty of Agriculture, University of Jordan.
[2]Department of Horticulture and Crop Science, Faculty of Agriculture, University of Jordan.
[3]Department of Land, Water, and Environment, Faculty of Agriculture, University of Jordan.

Received 9 August 2021; Accepted 13 January 2022

**Abstract**

This review addresses the growth and development of medicinal plants under arid land conditions and the potential use of remote sensing technologies to map their distribution, as well as morphological and physiological responses in Arid lands. Plant morpho-physiological variables including, chlorophyll content, and gas exchange (photosynthesis, transpiration, vapor pressure, and stomatal conductance) are linked to plant water status. Multispectral and hyperspectral remote sensing techniques are promising for detecting morphological physiological changes. Vegetation indices derived from hyperspectral and multispectral imagery makes it possible to assess medicinal plants' health through successful detection of the ground plant physiological variables and canopy cover including chlorophyll, canopy density, gas exchange (red, 600-700 nm, near-infrared spectrum, 700-1100 nm) as well as water status (shortwave infrared, 1300-2500 nm). Surface reflectance data within the shortwave infrared bands (water bands) revealed significant differences between well-watered and drought-stressed plants. However, the moderate spatial resolution (Sentinel-2: 20 m, Landsat: 30 m) for the space-born free sensors and the need for a cloud-free sky could be limitations. Overall, vegetation indices derived from remotely sensed data are a useful approach for estimating the physiology of plants (medicinal plants) especially those under drought stress.



**Keywords:** Medicinal Plants, Drought Stress, Water Status, Hyperspectral, Multispectral, Vegetation Index.

## 1. Introduction

Climate change is one of the major problems facing the world because it is foretelling climate patterns changes and a higher frequency of risky weather events. In recent years, the frequency and severity of droughts in the Mediterranean region have increased due to global warming (IPCC, 2013; Trenberth et al., 2014). Generally, climate change has a potential impact on agriculture, coastal areas, biodiversity, urban systems, society, water, and health sectors (FAO, 2008). In the agricultural sector, climate-change-related risks are represented by higher temperatures, rainfall decreases, the shift in the rainy season and seasonal alterations, heatwaves, and extreme events especially heavy rainfall and droughts (WB, 2021). Drought is a disastrous natural phenomenon that has negative impacts on plants and especially under the changing climate, it becomes more frequent and severe (Seneviratne et al., 2012). Drought has destructive effects on socioeconomic, plants, and the environment because it leads to insufficient precipitation, high evapotranspiration, and over-exploitation of water resources (Yurekli and Kurunc, 2004; Bhuiyan et al., 2006; García-Caparrós et al., 2019). Drought effects can be classified as direct and indirect (Van Lanen and Peters, 2000). Direct impacts of drought are the results of interactions among water deficiencies and environmental, and socio-economical components while indirect are a secondary result of water deficiency and are often occurred far away from the drought-impacted region (UNDRR, 2021).

Generally, drought can be categorized into three basic types in terms of measuring drought as a physical phenomenon; meteorological, agricultural, or hydrological drought (Wilhite and Glantz, 1985). Meteorological drought is a prolonged abnormal dryness period (compared to normal average precipitation), agricultural drought links meteorological variables (e.g., precipitation) to agricultural impacts such as soil water deficits while hydrological drought is associated with the influence of rainfall periods on the surface or groundwater supply (NDMC, 2021). In arid and semi-arid land, functional landscapes and their associated vegetation are ultimately dependent on water availability, which significantly affect vegetation distribution (Tardieu et al., 2018). Drought stress in plants (e.g., Thymus citriodorus) normally plants moisture content (dehydration) followed by a reduction in the metabolism process and photosynthesis and consequently plants death (Tátrai et al., 2016). However, the ability of plants to survive under stressed conditions depends on plant species, growth stage, duration, and the intensity of water deficit (Blum, 2017). Plant tolerance to abiotic stress such as water stress is unpredictable because of the complicated interactions between stress factors and plant molecular, biochemical, and physiological components associated with growth and development processes (Razmjoo et al., 2008).

Medicinal plants are the major sources of numerous valuable chemicals and/or drugs worldwide. According to the International Union for Conservation of Nature (IUCN)

* Corresponding author e-mail: Tewfik_Alhamad@mwi.gov.jo

and the World Wildlife Fund (WWF), about 50,000–80,000 flowering plants are used because of their medicinal values. In Europe, over 1300 medicinal plants are used, especially those from the wild sources which account for 90% of the total medicinal plants (Hao, 2019). Jordan is home to an abundance of flora and fauna, about 2978 plant species belonging to 120 families and 719 genera are recorded in Jordan (Abdelhalim et al., 2017). In addition, 20% of the total flora species in Jordan are classified as medicinal plants (Abdelhalim et al., 2017). High demand for medicinal plants coupled with unpredictable environmental stressors such as low rainfall has led to a significant reduction in their abundance worldwide. Cultural practices such as planting method and date, fertilizer application, irrigation regimes, and harvesting should be optimized to increase the growth and productivity of medicinal plants (Tanga et al., 2018). Efforts to conserve wildlife flora including medicinal plants have been observed recently including research studies focused on the growth (e.g soilless culture), physiology, production (yield, phenolic compounds, and oil content), and conservation of those plants (Al-Karaki and Othman 2009; Leskovar and Othman, 2016; Sharma et al., 2020).

Management and monitoring of wild plants including medicinal ones require frequent and consistent assessment of the canopy status and health over time. The main health indicators are morphology and physiological variables including chlorophyll contents, gas exchange [photosynthesis (Pn), transpiration (E), vapor pressure deficit (VPD), and stomatal conductance (gs)] as well as plant development and yield (Tahat et al., 2020). These morpho-physiological variables can provide accurate information about the plant carbon assimilation rate, leaf water level (Othman et al., 2014a; Tadros et al., 2021), plant nutrition, fruit quality, and consequently their health (Al-Ajlouni et al., 2017; A'saf et al., 2020; Ayad et al., 2018; Alsmirat et al. 2018; Leskovar and Othman, 2018, 2021; Tahat et al., 2020). However, these methods of assessment are time-consuming, labor intensive, and expensive. In addition, the distribution of some wildlife flora could be not accessible. Another possible alternative to assess plant health is through remote sensing techniques (Al-Kofahi et al., 2019; Othman et al., 2014b, 2021; Tadros et al., 2020). Remote sensing has potentially assessed chlorophyll content (Othman et al., 2019), canopy density (Othman and St. Hilaire, 2021; Tadros et al., 2020), gas exchange and water status (Othman et al., 2014b, 2015), and geographic distribution (Al-Bakri et al., 2011). Remotely sensed data are providing an upscale view of the land and a spatiotemporal context to measure drought impacts (Hazaymeh and Hassan, 2017). In addition, vegetation indices derived from space-borne sensors (e.g., Landsat and MODIS) such as Normalized Difference Vegetation Index (NDVI) and the Vegetation Condition Index (VCI) have been successfully linked to chlorophyll content and water content in the plants (Rousta et al., 2020). In this review, we evaluated the usefulness of using the remote sensing approach as an alternative for evaluating medicinal plants' morpho-physiological responses under drought conditions.

## 2. Evaluation of Eco-physiological Parameters of Medicinal Plants

In the developing world, local communities depend on traditional medicine for primary health care (Jeelani et al. 2018). In addition, developed countries heavily use medicinal plants for their pharmaceutical products (Chapman and Chomchalow, 2005). Medicinal plants have several phenolic and antioxidant compounds which used to support human health and cure some diseases. In Jordan, several medicinal plant species are native to Eastern and Northern rangelands (Badia) (Oran and Al-Eisawi, 2015). More than 49 plant families and 120 plant species found in Jordan are used by neighborhood people for medical purposes (Atta and Alkofahi, 1998). However, uncontrolled grazing and frequent drought periods in the last decade reduced their numbers (Oran and Al-Eisawi, 2015). Therefore, research studies that focus on improving the tolerance of the medicinal plant to harsh conditions as well as controlling grazing intensity are essential for the potential sustainability of those plants.

Abiotic, and biotic (soil microorganisms) factors can significantly affect medicinal plant metabolite biosynthesis. Abiotic stresses such as temperature extremes and water stress can negatively affect the physiology and chemical composition of plants, which as a result induce abnormalities in medicinal plant metabolic processes such as growth, photosynthesis performance, and yield (Zaid et al., 2021). Optimal environmental conditions tend to increase medicinal plant biomass rather than synthesizing secondary metabolites (Pavarini et al., 2012). Postharvest processing can also lead to an irreversible quality loss of medicinal plants (Tanga et al., 2018). Therefore, finding proper management practices to guarantee high plant growth, productivity and quality are critical for the medicinal plants industry. In this context, management practices including irrigation, fertilization, and pest control required frequent assessment and evaluation during the growing season to sustain plant health and productivity. To assess the growth performance in response to those cultural practices (irrigation, fertilization, pest management) several plant-base and soil-base measurements have been recommended including water status (e.g. midday stem water potential (Ψsmd), relative water content) and chlorophyll content (Othman et al., 2014b, 2015).

Plant-based measurements such as midday stem water potential, relative water content, gas exchange (Pn, gs, E, VPD, respectively), and leaf pigments are viable approaches to assess the physiology of plants which depict their health status (Jones, 2004; Khasawneh et al., 2021; Leskovar and Othman, 2019; Othman and Leskovar, 2018, 2019). This is because many features of the tree's physiology react immediately to changes in tree tissues including water status (Jones, 2004). For example, Othman et al., (2014a) reported that under deficit water stress, Ψsmd and gas exchange were significantly lower and resulted in lower growth rate and yield compared to non-water-stressed plants. Although total soluble sugars and proline concentration in chamomile (Matricaria chamomilla L.) was similar across water deficit regimes, the total chlorophyll concentration was significantly reduced in water deficit plants (55% of field capacity) compared to control (100% field capacity) (Pirzad et al., 2011).

Chlorophyll and carotenoids (carotenes and xanthophyll) are the major pigments of green leaves (Gitelson et al., 2002; Li et al., 2018). Pigment concentration inside the leaves potentially reflects the physiological performance of plants (Gamon and Surfus, 1999; Blackburn, 2007). This is because leaf pigments (chlorophyll, and anthocyanin) level in the leaves could act as a photoprotective mechanism that mitigates water deficit impact (Gamon and Surfus, 1999; Gori et al., 2021). Chlorophyll fluorescence (Fv/Fm) is a leaf-level physiological measurement that is used to study the performance of chlorophyll pigments under stress such as drought (Guidi et al., 2019). The decrease in Fv/Fm value is an indicator of low performance of photosynthetic pigments specifically, photosystem II (PSII) efficiency (Guidi et al., 2019). However, chlorophyll fluorescence measurements (re-emitted light from PSII) can interfere with the sunlight and thus many early systems had to be used in darkness and/or highly controlled light environments and it remains stable under mild and moderate drought stress and shows a significant decline only under severe drought conditions (Othman et al., 2014a). Gas exchange also is used in assessing plant performance including those studies focusing on plant growth and productivity as well as fruit quality (Leskovar and Othman, 2021; Kasaweneh et al., 2021). Gas exchange variables (Pn, gs, and E) normally decreased in parallel with increased stressors such as water deficit and nutrient deficiency (Ayad et al., 2018).

Water status is one of the most important factors limiting medicinal plant performance, especially those grown in an arid environment (Khorasaninejad et al., 2010; Pirzad et al., 2011). For example, drought stress significantly reduced the growth rate, essential oil, and yield of mint (Mentha piperita L.) compared to those grown under 100% field capacity (Khorasaninejad et al., 2010). Low soil moisture reduces stomatal conductance, total lipid content, photosynthetic capacity, chlorophyll content, transpiration, and the total dry matter (Guerfel et al., 2008; Grams et al., 2007; He et al., 2007; Warren et al., 2007; Damour et al., 2009; Arunyanark et al., 2008). At moderate drought, Pn decreased slightly because of the reduction of stomatal aperture that interacts with $CO_2$ diffusion as well as the intercellular $CO_2$ (Ci) inside the stomata; stomatal limitation effect (Cifre et al., 2005). However, at severe water deficits, Pn further declines and Ci increases indicating that non-stomatal limitations become significant (Tezara et al., 1999). Othman et al (2014a) screened leaf-level physiological changes that occurred during cyclic irrigation to determine parameters that best-represented changes in plants; the physiological variables included midday stem water potential ($\Psi_{smd}$), relative water content (RWC), the osmotic potential at full turgor ($\pi$), leaf area ratio (LAR), gas exchange (Pn, gs, and E) chlorophyll content and fluorescence (Fv/Fm). They found that $\Psi_{smd}$ was the best leaf-level physiological response to detect moisture status in plants. Although the study was on woody trees, a similar trend was found in medicinal plants (Kalamartzis et al., 2020). For example, water deficit stress increased leaf temperature, $\Psi_{smd}$, gas exchange parameters, and dry herb yield of Ocimum basilicum (Kalamartzis et al., 2020).

Although physiological measurements are a reliable source to assess plant health, the amount of time involved in data collection and the difficulties of automation of those instruments could be critical limitations to using ground physiological measurement to upscale the response to a large scale (Jones, 2004; Qarallah et al., 2021). In addition, physiological variables are at the leaf-level scale, which might be not representative of the whole tree's status (Othman et al., 2021). For example, high-performance liquid chromatography is usually used to measure pigment concentration inside the leaf, but the extraordinary cost and extraction time, along with the necessity of leaf destruction, limit its usage (Gamon and Surfus, 1999). Midday stem water potential equipment (pressure chamber) is not automated which requires the person to be onsite, requires leaf destruction, and might not be safe because of pressurized gas inside the instrument. Given that leaf-level physiological measurement is not easy, to upscale to a large scale, finding another alternative to estimate plant health is a critical issue for the plants in general and the medicinal plants' community specifically.

### 3. The role of remote sensing in assessing medicinal plants under drought conditions

The remote sensing approach involves the acquisition of information about an object without being in direct contact with it (Jensen, 2005). This technique enables researchers to collect information about plants in rugged topography places that are not accessible for plant-based measurements (Othman, 2014). Remote sensing is a promising approach for detecting and predicting plant morphological and physiological traits such as chlorophyll content, canopy density, and water status (Othman et al., 2014b; Santos et al., 2008). These techniques can detect, predict, and scale up leaf-level physiological responses to large areas without destroying leaves or plants (Ormeci et al., 2009). Multi-spectral satellite imagery can provide information covering large areas, while aerial photography with unmanned aerial vehicles (UAV) allows us to collect comprehensive biometric information from sites under investigation (Table 1). UAV created orthophoto with high quality that allowed confidently interprets the medicinal plants' communities during different growth stages including flowering (Fadeev et al., 2019). The combined use of multispectral aerial and satellite imagery and the high spatial resolution of UAV photography scaled up the vegetation (e.g., medicinal plants) in significant areas and accelerated the work in large areas (Fadeev et al., 2019; Qarallah et al., 2021). The age of an endangered medicinal and aromatic plant species Valeriana jatamansi was successfully identified using field hyperspectral remote sensing and machine learning techniques. This combined approach provides a scientific way for harvesting this plant at its optimum age avoiding its wastage (Kandpal et al., 2021). A multilevel monitoring system including spaceborne (Landsat), aerial remote sensing, and field measurement was conducted to monitor the medicinal plant (Rheum tanguticum) resource in Sichuan Province, China (Xie et al., 2014). They found that only the R. tanguticum with canopy coverages of more than 1 $m^2$ could be detected from the aerial of 10 cm resolution. Landsat alone has limited capability of detecting the scattered R. tanguticum plants.

**Table 1.** Satellite and field sensor spectral, spatial, and radiometric data and their application in vegetation studies.

| Platform | Sensor | Revisit time (day) | Spatial Resolution (m) | Variable | Example |
|---|---|---|---|---|---|
| Sentinel-2A | MSI | 5 | 10 -20 | Leaf area, productivity | Cerasoli et al., (2018). |
| Landsat 8 | OLI | 16 | 30 | Leaf area, chlorophyll, photosynthesis, water stress. | Othman et al., (2014b, 2018, 2020, 2021); Tadros et al., (2020), Sawalhah et al., (2018; 2021). |
| NOAA-15 | AVHRR/3 | 1 | 1090 | Leaf area index | Liu et al., (2012) |
| TERRA / AQUA | MODIS | 1 – 2 | 250-1000 | Equivalent water thickness, leaf area index, chlorophyll-*a*, fraction of photosynthetically active radiation | Cheng et al., (2013), Liu et al., (2012), Moses et al., (2009),Qu et al., (2014), Yang et al., (2006). |
| SPOT-5 | HRS | 27 | 5 | Leaf area index and soil moisture. | Soudani et al., (2006), Gouveia et al., (2009). |
| | HRG | 27 | 10 | | |
| | VEGETATION | 1 | 165 | | |
| IKONOS-2 | OSA | 11- 14 | 4 | Leaf area index, and chlorophyll-*a*. | Soudani et al., (2006), Ormeci et al., (2009). |
| ASD Fieldspec Pro Full Range Spectroradiometer | - | | ≈ 1.0 $m^2$ at 1m nadir view (25° field-of-view) | Relative water content, chlorophyll florescent, photosynthesis, and leaf water content. | Matsushita et al., (2010), Othman et al., (2015, 2020). |

The water content of plants is an essential variable for the growth and productivity of medicinal plants. The water status of plants can be monitored with surface reflectance data. Generally, canopy reflectance at near infrared (NIR, 700 – 1200 nm) is higher than at shortwave infrared (SWIR; 1300 – 2500 nm) (Figure 1). This is because leaf water status has a dominant influence in the SWIR wavelengths by strongly absorbing spectral reflectance in this spectra region (Pu et al., 2003; Eitel et al., 2006). Water status (drought) indices are commonly used to detect the potential risk of occurrence and severity of drought, and to study spatial–temporal reasoning. Remotely-sensing indices such as water band index (WBI) and band ratio (NIR/SWIR) response to water status in the plant by detecting the canopy surface reflectance in the “water bands” spectrum (1200 to 2500 nm spectral range) during drought and recovery cycles (Claudio et al., 2006; Othman et al., 2014b). Under drought conditions, the spectral reflectance in the SWIR region (water absorption region) increased and change the vegetation values of indices that rely on these bands (Eitel et al., 2006). Up to now, several remote sensing methods have been established and used for agricultural drought monitoring such as vegetation indices, band ratio and empirical remote sensing algorithms (Ligi et al., 2017; Zargar et al., 2011). These methods showed the potential results in terms of detecting drought conditions in plants (Faragó et al., 1993; Zargar et al., 2011).

The use of remote sensing techniques to monitor drought and assess its influence has been widely adopted recently (Manesh et al., 2019). It is possible to observe the intensity of plant water stress and to detect the damage in crop areas using various agricultural drought indices (Ryu et al., 2019). This directly affects agricultural production (agricultural drought), which is most often visible in the physiological condition of plants and can be assessed from ground or satellite sensors (Wu et al., 2015; Othman et al., 2015, 2021). Using these land-surface properties, numerous satellite-based water stress indices (drought) have been developed for effective monitoring (AghaKouchak et al., 2015). However, the correlations among this vegetation are not always accurate because the definitions of indices are conceptually different based on the indicated drought phenomenon and the time scale for observing the progress (Zhang et al., 2017). In addition, the parameters used in the calculation of each index differ according to the meteorological, agricultural, and hydrological drought concepts (Anggraini et al., 2016). For example, while meteorological drought considers only atmospheric dry conditions, agricultural, and hydrological droughts are highly related to land conditions. In Iaşi region/Romania, the land of several aromatic and medicinal plants including Verbena Officinalis, Macarof and Stătescu (2017) found that Normalized Vegetation Supply Water Index (NVSWI) derived from Landsat 8 Operational Land Imager (OLI) were able to detect drought stress. Karnaris and Asimopoulos (2020) reviewed the use of the unmanned aerial vehicle for detecting aromatic plant growth change and response to harsh micro-climate in Greece. They find that UAV were able to detect vegetation cover changes (NDVI). However, more studies and vegetation indices should be developed for the Western Macedonia region to successfully detect the response of the aromatic-medicinal plants to harsh conditions (cold-dry).

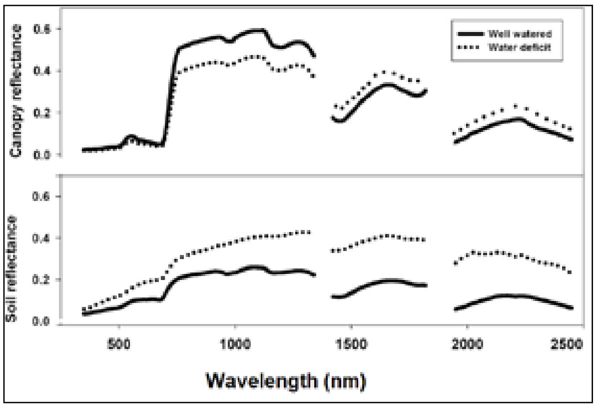


**Figure 1.** Canopy and soil surface reflectance under well-water and drought stress conditions for woody plants. Source: Canopy reflectance data were from Bayat et al. (2016) and soil data were from Othman (2014).

Leaf pigments including chlorophyll and carotenoids are essential for several plant processes such as carbon assimilation. Chlorophyll is a green pigment found in chloroplast and present in green algae and terrestrial plants in two forms, chlorophyll, a and b. This pigment absorbs light mainly in the red (650 – 700 nm) and the blue (400 – 500 nm) and reflects the green light (~550 nm) (Jones and Vaughan, 2010). Remotely sensed data of leaf pigments especially chlorophyll can predict the leaf's physiological status and consequently the plants' health (Gamon and Surfus, 1999).Surface reflectance at 510, 550, 700 and 750 nm significantly correlated ($R^2 > 0.75$) with the total carotenoids in the leaves (Gitelson et al., 2002). Othman et al. (2018) found that multispectral data from Landsat ETM+ are a reliable source to detect chlorophyll content in the plant. In addition, Ormeci et al. (2009) concluded that IKONOS data are a reliable source for detecting chlorophyll-a in large areas even if the in-situ measurements are limited. At drought stress, excess light energy migrates from the chlorophyll molecules to the xanthophyll cycle to protect the system from damage (Grace et al., 2007). This energy causes a shift in the xanthophyll cycle, at which point violaxanthin is converted into zeaxanthin causing excess energy dissipation (Naumann et al., 2009). The hyperspectral vegetation index, and photochemical reflectance index (PRI) successfully measured the efficiency of the xanthophyll (Naumann et al., 2009).Suàrez et al. (2008) found that canopy-PRI derived from Airborne Hyperspectral Scanner (AHS) sensor was able to detect the physiological responses (xanthophyll pigment cycle, stomatal conductance, and stem water potential) of plants (Suàrez et al., 2008). In addition, Thenot et al. (2002) revealed that PRI could be a non-destructive, cost-effective method for detecting water stress in Chenopodium quinoa. Considering the previous studies that showed a significant relationship between remotely sensed data and leaf pigments, especially chlorophyll (content and fluorescence), we believe that remote sensing data are a reliable source to assess plant chlorophyll and hence plant health.

Precision agriculture of woody and herbaceous crops including medicinal plants requires a piece of accurate information about the canopy, specifically coverage percentage. Leaf area index (LAI) is an essential variable that is used to estimate vegetation cover and productivity and as an input to water and energy budgets and ecosystem process models (Butson et al., 2002; Fernandes et al., 2004). When LAI strongly correlates with remotely sensed vegetation indices, these indices can be used to scale up those variables over large regions (Treitz et al., 2010).Othman and St. Hilaire (2021) found that three vegetation indices derived from Landsat ETM+ were able to estimate LAI correctly. The vegetation indices were normalized difference infrared Index-band 5 (NDII5), enhanced vegetation index (EVI), and green normalized difference vegetation index (GNDVI). In addition, Liu et al. (2012) concluded that vegetation indices from Landsat TM/ETM$^+$ including normalized difference vegetation index (NDVI), the optimized soil adjusted vegetation index (OSAVI), the two bands enhanced vegetation index (EVI2) and the modified triangular vegetation index (MTVI2) can be used to derive LAI map for seasonal crop growth monitoring. Considering the finding of previous studies, the use of datasets from high-resolution aerial sensors and moderate satellites images are holding promises for detecting medicinal plants' health status by estimating canopy cover and chlorophyll content (red, 600-700 nm; near-infrared spectrum, 700-1100 nm) as well as water status (shortwave infrared, 1300-2500 nm).

## 4. Remote sensing limitations

The current limitations for using remotely sensed data are mainly due to restricted spectral range, coarse spatial resolution (more than 30 m), low temporal resolution (revisit time) as well as inadequate repeat coverage during the growing season (Moran et al., 1997). In addition, image pre-processing of aircraft- and satellite-based images required specialized software and workers. For example, satellite sensor data requires atmospheric and geometric correction before utilization using special software such as ENVI and ERDAS IMAGINE (Othman et al., 2018; Sawalhah et al., 2018, 2021). In addition, the acquisition of cloud-free space-born images (e.g., MODIS, Landsat) is one of the biggest challenges (Whitcraft et al., 2015). During the satellite overpass, the area should be cloud-free to guarantee meaningful images. Therefore, this tool could be inefficient during winter and early spring; the time when clouds cover percentage is extremely high. Although multispectral remotely sensed data such as Landsat series and Sentinel-2, hyperspectral remote sensing equipment is extremely expensive. In terms of physiological assessment, data from several remote sensing studies could show a pattern of difficulties in predicting or detecting the plant response. For example, when plants are under moderate water stress the difference in reflectance is quite narrow. As a result, the plant could be exposed to water stress through the surface reflectance is almost similar. At the field scale, both high spatial and high temporal data are required due to the small size of agricultural fields and the quick changes in plants through the growing season (Becker-Reshef et al., 2010; Rocha et al., 2012; Atzberger, 2013). For example, moderate spatial resolution data (i.e., 30 m) is essential for studying plant responses at a field scale (Roy et al., 2014), and high temporal resolution data (i.e., weekly) is obligatory for monitoring quick changes during the growing season (Zhang et al., 2003; Kovalskyy et al., 2012). These variations, in some cases, may reflect specific agricultural difficulties such as drought (McVicar and Jupp, 1998). Generally, if the spatial resolution is high enough (e.g., less, or equal to 30 m), then it is reasonably easy to compare with ground-based measurements. When the coarse spatial resolution is used, a combined airborne and space-borne remote sensing datasets might be used for favorable accuracy (Hazaymeh and Hassan, 2016).

## 5. Conclusions

Plant-based measurements including midday stem water potential, relative water content, gas exchange (Pn, gs, E and VPD), and leaf pigments (chlorophyll and carotenoids) are the best physiological measurements to assess the response of plants to environmental stresses including those planted for medicinal usage. However, those measurements are time consuming and expensive. Remotely sensed data from hyperspectral and multispectral sensors make it possible to assess medicinal plant physiology through successful detection of the ground leaf and canopy physiological variables including water status, chlorophyll, and LAI. Shortwave infrared indices such as vegetation water stress index are useful for estimating medicinal plant water status especially when ground physiological measurements (e.g., midday stem water potential) are limited. However, those remotely sensed indices can markedly predict water levels in medicinal plants under severe water stress conditions. Surface reflectance vegetation indices can be used in estimating water status in vegetation including medicinal plants when rainfall is the only source of water and when plants are exposed to severe water stress. Under commercial production of medicinal plants, the use of those indices could be not accurate because growers will not allow them to fully dry, exposing plants to severe water stress. Despite being inefficient occasionally, remote sensing sensors are a viable and accurate tool; and hold promise for assessing vegetation health including medicinal plants.

## References


Abdelhalim, A., Aburjai, T., Hanrahan, J., Abdel-Halim, H. (2017). Medicinal plants used by traditional healers in Jordan, the Tafila region. Pharmacognosy Magazine 13: S95-S101. doi:10.4103/0973-1296.203975.

AghaKouchak, A., Farahmand, A., Melton, F.S., Teixeira, J., Anderson, M.C., Wardlow, B.D., Hain, C.R. (2015). Remote sensing of drought: Progress, challenges and opportunities. Reviews of Geophysics 53: 452–480.

Al-Ajlouni, M., Ayad, J., Othman, Y. (2017). Increasing nutrient levels promote growth and flower quality in lilies grown under soilless culture. Horticultural Science 44(4):171-177.

Al-Bakri, J., Al-Eisawi, D., Damhoureyeh, S., Oran, S. (2011). GIS-Based analysis of spatial distribution of medicinal and herbal plants in arid and semi-arid zones in the North-west of Jordan. Annals of Arid Zone 50(2): 99-115.

Al-Karaki, G. and Othman, Y. (2009). Soilless cultivation of some medicinal and aromatic herb plants under the conditions of Arabian Gulf region. Emirate Journal of Food Agriculture 21 (2): 64-70. 3.

Al-Kofahi, S., Gharaibeh, A., Bsoul, E., Othman, Y., St. Hilaire, R. (2019). Investigating domestic gardens' densities, spatial distribution and types among city districts. Urban Ecosystems 22(2). https://doi.org/10.1007/s11252-019-0833-7.

Alsmirat, N., Al-Ajlouni, M., Ayad, J., Othman, Y., St. Hilaire, R. (2018). Composition of soilless substrates affect the physiology and fruit quality of two strawberry (Fragaria × ananassa Duch.) cultivars. Journal of Plant Nutrition 41(18): 2356-2364.

Anggraini, N., Faridah, E., Indrioko, S. (2016). The effect of drought stress on physiological behavior and growth of black locust seedlings (Robinia pseudoacacia). Journal of Forest Science 9 (1): 40-56 (17).

Arunyanark, A., Jogloy, S., Akkasaeng, C., Vorasoot, N., Kesmala, T., Rao, R., Wright, G., Patanothai, A. (2008). Chlorophyll stability is an indicator of drought tolerance in peanut.Journal of Agronomy and Crop Science 194: 113–125.

A'saf, T., Al-Ajlouni, M., Ayad, J., Othman, Y., St. Hilaire, R. (2020). Performance of six different soilless green roof substrates for the Mediterranean region. Science of the Total Environment 730:139182. https://doi.org/10.1016/j.scitotenv.2020.139182.

Atta, A.H. and Alkofahi, A. (1998). Anti-nociceptive and anti-inflammatory effects of some Jordanian medicinal plant extracts. Journal of Ethnopharmacology 60:117-124.

Atzberger, C. (2013). Advances in remote sensing of agriculture: Context description, existing operational monitoring systems and major information needs. Remote Sensing 5: 949-981.

Ayad, J., Othman, Y., Al-Ajlouni, M., Alsmirat, N. (2018). Photosynthesis, gas exchange and yield of two strawberry (Fragaria × ananassa duch.) cultivars in response to gibberellic acid. Fresenius Environmental Bulletin 27: 9127-9134.

Bayat, B.; Van der Tol, C.; Verhoef, W. (2016). Remote sensing of grass response to drought stress using spectroscopic techniques and canopy reflectance model inversion. Remote Sensing 8, 557. https://doi.org/10.3390/rs8070557.

Becker-Reshef, I., Justice, C., Sullivan, M., et al. (2010). Monitoring global croplands with coarse resolution earth observations: The global agriculture monitoring (GLAM) project. Remote Sensing 2: 1589-1609.

Bhuiyan, C., Singh, R. P., Kogan, F. N. (2006). Monitoring drought dynamics in the Aravalli region (India) using different indices based on ground and remote sensing data. International Journal of Applied Earth Observation and Geoinformation 8:289–302.

Blackburn, G. (2007).Hyperspectral remote sensing of plant pigments. Journal of Experimental Botany 58(4): 855-867.

Blum, A. (2017). Osmotic adjustment is a prime drought stress adaptive engine in support of plant production. Plant, Cell and Environment 40: 4–10.

Butson, C., Fernandes, R., Latifovic, R., Wenjun, C. (2002). A robust approach for estimating LAI from Landsat TM/ETM + imagery. Proceedings of the IEEE Int. Geosciences Remote Sensing 4: 2328–2330. DOI: 10.1109/IGARSS.2002.1026534.

Cerasoli, S., Campagnolo, M., Faria, J., Nogueira, C., Caldeira, M. (2018). On estimating the gross primary productivity of Mediterranean grasslands under different fertilization regimes using vegetation indices and hyperspectral reflectance. Biogeosciences 15: 5455–5471.

Chapman, K. and Chomchalow, N. (2005). Production of medicinal plants in Asia. Acta Horticulturae: 679: 45–59.

Cheng, T., Riano, D., Koltunov, A., Whiting, M., Ustin, S., Rodriguez, J. (2013). Detection of diurnal variation in orchard canopy water content using MODIS/ASTER airborne simulator (MASTER) data. Remote Sensing of Environment 132:1–12.

Cifre, J., Bota, J., Escalona, J., Medrano, H., Flexas, J. (2005). Physiological tools for irrigation scheduling in grapevine (Vitis vinifera L.) An open gate to improve water-use efficiency. Agriculture, Ecosystems and Environment 106:159–170.

Claudio, H., Cheng, Y., Fuentes, D., Gamon, J., Luo, H., Oechel, W., Qiu, H., Rahman, A., Sims, D. (2006). Monitoring drought effects on vegetation water content and fluxes in chaparral with the 970 nm water band index.Remote Sensing of Environment 103:304–311.

Damour, G., Vandame, M., Urban, L. (2009). Long-term drought results in a reversible decline in photosynthetic capacity in mango leaves, not just a decrease in stomatal conductance.Tree Physiology 29: 675–684.

Eitel, J., Gessler, P., Smith, A., Robberecht, R. (2006).Suitability of existing and novel spectral indices to remotely detect water stress in Populus spp.Forest Ecology and Management 229:170–182.

Fadeev, N., Skrypitsyna, T., Kurkov, V., Sidelnikov, N. (2019). Use of remote sensing data and GIS technologies for monitoring stocks of medicinal plants: Problems and Prospects Information Technologies in the Research of Biodiversity, SPEES 4-21.

FAO (Food and Agriculture Organization, 2008). Climate change, water, and food security. Land and Water Division.

Faragó, T., Kozma, E., Nemes, Cs. (1993). Drought indices in meteorology. Quarterly Journal of the Hungarian Meteorological Service 93(1): 45–60.

Fernandes, R. A., Miller, J. R., Chen, J. M., Rubinstein, I. G. (2004). Evaluating image-based estimates of leaf area index in boreal conifer stands over a range of scales using high-resolution CASI imagery. Remote Sensing of Environment 89: 200-216. https://doi.org/10.1016/j.rse.2002.06.005.

Gamon, J. and Surfus, J. (1999).Assessing leaf pigment content and activity with a reflectrometer. New Phytology 143(1): 105-117.

García-Caparrós, P., Romero, M.J., Llanderal, A., Cermeño, P., Lao, M.T., Segura, M.L. (2019). Effects of drought stress on biomass, essential oil content, nutritional parameters, and costs of production in six Lamiaceae species. Water 11: 573. https://doi.org/10.3390/w11030573.

Gitelson, A., Zur, Y., Chivkunova, O., Merzlyak, M. (2002). Assessing carotenoid content in plant leaves with reflectance spectroscopy. Photochemistry and Photobiology 75(3): 272-281.

Gori, A., Brunetti, C., dos Santos Nascimento, L.B., Marino, G., Guidi, L., Ferrini, F., Centritto, M., Fini, A., Tattini, M. (2021). Photoprotective role of photosynthetic and non-photosynthetic pigments in Phillyrea latifolia: Is their "Antioxidant" function prominent in leaves exposed to severe summer drought? International Journal of Molecular Sciences 22: 8303, https://doi.org/10.3390/ijms22158303.

Gouveia, C., Trigo, R., Dacamara, C. (2009). Drought and vegetation stress monitoring in Portugal using satellite data. Natural Hazards and Earth System Sciences 9:185–195.

Grace, J., Nichol, C., Disney, M., Lewis, P., Quaife, T., Bowyer, P. (2007). Can we measure terrestrial photosynthesis from space directly, using spectral reflectance and fluorescence? Global Change Biology 13(7): 1484-1497.

Grams, T., Koziolek, C., Lautner, S., Matyssek, R., Fromm, J. (2007). Distinct roles of electric and hydraulic signals on the reaction of leaf gas exchange upon re-irrigation in Zea mays L. 2007. Plant, Cell and Environment 30(1): 79-84.

Guerfel, M., Baccouri, O., Boujnah, D., Zarrouk, M. (2008). Changes in lipid composition, water relations and gas exchange in leaves of two young 'Chmlali' and 'Chetoui' olive trees in response to water stress.Plant Soil 311: 121–129.

Guidi, L., Lo Piccolo, E., Landi, M. (2019). Chlorophyll fluorescence, photoinhibition and abiotic stress: does it make any difference the fact to be a C3 or C4 species? Front. Plant Science 10:174. doi: 10.3389/fpls.2019.00174.

Hao, D. (2019). Genomics and Evolution of Medicinal Plants. In: Ranunculales Medicinal Plants Biodiversity, Chemodiversity and Pharmacotherapy pp 1-33.

Hazaymeh, K. and Hassan, Q. K. (2017). A remote sensing-based agricultural drought indicator and its implementation over a semi-arid region, Jordan. Journal of Arid Land 9:319–330.

Hazaymeh, K. and Hassan, Q.K. (2016). Remote sensing of agricultural drought monitoring: A state of art review. AIMS Environmental Science 3(4): 604-630. doi: 10.3934/environsci.2016.4.604.

He, C., Zhang, J., Duan, A., Sun, H., Fu, L., Zheng, S. (2007). Proteins responding to drought and high temperature stress in Pinus armandii Franch. Canadian Journal for Research 85: 994-1002.

IPCC. (2013). Intergovernmental Panel on Climate Change. Climate change: the physical science basis. In: Stocker, T.F., Qin, D., Plattner, M., Tignor, S.K., Allen, et al. (eds.), Working group I contribution to the fifth assessment report of the Intergovernmental Panel on Climate Change. Cambridge University Press, Cambridge, United Kingdom and New York, NY, USA.

Jeelani, S.M., Rather, G.A., Sharma, A., Lattoo, S.K. (2018). In perspective: Potential medicinal plant resources of Kashmir Himalayas, their domestication and cultivation for commercial exploitation. Journal of Applied Research on Medicinal and Aromatic Plants 8:10–25.

Jensen, J. (2005). Introductory digital image processing: A remote sensing perspective. Pearson Prentice Hall. Third edition. USA.

Jones, H. (2004). Irrigation scheduling: Advantages and pitfalls of plant-based methods. Journal of Experimental Botany 55:2427–2436.

Jones, H. and Vaughan, R. (2010). Remote sensing of vegetation, principles, techniques, and applications. Oxford University Press. USA.

Kalamartzis, I., Menexes, G., Georgiou, P., Dordas, C. (2020). Effect of water stress on the physiological characteristics of five Basil (Ocimum basilicum L.) Cultivars. Agronomy 10: 1029. https://doi.org/10.3390/agronomy10071029.

Kandpal K., Kumar S., Venkat G., Meena R., Pal P., Kumar, A. (2021). Onsite age discrimination of an endangered medicinal and aromatic plant species Valeriana jatamansi using field hyperspectral remote sensing and machine learning techniques, International Journal of Remote Sensing 42(10): 3777-3796, DOI: 10.1080/01431161.2021.1881184.

Karnaris, I., and Asimopoulos, N. (2020). Overview of Aromatic Plants Precision Agriculture with the use of UAV. Proceeding of the 9th International Confernce on Information and Communication Technologies, Agriculture, Food and Environment (HAICTA, 2020), Thessaloniki, Greece, pages 24-27.

Khasawneh, A., Alsmairat, N., Othman, Y., Ayad, J., Al-Qudah T., Leskovar, D. (2021). Influence of nitrogen source on physiology, yield and fruit quality of young apricot trees. Journal of Plant Nutrition https://doi.org/10.1080/01904167.2021.1918718.

Khorasaninejad, S., Mousavi, A., Soltanloo, H., Hemmati, K., Khalighi, A. (2010).The effect of salinity stress on growth parameters, essential oil yield and constituent of peppermint (Mentha piperita L.). World Applied Sciences Journal 11 (11): 1403-1407.

Kovalskyy, V., Roy, D.P., Zhang, X. Y., et al., (2012). The suitability of multi-temporal web-enabled Landsat data NDVI for phenological monitoring—a comparison with flux tower and MODIS NDVI. Remote Sensing Letters 3: 325-334.

Leskovar, D. and Othman Y. (2018). Organic and conventional farming differentially influenced soil respiration, physiology, growth and head quality of artichoke cultivars. Journal of Soil Science and Plant Nutrition 18 (3), 865-880.

Leskovar, D. and Othman, Y. (2016). Low nitrogen and fertigation practices can improve artichoke transplant quality and yield. HortScience 51(5):567-572. https://doi.org/10.21273/HORTSCI.51.5.567.

Leskovar, D. and Othman, Y. (2019). Nitrogen management for improving root and shoot components of young 'Arbequina' Olives. HortScience 54(1):175-180. https://doi.org/10.21273/HORTSCI13397-18.

Leskovar, D. and Othman, Y. (2021). Direct Seeding and transplanting influence root dynamics, morpho-physiology, yield, and head quality of globe artichoke. Plants 10, 899. https://doi.org/10.3390/plants10050899.

Li, Y., He, N., Hou, J., Xu, L., Liu, C., Zhang, J., Wang, Q., Zhang, X., Wu, X. (2018). Factors influencing leaf chlorophyll content in natural forests at the biome scale. Frontiers in Ecology and Evolution 6:64. doi:10.3389/fevo.2018.00064.

Ligi, M., Kutser T., Kallio K, Attila J., Koponen S., Paavel B., Soomets T., Reinart A. (2017). Testing the performance of empirical remote sensing algorithms in the Baltic Sea waters with modelled and in situ reflectance data. Oceanologia 59: 57-68.

Liu, J., Pattey, E., Jégo, G. (2012). Assessment of vegetation indices for regional crop green LAI estimation from Landsat images over multiple growing seasons. Remote Sensing of Environment 123: 347–358. https://doi.org/10.1016/j.rse.2012.04.002.

Macarof, P., and Stătescu F. (2017). Identification drought extent based on NVSWI using Landsat data: a case study of Iași County. Lucrări Științifice 60:221-224.

Manesh, M.B., Khosravi, H., Alamdarloo, E. H., Alekasir, M. S., Gholami, A., Singh, V.P. (2019). Linkage of agricultural drought with meteorological drought in different climates of Iran. Theoretical and Applied Climatology 1–9.

Matsushita, B., Xu, M., Onda, Y., Otsuki, Y., Toyota, M. (2010). Detecting forest degradation in Kochi, Japan: ground-based measurements versus satellite (Terra/ASTER) remote sensing. Hydrological Processes 24:588–595.

McVicar, T. R. and Jupp, D. L. (1998). The current and potential operational uses of remote sensing to aid decisions on drought exceptional circumstances in Australia: A review. Agricultural Systems 57: 399-468.

Moran, M., Inoue Y. and Barnes E. (1997). Opportunities and limitations for image-based remote sensing in precision crop management. Remote Sensing of Environment 61:319-346.

Moses, W., Gitelson, A., Berdnikov, S., Povazhnyy, V. (2009). Estimation of chlorophyll-a concentration in case II waters using MODIS and MERIS data successes and challenges. Environmental Research Letters 4:1–8.

Naumann, J., Young, D., and Anderson, J. (2009). Spatial variations in salinity stress across a coastal landscape using vegetation indices derived from hyperspectral imagery. Plant Ecology 202: 285-297.

NDMC. (2021). Type of drought.National Drought Mitigation Center. University of Nebraska. Accessed, October 25, 2021, https://drought.unl.edu/Education/DroughtIn-depth/TypesofDrought.aspx.

Oran S. A. and Al-Eisawi D. M. (2015). Ethnobotanical survey for the medicinal plants in the high mountains of Jordan. Journal of Biodiversity and Environmental Sciences 6 (3), 381-400.

Ormeci, C., Sertel, E., Sarikaya, O. (2009). Determination of chlorophyll-a amount in golden Horn, Istanbul, Turkey using IKONOS and in situ data.Environmental Monitoring Assessment 155:83–90.

Othman, Y. (2014). Detecting moisture status of pecan orchards and the potential of remotely-sensed surface reflectance data. New Mexico State University, NM, USA.

Othman, Y. and Leskovar D. (2018). Organic soil amendments influence soil health, yield, and phytochemicals of globe artichoke heads, Biological Agriculture and Horticulture 34:4, 258-267. DOI:10.1080/01448765.2018.1463292.

Othman, Y. and Leskovar, D. (2019). Nitrogen management influenced root length intensity of young olive trees. Scientia Horticulturae 246:726–733.

Othman, Y. and St. Hilaire, R. (2021). Using multispectral data from Landsat ETM+ to estimate leaf area index of pecan orchards. Fresenius Environmental Bulletin 30:2613-2618.

Othman, Y., Al-Ajlouni, M., A'saf, T., Sawalhah, H., Bany Hani, M. (2021). Influence of gibberellic acid on the physiology and flower quality of gerbera and lily cut flowers. International Journal of Agriculture and Natural Resources 48(1): 21-33, http://dx.doi.org/10.7764/ijanr.v48i1.2218.

Othman, Y., Al-Ajlouni, St. Hilaire, R. (2019). Using hyperspectral surface reflectance data to detect chlorophyll content in pecans. Fresenius Environmental Bulletin 28(8): 6117-6124.

Othman, Y., Steele, C., St. Hilaire, R. (2018). Surface Reflectance Climate Data Records (CDRs) is a reliable Landsat ETM+ source to study chlorophyll content in pecan orchards. Journal of the Indian Society of Remote Sensing 46(2): 211–218.

Othman, Y., Steele, C., Van Leeuwen, D., St. Hilaire, R. (2015). Hyperspectral surface reflectance data used to detect moisture status of pecan orchards during flood irrigation. Journal of the American Society for Horticultural Science 140(5): 449-458.

Othman, Y., Van Leeuwen, D., Heerema, R., St. Hilaire, R. (2014a). Midday stem water potential values needed to maintain photosynthesis and gas exchange established for pecans. Journal of the American Society for Horticultural Science 139(5): 537–546.

Othman, Y., Steele, C., Van Leeuwen, D., Heerema, R., Bawazir, S., St. Hilaire, R. (2014b). Remote sensing used to detect moisture status of pecan orchards grown in a desert environment. International Journal of Remote Sensing 35(3): 949-966.

Pavarini, D. P., Pavarini, S. P., Niehues, M., Lopes, N. P. (2012). Exogenous influences on plant secondary metabolite levels. Animal Feed Science and Technology 176(1-4): 5–16.

Pirzad, A., Shakiba, M., Zehtab-Salmasi, S., Mohammadi, S., Darvishzadeh, R., Samadi, A. (2011). Effect of water stress on leaf relative water content, chlorophyll, proline and soluble carbohydrates in Matricaria chamomilla L. Journal of Medicinal Plants Research 5(12): 2483-2488.

Pu, R., Ge, S., Kelly, N., Gong, P. (2003). Spectral absorption features as indicators of water status in coast live oak (Quercus agrifolia) leaves. International Journal of Remote Sensing 24:1799–1810.

Qarallah, B., Al-Ajlouni, M., Al-Awasi, A., Alkarmy, M., Al-Qudah, E., Bani Naser, A., Al-Assaf, A., Gevaert, C., Al Asmar, Y., Belgiu, M., Othman, Y. (2021). Evaluating post-fire recovery of Latroon dry forest using Landsat ETM+, unmanned aerial vehicle and field survey data. Journal of Arid Environments 193:104587.

Qu, Y., Zhu, Y., Han, W., Wang, J., Ma, M. (2014). Crop leaf area index observations with a wireless sensor network and its potential for validating remote sensing products. IEEE Journal of Selected Topics in Applied Earth Observations and Remote Sensing 7:431–443.

Razmjoo, K. P., Heydarizadeh, Sabzalian, M. R. (2008). Effect of salinity and drought stresses on growth parameters and essential oil content of Matricaria chamomila, International Journal of Agriculture and Biology.

Rocha, J., Perdigão, A., Melo, R., et al. (2012). Remote sensing based crop coefficients for water management in agriculture. In: Curkovic, S. Sustainable Development—Authoritative and Leading Edge Content for Environmental Management 167-192.

Rousta, I., Olafsson, H., Moniruzzaman, M., Zhang, H., Liou, Y., Mushore, T.D., Gupta, A. (2020) Impacts of drought on vegetation assessed by vegetation indices and meteorological factors in Afghanistan. Remote Sensing 12: 2433. https://doi.org/10.3390/rs12152433.

Roy, D. P., Wulder, M. A., Loveland, T. R., et al. (2014). Landsat-8: Science and product vision for terrestrial global change research. Remote Sensing of Environment 145: 154-172.

Ryu, J., Han, K., Lee, Y., Park, N., Hong, S., Chung, C., Cho, J. (2019). different agricultural responses to extreme drought events in neighboring counties of south and north Korea. Remote Sensing 11:1773. https://doi.org/10.3390/rs11151773.

Santos, C., Lorite, J., Tasumi, M., Allen, R., Fereres, E. (2008). Integrating satellite-based evapotranspiration with simulation models for irrigation management at the scheme level. Irrigation Science 26(3):277–288.

Sawalhah, M., Al-Kofahi, S., Othman, Y., Cibils, A. (2018). Assessing rangeland cover conversion in Jordan after the Arab spring using a remote sensing approach. Journal of Arid Environments 157:97–102.

Sawalhah, M., Othman, Y., Abu Yahya, A., Al-Kofahi, S., Al-Lataifeh, F., Cibils, A. (2021). Evaluating the influence of COVID-19 pandemic lockdown on Jordan Badia rangelands, Arid Land Research and Management, 35: 483–495, DOI: 10.1080/15324982.2021.1921071.

Seneviratne, S. I., Nicholls, N., Easterling, D. C., Goodess, M., Kanae, S., Kossin, J., Luo, Y., Marengo, J., McInnes, K., Rahimi, M., Reichstein, M., Sorteberg, A., Vera, C., Zhang, X. (2012). Changes in climate extremes and their impacts on the natural physical environment. Cambridge, UK, and New York, NY, USA, pp. 109-230.

Sharma, T., Kaur, A., Saajan, S., Thakur, R. (2020). Effect of nitrogen on growth and yield of medicinal plants: A review paper. European Journal of Molecular and Clinical Medicine 7: 2771-2776.

Soudani, K., Francois, C., Maire, G., Dantec, V., Dufrene, E. (2006). Comparative analysis of IKONOS, SPOT, and ETM+ data for leaf area index estimation in temperate coniferous and deciduous forest stands. Remote Sensing of Environment 102:161–175.

Suárez, L., Zarco-Tejada, P. J., Sepulcre-Cantó, G., Pérez-Priego, O., Miller, J.R., Jiménez-Muñoz, J.C., Sobrino, J. (2008). Assessing canopy PRI for water stress detection with diurnal airborne imagery. Remote Sensing of Environment 112: 560–575.

Tadros, M. J., Al-Mefleh, N., Othman, Y., Al-Assaf, A. (2021). Water harvesting techniques for improving soil water content, and morpho-physiology of pistachio trees under rainfed conditions. Agricultural Water Management 243: 106464. https://doi.org/10.1016/j.agwat.2020.106464.

Tadros, M.J., Al-Assaf, A., Othman, Y.A., Makhamreh, Z., Taifour, H. (2020). Evaluating the effect of Prosopis juliflora, an alien invasive species, on land cover change using remote sensing approach. Sustainability 12:5887, https://doi.org/10.3390/su12155887.

Tahat, M., Alananbeh, K., Othman, Y., Leskovar, D. (2020). Soil health and sustainable agriculture. Sustainability 12: 4859. https://doi.org/10.3390/su12124859.

Tanga, M., Lewu, F., Oyedeji, O., Oyedeji, O. (2018). Cultivation of medicinal plants in South Africa: A solution to quality assurance and consistent availability of medicinal plant materials for commercialization. Academia Journal of Medicinal Plants 6: 168-177.

Tardieu, F., Simonneau, T., Muller, B. (2018). The physiological basis of drought tolerance in crop plants: A scenario-dependent probabilistic approach. Annual Review of Plant Biology 69: 733–759.

Tátrai, Z., Sanoubar, R., Pluhár, Z., Mancarella, S., Orsini, F., Gianquinto, G. (2016). Morphological and physiological plant responses to drought stress in Thymus citriodorus. International Journal of Agronomy, 4165750: 8 https://doi.org/10.1155/2016/4165750.

Tezara, W., Mitchell, V., Driscoll, S., Lawlor, D. (1999). Water stress inhibits plant photosynthesis by decreasing coupling factor and ATP. Nature 401: 914-917.

Thenot, F., Methy, M., Winkel, T. (2002). The Photochemical Reflectance Index (PRI) as a water-stress index. International Journal of Remote Sensing 23(23): 5135–5139.

Treitz, P., Thomas, V., Zarco-Tejada, P., Gong, P., Curran, P. (2010). Hyperspectral remote sensing for forestry. American Society for Photogrammetry and Remote Sensing (ASPRS). USA.

Trenberth, K.E., Dai, A., van der Schrier, G., Jones, P. D., Barichivich, J., Briffa, K. R., Sheffield, J. (2014). Global warming and changes in drought. Nature Climate Change 4: 17–22. DOI: 10.1038/nclimate2067.

UNDRR, 2021. United Nations Office for Disaster Risk Reduction. GAR Special Report on Drought 2021. Geneva. Accessed October 26, 2021, https://www.undrr.org/publication/gar-special-report-drought-2021.

Van Lanen and Peters, E. (2000). Definition, Effects and Assessment of Groundwater Droughts. In Vogt, J., Somma, F.Drought and drought mitigation in Europe. Pages 49-61.

Warren, C., Bleby, T., Adams, M. (2007). Changes in gas exchange versus leaf solutes as a means to cope with summer drought in Eucalyptus marginata.Oecologia 154:1–10.

WB. 2021. The world bank. climate-smart agriculture. accessed September 3, 2021. https://www.worldbank.org/en/topic/climate-smart-agriculture.

Whitcraft A.K., Vermote E.F., Becker-Reshef I., Justice C.O. (2015). Cloud cover throughout the agricultural growing season: impacts on passive optical earth observations. Remote Sensing of Environment 156: 438-447.

Wilhite, D.A., Glantz, M. (1985). Understanding the drought phenomenon: The role of definitions. Water International 10(3):111–120.

Wu, D., Qu, J. J., Hao, X. (2015). Agricultural drought monitoring using MODIS-based drought indices over the USA Corn Belt. International Journal of Remote Sensing 36: 5403–5425.

Xie, C., Song, J., Suo, F., Li, X., Li, Y., Yu, H., Xu, X., Luo, K., Li, Q., Xin, T., Guan, M., Xu, X., Miki, E., Takeda, Q., Chen, S. (2014). Natural resource monitoring of Rheum tanguticum by multilevel remote sensing. Evidence-Based Complementary and Alternative Medicine 618902: 9 https://doi.org/10.1155/2014/618902.

Yang, W., Tan, B., Huang, D., Rautiainen, M., Shabanov, N., Wang, Y., Privette, J., Huemmrich, K., Fensholt, R., Sandholt, I., Weiss, M., Ahl, D., Gower, S., Nemani, R., Knyazikhin, Y., Myneni, R. (2006). MODIS leaf area index products: from validation to algorithm improvement. IEEE Transactions on Geosciences and Remote Sensing 44:1885–1897.

Yurekli, K. and Kurunc, A. (2004). Simulation of drought periods using stochastic models. Turkish Journal of Engineering and Environmental Sciences 28:181–190.

Zaid, A., Ahmad, B., Wani, S.H. (2021) Medicinal and Aromatic Plants Under Abiotic Stress: A Crosstalk on Phytohormones' Perspective. In: Aftab T., Hakeem K.R. (eds) Plant Growth Regulators. Springer, Cham. https://doi.org/10.1007/978-3-030-61153-8_5.

Zargar, A., Sadiq, R., Naser, B., Khan, F. I. (2011). A review of drought indices. Environmental Reviews 19: 333–349. DOI: 10.1139/a11-013.

Zhang, X., Friedl, M. A., Schaaf, C. B., et al. (2003). Monitoring vegetation phenology using MODIS. Remote Sensing of Environment 84: 471-475.

Zhang, X., Wu, S., Yan, X., Chen, Z. (2017). A global classification of vegetation based on NDVI, rainfall and temperature. International Journal of Climatology 37: 2318–2324.

JJEES

Jordan Journal of Earth and Environmental Sciences

JJEES (2022) 13 (2): 114-121
ISSN 1995-6681

# Ecotoxicological Consequences and Hyper-accumulative Potentials of Beans (Phaseolus vulgaris) Exposed to Heavy Metals Spiked in Native Soils

Doris Fovwe Ogeleka*[1] and Gloria Omorowa Omoregie[2]

[1]*Department of Chemistry, Federal University of Petroleum Resources, Effurun, Delta State, Nigeria*
[2]*Department of Environmental Management and Toxicology, Federal University of Petroleum Resources, Effurun, Delta State, Nigeria*

*Received 29 March 2021; Accepted 20 January 2022*

**Abstract**

Heavy metals from anthropogenic sources in Nigeria are daily on the increase. This research was to ascertain the adverse effects of cadmium, zinc, and lead on the morphology of beans (*Phaseolus vulgaris*) with a secondary aim to evaluate the hyper-accumulative potentials of the plant. Bean seeds were planted in cadmium, zinc, and lead spiked soil with a heavy metal concentration in the soil was 0.1 mg/kg, 1.0 mg/kg, and 10 mg/kg respectively. The control experiment consisted of beans seed grown in metal-free soil. Metals in the soil were significantly reduced in the various treatment groups indicating uptake of metals by the plant. Morphological response to this environmental stress indicated that the leaves of some of the exposed concentrations showed necrosis, chlorosis, and reduced root, length, especially in the higher concentrations. Plant height, leaf an area, leave a number, and senescence were indicators used to measure morphological response to heavy metal stress. *Phaseolus vulgaris* is capable of metal uptake, and the highest concentration from the soil was recorded in Zn (32%) while the highest metal accumulation/bioaccumulation factor (BAF) was 0.206 ± 0.042. This capacity was indicative of hyperaccumulation potential.



**Keywords:** *Phaseolus Vulgaris*, Heavy Metals, Hyper-Accumulative Potential, Natural Soils.

## 1. Introduction

In most conurbations in the world, there is a great risk of chemical contamination, especially in peri-urban settlements due to intensive anthropogenic processes and actions. Sometimes, the environmental bodies (soils, sediments, water, etc.) within the region of organizations can be contaminated with metals namely from batteries (Cd, Pb, Zn), paint (Pb), steel (Zn), wires (Cu), crude oil gas flaring (heavy metals) and waste disposal (Kacholi and Sahu, 2018).In addition, the utilization of untreated sewage and wastewater for irrigation could discharge effluents containing heavy metals which could lead to the absorption of these metals by plants (Ogeleka *et al*., 2018).

Exposure of metals to humans could occur through various pathways, including inhalation of air, and ingestion through food, water, soil, or dust. The high concentration of heavy metals in the environmental bodies is of great concern because they are recalcitrant and could bioaccumulate in organisms along the food chains with disastrous consequences on the environment and human health (Ikhajiagbe *et al*., 2014). To this end, metals in the environment above recommended levels can increase the risk of illness and death among consumers of items (food, water, etc.) as in the case of Itai-Itai disease caused by consuming rice containing excess cadmium concentrations and poisoning from other sources (Kobayashi 2006). Chronic ailments and consequences resulting from contact with heavy metals include cancer and organ (heart and kidney) malfunction, diseases, seizures, mental retardation, behavioral disorders among others (Santos *et al*., 2006). In addition, soil polluted with heavy metals can impact toxic consequences on sensitive organisms (Ogeleka *et al*., 2016).

The most common heavy metal contaminants include copper, cadmium, lead chromium, and zinc. Metals are natural components in soil; however, due to the toxicity trace metals may impact, it is important to use phytoremediation to remove the excess amount from the environment and eliminate the risk to humans/environment from the damaging consequences. Soil washing, burning, and excavation is engineering techniques used to remediate heavy metal contaminated soil; however, the techniques are cost-intensive and time-consuming with lots of damage to the soil structure and soil-dwelling organisms (Pilon-Smits and Freeman, 2006). For this reason, the development of low-cost, effective, and sustainable technologies to remediate heavy metal contaminated soils is very important and had been given considerable attention (LeDuc and Terry, 2005). The phytoremediation process can be divided into different classes namely, phytostabilisation, phytostimulation / rhizodegradation, phytovolatilization, phytodegradation, and phytoextraction (Pilon-Smits and Freeman, 2006). Several plants have been widely used for removing contaminants from environmental bodies and some have achieved success recorded (Cho-Ruk *et al*., 2006). Phytoremediative plants also suffer some level of phytotoxic impacts of the remediated heavy metal. These plants first show a significant level of

* Corresponding author e-mail: dorysafam@yahoo.com

tolerance to the accumulated metal (Ikhajiagbe, 2016). In the present study, the capacity for phytoremediation of selected metal by *Phaseolus vulgaris* is investigated vis-à-vis its morphological adaptive capacities.

## 2.0 Materials and Methods

### *2.1 Study Area*

The sample location is in Ugbomro, a community in Effurun, Delta State, Nigeria. The community houses the Federal University of Petroleum Resources, Effurun (FUPRE). The surrounding towns in Effurun include Ekpan, Enerhen, Edjeba, Ogunu, Jakpa, Ovwian-Aladja, and Udu. Anthropogenic activities in this region include but are not limited to gas flaring, refinery, acid rain/ precipitation, farming, fishing and burning of wood, fossil fuels, commercial, and so on. The area is characterized by a tropical equatorial climate with a mean annual temperature of 32.8°C and rainfall amount of 3000 mm. The rainfall period ranges from January to December. However, double rain maxima between the months of July and September are observed. There is a little dry spell in the month of August called — August break. Convectional type of rainfall is predominant in the city (Figure 1) (Ojeh, 2011).

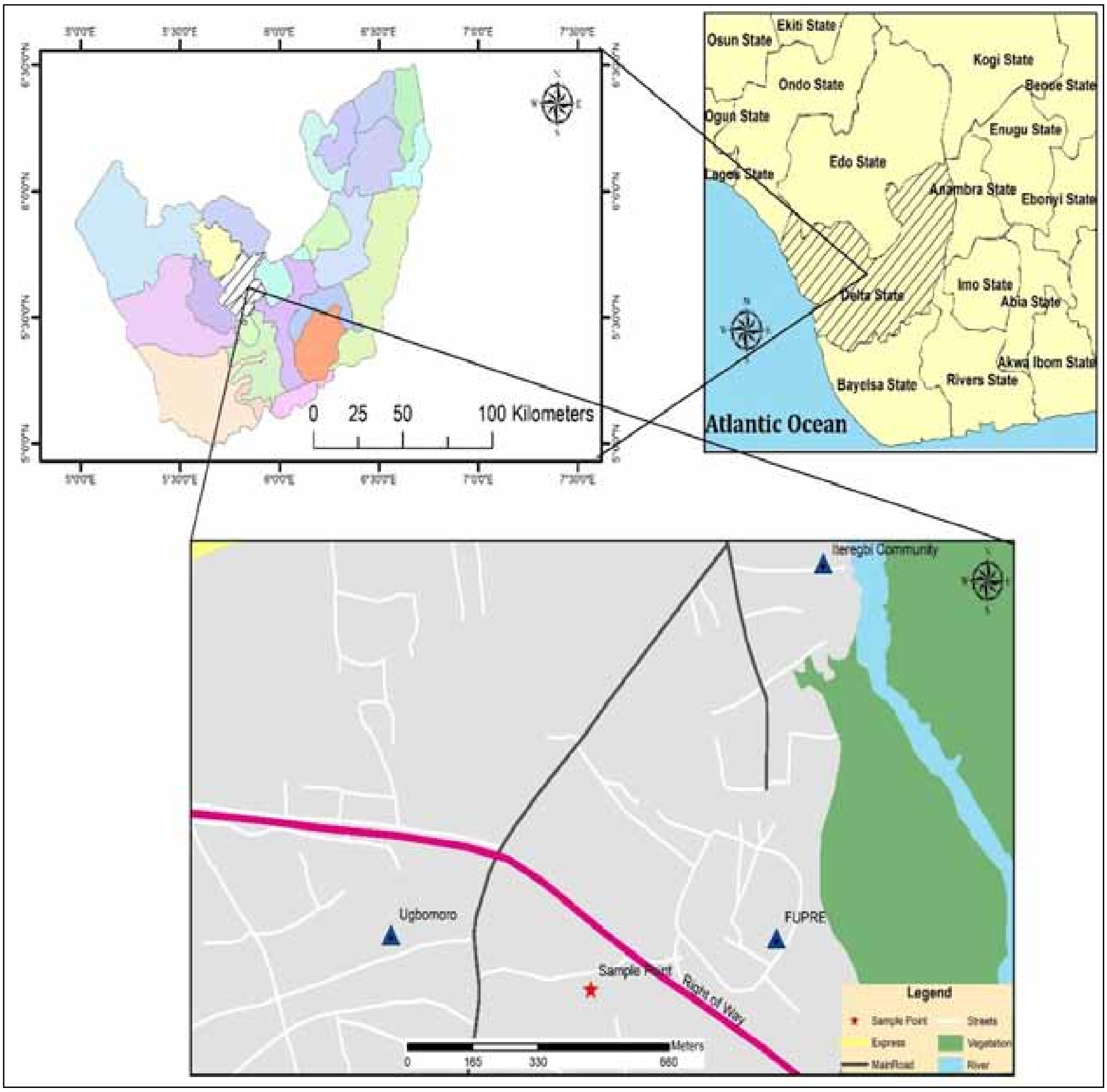


**Figure 1.** Map of the study area.

### *2.2 Soil Sampling*

The native (indigenous) soil samples used for the study were randomly collected from farm sites in the Federal University of Petroleum Resources, Effurun Delta State, Nigeria. The soil samples were taken from the surface and the first sub-surface horizon (0 – 30 cm). After collection, objects such as dead weeds, stems, leaves, sticks, and stones were carefully removed, and the soil samples were transferred into labeled aluminum foils/containers in the laboratory. The uncontaminated soils were kept for planting and analysis of the different components needed for the experimental bioassay procedure and analysis.

### *2.3 Chemical preparation*

Cadmium, lead, and zinc metals of Analar grade were used for the toxicity assessment. Pre-determined amounts of the test compounds were weighed, dissolved in a small quantity of deionized water, and the solution made up to a fixed volume by adding an appropriate volume of deionized water as diluents to achieve a stock solution of 1000 mg/L of Cd, Pb, and Zn. The resultant stocks were then serially diluted to obtain solutions of the required concentrations of the various metals used for the experiment.

**2.4 Test specie -*Phaseolus vulgaris***

A healthy seedling of the test specie was obtained from the International Institute of Tropical Agriculture (IITA), Ibadan, Nigeria. Before the experiment, the seedlings were wetted approximately 24 hours before planting and three seedlings per test tank were planted.

***2.5 The Physico-chemical properties of soils used for the study***

The soils used in planting the test toxicants were assessed before they were used for the photo-toxicity experiment. The Physico-chemical analysis determined includes soil pH, total organic carbon (TOC), soil texture, particle size, moisture content, and heavy metals (cadmium, lead, and zinc).

**Table 1.** Specific soil quality parameters and methods used for the study

| Parameters | Analytical Methods |
|---|---|
| pH | pH, (APHA 4500 $H^+$), APHA, 2017 |
| Total organic content (%) | Walkey Black, 1937 |
| Metals (Cd, Pb, and Zn) | Extraction and Atomic Absorption Spectrophotometer (Shimazu 6701 F model) |
| Soil texture | (IITA, 1984) |
| Soil particle size | (IITA, 1984) |
| Moisture content | Gravimetry |
| Water holding capacity | Gravimetry |

***2.6 Experimental bioassay procedure for the hyper-accumulation of Phaseolus vulgaris***

The experimental procedure was carried out for 90 days using the Organization for Economic Co-operation and Development, (OECD) protocol #208 (OECD, 2003). From the prepared stock solutions of the test chemicals, serial dilutions were made to obtain concentrations in the range of 10 mg/L (0.001%), 1.0 mg/L (0.0001%), and 0.1 mg/L (0.00001%) of Cd, Pb, and Zn. When these concentrations were spiked with 1.0 kg of natural soil, the resultant concentrations were 10mg/kg, 1.0 mg/kg, and 0.1 mg/kg of Cd, Pb, and Zn, respectively.

Ten kg (10 kg) of uncontaminated soil samples were accurately weighed into large containers and the soil samples were spiked with 850 mL of the test toxicants. Seeds of the test plants were sown in the soils spiked with metals at 5 different concentrations of the heavy metals each treatment was replicated 5 times. The control setup was prepared in conjunction with the test metals as described above except that the seedlings were planted on a clean substrate and sprinkled with 800mL of water (i.e., without the toxicants) after being homogenized. Daily or every other day 100 mL of the toxicants were irrigated into the treatment tanks and the control was based on the water holding capacity of the soil. Observations for germination, leaves, stem, and root were taken daily / weekly depending on the parameter. Similarly, soil samples were randomly collected and analyzed for individual metal residues for the hyper-accumulative endpoint assessment and other ecological effects.

***2.7 Heavy metal analyses***

Two (2) g of sieved air-dried soil and plant samples (air-dried plant leaves) was digested in a mixture of 7 mL concentrated nitric acid ($HNO_3$) and 2 mL sulphuric acid ($H_2SO_4$). Digestion was done on a hot plate and continued until brown fumes of nitric acid were no longer seen. When white fumes started coming out the heat was turned off. The solution was cooled, and the filtrate was made up to the mark in a volumetric flask of 100 mL with double distilled water. The level of the metals (cadmium, lead, and zinc) was estimated with a Flame Atomic Absorption Spectrophotometer (AAS) with a Shimadzu 6701F model.

***2.8 Leaf Area***

By multiplying leaf length by leaf width with a correlation coefficient (r) of 0.72, the leaf area (LA) was calculated according to the methods of Hoyt and Bradfield, (1962) and Udo and Oputa, (1984).

***2.9 Bioaccumulation factor (BAF)***

The ability of specie to bioaccumulate toxicants from a medium can be estimated using the BAF, which is given as the ratio of metal concentration in the specie (e.g., plant) to that in the medium (soil). This can be used to determine the extent of hyperaccumulation of the plant. Bio-concentration factor of metal in the plant was calculated with the formula below:

$$BAF = \frac{\text{Metal concentration in plant}}{\text{metal concentration in soil}}$$

***2.11 Statistical analysis***

All experiments were conducted in triplicate and used for the calculation of the mean of the various endpoints including germination, plant height, leaves number, stem girth, and metal levels. The statistical analysis was performed to obtain the significant variation between the treated and untreated groups at a probability level of 5%. In addition, bar, line, and XY-scattered graphs were used to depict the various endpoint parameters.

## 3.0 Results

Tables 2–6 and Figures 2–5 described the results of *Phaseolus vulgaris* exposed to varying concentrations of cadmium, lead, and zinc spiked in natural soils for a period of 7 weeks. Plant height, leave length (area), leave number, stem girth, and senescence were assessed to monitor the morphological response of plant species. Chlorosis, necrosis, and growth retardation (inhibition) were observed daily and weekly depending on the parameter.

**Table 2.** Physico-chemical properties of natural soil quality used for the study

| Parameter | Results |
|---|---|
| pH | 5.79 ± 0.23 |
| Total organic content (TOC), (%) | 0.49 ± 0.01 |
| Cation exchange capacity (CEC), (meq/L) | 1.353 |
| Soil texture | Sand |
| Sand (%) | 86.24 |
| Clay (%) | 9.20 |
| Silt (%) | 4.56 |
| Moisture content, (%) | 1.29 ± 0.20 |
| Water holding capacity, (%) | 7.83 ± 0.12 |
| Cadmium (mg/kg) | <0.001 |
| Lead (mg/kg) | <0.001 |
| Zinc (mg/kg) | <0.001 |

***3.1 Growth Retardation***

For the period under study, growth was more inhibited at the higher concentrations of 10 mg/kg than the lower concentrations of 1.0 and 0.1 mg/kg. Similarly, there was reduced root length at the higher concentration. Although there was measurable growth in all the concentrations, the heavy metals were reduced in the various treatment groups.

***3.2 Necrosis***

Morphological studies indicated that the leaves of some of the exposed concentrations showed necrosis, a condition when a biological species' cells degenerate and die. Plants affected show signs of change in coloration (green to yellow to brown) as was observed at the higher concentrations of heavy metals exposure in this assessment (Figure 2).

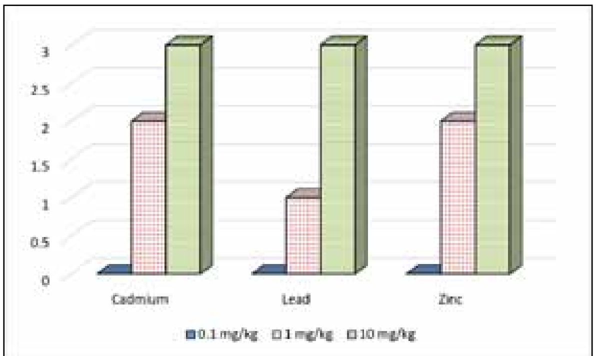


**Figure 2.** Mean results of the effect of heavy metals on necrosis of *Phaseolus vulgaris*

***3.3 Chlorosis***

The results also indicate that the leaves of some of the exposed concentrations showed chlorosis. Chlorosis, is a condition involving the yellowing of the leaf tissue due to a lack of chlorophyll. Chlorophyll is responsible for the green coloration of the leaves. Some of the chlorotic leaves observed in this research were pale, yellow, or yellow white. There was yellowing in the highest heavy metal exposures (Figure 3).

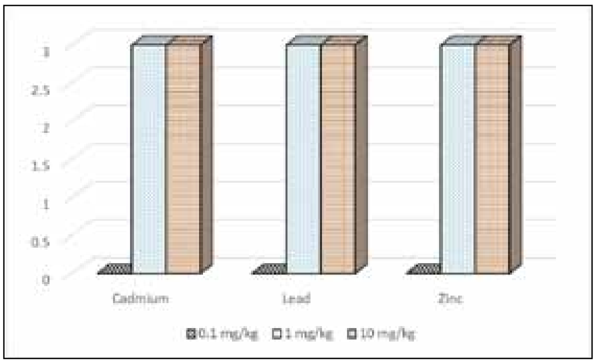


**Figure 3.** Mean results of the effect of heavy metals on chlorosis of *Phaseolus vulgaris*

***3.4 Plant Height***

The plant height is a measure from the soil level to the terminal leaf. At the end of the experiment, the mean results for control were 89.4 ± 5.6 cm, Cd in soil was52.6 ± 4.9 cm, 33.2 ± 4.2 cm, 13.5 ± 2.9 cm for the control, 0.1, 1, and 10 mg/kg respectively. Also, the mean value of Pb was57.6 ± 2.4 cm, 37.1 ± 7.2 cm, and 19.0 ± 3.2 cm in the respective concentrations. Furthermore, Zn was62.4 ± 4.1 cm, 38.0 ± 0.9 cm, 19.0 ± 3.2cm in the respective order (Table 3). These results showed that the plant height of *Phaseolus vulgaris* was greatly affected by metal concentration (the higher concentration of heavy metal resulted in a decrease in plant height).

***3.5 Leaf Area***

The results for the leaf area for *Phaseolus vulgaris* seedling revealed 51.3 ± 6.4 cm$^2$ in the control, while the average concentration of Cd in soil was 41.6 ± 7.6 cm$^2$, 13.5 ± 2.9 cm$^2$, 16.4 ± 3.9 cm$^2$ for 0.1, 1 and 10 mg/kg respectively. Also, Pb values was44.2 ± 3.4 cm$^2$, 28.3 ± 8.1 cm$^2$, 17.0 ± 4.6 cm$^2$while Zn in soil had47.0 ± 0.9 cm$^2$, 25.1 ± 4.2 cm$^2$, 15.6 ± 0.1 cm$^2$in the order mentioned above (Table 4). These results showed a reduction when compared to the control.

**Table 3.** Mean weekly results of the effect of heavy metals on plant height of *Phaseolus vulgaris*

| TIME (Days) | | 7 | 14 | 21 | 28 | 35 | 42 | 49 |
|---|---|---|---|---|---|---|---|---|
| CONTROL | | 14.2 ± 0.4 | 20.3± 1.5 | 23.2± 3.5 | 31.4 ± 2.1 | 38.1 ± 4.3 | 42.3 ± 4.5 | 89.4 ± 5.6 |
| Cd | 0.1 mg/kg | 11.5 ± 3.8 | 16.9 ± 3.2 | 19.3 ± 3.0 | 26.9 ± 4.4 | 34.9 ± 5.4 | 46.3 ± 3.5 | 52.6 ± 4.9 |
| | 1 mg/kg | 10.8 ± 0.3 | 13.9 ± 6.2 | 17.6 ± 1.5 | 18.4 ± 2.4 | 23.9 ± 5.0 | 32.1 ± 2.4 | 33.2 ± 4.2 |
| | 10 mg/kg | 7.2 ± 1.3 | 10.3 ± 2.1 | 12.1 ± 1.4 | 12.4 ± 1.6 | 12.7 ± 1.4 | 13.2 ± 3.0 | 13.5 ± 2.9 |
| Pb | 0.1 mg/kg | 13.9± 2.0 | 16.7 ± 2.1 | 18.9± 3.2 | 23.1± 1.5 | 26.8± 1.7 | 44.0± 1.3 | 57.6± 2.4 |
| | 1 mg/kg | 11.6 ± 2.1 | 14.0 ± 3.0 | 17.3 ± 2.8 | 18.7 ± 3.4 | 23.9 ± 6.5 | 32.5 ± 6.2 | 37.1 ± 7.2 |
| | 10 mg/kg | 7.6 ± 1.7 | 11.2 ± 1.1 | 11.9 ± 1.9 | 12.3 ± 1.8 | 13.2 ± 1.3 | 13.9 ± 1.3 | 14.0 ± 1.3 |
| Zn | 0.1 mg/kg | 11.2 ± 1.3 | 17.3 ± 3.8 | 21.3± 4.2 | 28.9 ± 4.0 | 41.8± 3.8 | 56.3± 3.3 | 62.4± 4.1 |
| | 1 mg/kg | 9.4± 0.7 | 13.5 ± 1.8 | 16.0 ± 1.7 | 17.1 ± 3.1 | 26.6 ± 3.8 | 33.9 ± 3.1 | 38.0 ± 0.9 |
| | 10 mg/kg | 8.4 ± 1.3 | 10.4 ± 0.3 | 12.8 ± 1.9 | 14.2 ± 2.7 | 15.4 ± 2.8 | 16.3 ± 2.4 | 19.0 ± 3.2 |

**Table 4.** Mean weekly results of the effect of heavy metals on leaf area of *Phaseolus vulgaris*

| TIME (Days) | | 7 | 14 | 21 | 28 | 35 | 42 | 49 |
|---|---|---|---|---|---|---|---|---|
| Control | | 14.2 ± 2.1 | 19.2 ± 3.0 | 22.0 ± 3.0 | 26.5 ± 2.4 | 36.0 ± 3.6 | 43.6 ± 2.4 | 51.3 ± 3.4 |
| Cd | 0.1 mg/kg | 10.6 ± 2.1 | 16.0 ± 3.0 | 18.3 ± 3.8 | 22.3 ± 2.4 | 28.3 ± 2.6 | 40.5 ± 3.2 | 41.6 ± 2.6 |
| | 1 mg/kg | 8.7 ± 0.8 | 12.2 ± 2.2 | 15.9 ± 2.8 | 17.1 ± 1.8 | 17.6 ± 3.3 | 18.2 ± 0.2 | 20.6 ± 3.6 |
| | 10 mg/kg | 7.6 ± 0.3 | 9.6 ± 1.7 | 11.8 ± 1.4 | 13.7 ± 3.7 | 15.4 ± 3.2 | 15.9 ± 2.4 | 16.4 ± 3.9 |
| Pb | 0.1mg/kg | 11.2 ± 3.1 | 17.3 ± 3.0 | 19.5 ± 2.8 | 21.3 ± 4.1 | 28.4 ± 3.3 | 40.6 ± 4.4 | 44.2 ± 3.4 |
| | 1 mg/kg | 10.3 ± 0.9 | 14.7 ± 3.9 | 16.7 ± 3.0 | 17.5 ± 2.8 | 20.3 ± 3.1 | 22.4 ± 2.3 | 28.3 ± 3.1 |
| | 10 mg/kg | 10.3 ± 0.7 | 10.9 ± 2.4 | 12.7 ± 1.3 | 13.7 ± 2.5 | 15.0 ± 1.9 | 15.3 ± 3.2 | 17.0 ± 2.6 |
| Zn | 0.1mg/kg | 12.6 ± 1.7 | 18.1 ± 5.4 | 20.8 ± 2.8 | 23.0 ± 2.7 | 26.6 ± 2.8 | 44.9 ± 0.2 | 47.0 ± 0.9 |
| | 1 mg/kg | 11.8 ± 0.3 | 15.5 ± 2.8 | 17.0 ± 2.7 | 20.0 ± 2.2 | 22.1 ± 1.2 | 22.5 ± 2.7 | 25.1 ± 4.2 |
| | 10 mg/kg | 8.6 ± 1.5 | 12.4 ± 2.1 | 13.0 ± 2.4 | 14.1 ± 1.6 | 14.6 ± 1.1 | 14.8 ± 3.7 | 15.6 ± 0.1 |

### 3.6 Leaf Number

The number of leaves was determined by visual counting of the number of leaves per seedling per treatment. The results at day 7 for each treatment was 2 ± 0.0, 2 ± 0.0, 2 ± 0.0, 0.0 ± 0.0 for the 0.1, 1 and 10 mg/kg respectively except for the control which showed 5 ± 0.0. These results showed the emergence of the first leaf at the same interval, however, as the days progressed there was variation amongst treatments. At the end of the experiment, the results varied for the different concentrations - control was 26 ± 1.4, Cdwas20 ± 2.1, 17± 2.5, 15 ± 0.7 respectively, While Pb was20 ± 4.3, 18 ± 0.9, 16 ± 3.2, Zn was20 ± 4.6, 19 ± 1.0, 17 ± 2.1in the above-mentioned order, the results could be due to the likely effect of the metals on the plants (Figure 4).

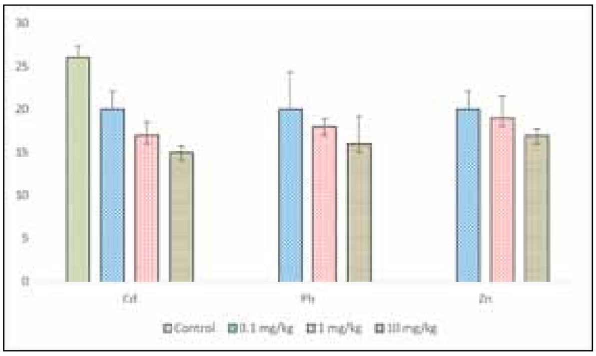


**Figure 4.** Effect of heavy metals on leaf number of P*haseolus vulgaris* at 49 days

### 3.7 Senescence

The number of senescence leaves was determined by visual counting of the number of dead leaves per seedling per treatment. At the end of the experiment (49 days), the results varied for the different concentrations. The control was 0.0 ± 0.0, Cd was 7.3 ± 2.1, 8.0 ± 0.0, 12 ± 1.2, Pb was 3.7 ± 2.9, 8.5 ± 0.7, 8.8 ± 1.4 while Zn was 3.5 ± 0.1, 7.0 ± 4.2, 7.4 ± 1.3 for 0.1, 1 and 10 mg/kg respectively (Figure 5).

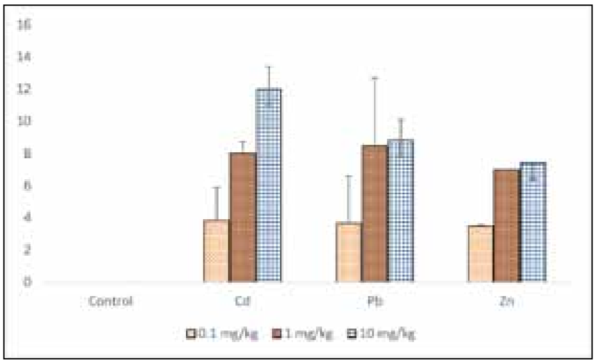


**Figure 5.** Effect of heavy metals on senescence of *Phaseolus vulgaris* at test termination

### 3.8 Residual concentration in soil and uptake in plant

The exposed plants' accumulated metals from the soil for the period under study as indicated in Table 5.

### 3.9 Bioaccumulation factors (BAFs) of heavy metals in the plant

Significant differences were found in the BAF of heavy metals in the exposed plants. The order of the heavy metal (Zn, Pb, Cd) for BAF was similar to that obtained for the metal concentrations in plants (Figure 6). There was a significant difference at a probability value of 5% between the control samples and the exposed samples.

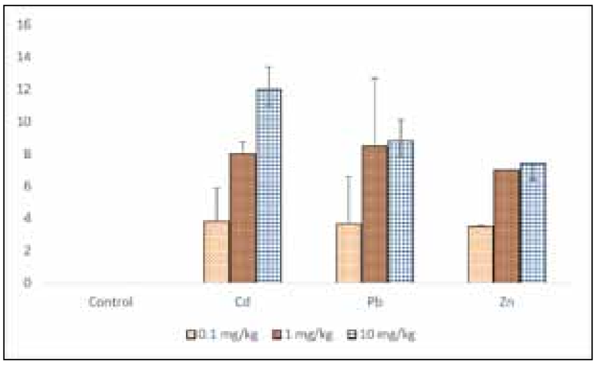


**Figure 6.** Bioaccumulation factors (BAFs) of heavy metals in different accessions. Error bars indicate the standard error of five replicates.

**Table 5.** Mean results of heavy metal in soil and plant at test termination

| | Residual concentration in soil (mg/kg) | | | Uptake in plant leaves (mg/kg) | | | Removal of heavy metal (%) | | |
|---|---|---|---|---|---|---|---|---|---|
| Test concentration (mg/kg) | Cd | Pb | Zn | Cd | Pb | Zn | Cd | Pb | Zn |
| 0.1 | 0.079 ± 0.001 | 0.072 ± 0.001 | 0.068 ± 0.003 | 0.0108 | 0.012 | 0.014 | 21 | 28 | 32 |
| 1.0 | 0.837± 0.06 | 0.79 ± 0.04 | 0.73 ± 0.02 | 0.065 | 0.079 | 0.083 | 16 | 21 | 27 |
| 10 | 8.85 ± 0.60 | 8.55 ± 1.2 | 8.4± 0.51 | 0.59 | 0.62 | 0.71 | 11.5 | 14.5 | 16 |

## 4. Discussion

The growth of plants and their life cycles are associated with survival, and this is used to assess the potential of plants to grow in contaminated soil (Spiares *et al.,* 2001). The survival of plants on contaminated soils may be ascribed to several factors that either help to reduce the effects of the contaminants by rendering them immobile (Ikhajiagbe *et al.,* 2017) or directly by accumulating the contaminants and stirring them in harvestable plant parts. The presence of microbes in the rhizosphere confers such capabilities (Nwoko *et al.,* 2007).

Heavy metals are among the environmental pollutants. Aside from natural activities, practically all human activities have the potential to produce heavy metals as byproducts. The migration of these contaminants into noncontaminated areas as dust or leachates through the soil, as well as the spread of heavy metals containing sewage sludge, are only a few instances of occurrences that contribute to ecosystem contamination.

Heavy metals are a type of pollutant that can be found in the environment. Aside from natural activities, practically every human activity has the potential to produce heavy metals as a byproduct. The spread of heavy metals containing sewage sludge and the migration of these contaminants into non-contaminated areas as dust or leachates through the soil are two examples of occurrences that contribute to ecosystem contamination.

Plants can endure relatively high concentrations of organic and inorganic chemicals without toxic effects, and they can take up and convert these contaminates swiftly to less toxic metabolites in some cases by rhizodegradation (Nwoko *et al.,* 2007). Like other plants, Phaseolus *vulgaris* have been previously reported to have the ability to accumulate metals in their roots and stem tissues with remarkably high tolerance to heavy metals (Malairajan *et al.,* 2015; Ohanmu et al., 2018). Elevated amounts of essential and non-essential heavy metals present in soils can result in toxic symptoms including growth retardation in most plants.

Transfer, translocation, and accumulation of toxicants (heavy metals) by plants can reduce the quality and quantity of viable species, which can lead to serious health hazards for humans who consume contaminated food along the food chain (Axtell *et al.,* 2003; Sathawara *et al.,* 2004).

During the last three decades, environmental degradation has gotten increasingly severe because of fast economic expansion. Soil degradation from hazardous organic chemicals and heavy metals would put enormous strain on an already fragile planet.

Because of its importance to humanity's sustainability and well-being, food security and safety have been designated as one of the most important sustainable goals. From the point of view of plant-based food security, a significant reduction would lead to a concomitant decrease in food availability. The capability of the *P. Vulgaris* to take up heavy metals reflects their tolerance capacities. Whereas some plants accumulate metals and do not show any phytotoxic symptoms; others are highly sensitive. Soil matrices naturally contain heavy metals; however, some anthropogenic, geologic, industrial, and agricultural practices increase the levels to the extent that they could cause deleterious effects on humans, flora, and fauna (Bonnail *et al.,* 2016). Sometimes, even when soils are naturally high in a certain metal, the plant may adapt over time to these elevated levels but with a limited amount of growth and other metabolic processes. Toxicity because of metal exposure usually occurs from repeated anthropogenic alterations and perturbation (Ata et al., 2009).

Plants need both essential macronutrients (N, P, K, S, Ca, and Mg) and essential micronutrients (Fe, Zn, Mn, Ni, Cu, and Mo) to grow and function. Plants have a specific capability to take up, translocate and store these required nutrients. The ability of a plant to remove metals from environmental matrices is limited by the plant's ability to take up and tolerate such an exposed amount. Trace metals can exact toxic effects (cytotoxic) at relatively low concentrations, even though only very few are needed for metabolic processes (Kabata-Pendias and Pendias, 2001). According to Linger *et al*., (2005) and Khan *et al*., 2015), metal toxicity reduces plant functions and growth, which could cause the death of the plant in extreme cases. Reduced growth due to exposure to heavy metals was reported in the study.

Although the report from the study showed a significant reduction in plant morphological parameters, most plants still show tolerance capacities. Heavy metal contaminated settings, according to Levitt (1980), act as stress factors on plants, causing physiological response changes that diminish or limit plant vigor and growth. A plant that has been injured or died as a result of metal stress is said to be sensitive to its surroundings. Resistant plants, on the other hand, can survive and reproduce in metal-stressed environments (Ernst *et al.,* 2008). Plants can withstand heavy metals in general by avoiding or tolerating them.

Plants use a variety of techniques to prevent metals from entering root tissue, which is known as avoidance. Plants can avoid metal uptake in circumstances where soil metal pollution is unevenly distributed by exploring less contaminated soil. Mycorrhizal fungi, which may stretch their hyphae up to many tens of meters outside the plant's rooting zone and transmit the necessary materials to the plant, are another avoidance method.

It becomes clear that different mechanisms of metal accumulation, exclusion, and compartmentation exist in various plant species; this may have accounted for the survival of *P. vulgaris* even when the exogenous elevation of soil Zn led to stunted growth presentation. In *T. caerulescens*, Zn is sequestered preferentially in vacuoles of epidermal cells in a soluble form (Frey *et al.,* 2000).

Most metals are too insoluble to flow freely in the vascular system once within the plant, thus they precipitate as carbonate, sulfate, or phosphate, which immobilizes them in apoplastic (extracellular) and symplastic (intracellular) compartments (Raskin *et al.,* 1997). The high cation exchange capacity of cell walls further limits apoplastic transport unless the metal ion is carried as a non-cationic metal chelate (Raskin *et al.,* 1997; 2000).

Non-essential heavy metals may compete efficiently for the same transmembrane transporters employed by necessary heavy metals, causing chlorotic and necrotic signs. Toxic heavy metals like cadmium may effectively compete with micronutrient heavy metals for the same transmembrane carrier. This lack of selectivity in transmembrane ion transport could help explain why non-essential heavy metals can still enter cells despite a concentration gradient. Kinetic studies, for example, show that necessary Cu2+ and Zn2+ fight for the same transmembrane carrier as non-essential $Cd^{2+}$ (Crowley et al., 1991). Metal chelate complexes can also be transported across the plasma membrane using specific carriers, as Fe–phytosiderophore transport in graminaceous species is (Cunningham and Berti, 1993).

## 5. Conclusion

The study corroborates previous reports on the phytotoxic impact of heavy metals growth and development of *Phaseolus vulgaris*. The study also suggested the ability of *P. vulgaris* to survive in the metal-contained media. This implies the need to ensure extreme care during crop husbandry.

## References

American Public Health Association/American Water Works Association/Water Environment Federation. 2017. Standard methods for the examination of water and wastewater. 23rd edn, Washington DC, USA.

Ata S., Farid M., and Soroush M. (2009). Heavy metal contamination and distribution in the Shiraz industrial complex zone soil, South Shiraz, Iran. World Applied Sciences Journal. 6(3): 413-425.

Axtell, N. R., Sternberg, S. P. K., Claussen, K., (2003). Lead and nickel removal using Microspora and Lemna minor, Bioresour. Technol. 89: 41-48.

Bonnail E., Sarmiento A.M., Del Valls T.A., Nieto J.M., Riba I (2016). Assessment of metal contamination, bioavailability, toxicity, and bioaccumulation in extreme metallic environments (Iberian Pyrite Belt) using Corbicula fluminea. Sci. Total. Environ. 544: 1031-1044,

Cho-Ruk K., Kurukote J., Supprung P., and Vetayasuporn S. (2006) "Perennial plants in the phytoremediation of lead-contaminated soils," Biotechnology. 5(1):1–4

Crowley, D.E., Wang, Y.C., Reid, C.P.P., and Szansiszlo, P.J. (1991). Mechanism of iron acquisition from siderophores by microorganisms and plants. Plant and Soil, 130: 179-198. Cunningham, S.C. and Berti, W.R. (2000). Phytoextraction and Phytostabilization: Technical, Economic, and Regulatory Considerations of the Soil-Lead Issue. In: Terry, N. and Banuelos, G. (eds.) Phytoremediation of Contaminated Soil and Water. Boca Raton, Florida, USA: Lewis Publishers; 2000. pp. 359–376.

Frey, B., Keller, C. and Zierold, K. (2000). Distribution of Zn in functionally different leaf epidermal cells of the hyperaccumulator Thlaspi caerulescens. Plant Cell Environment, 23: 675–687.

Hoyt, P. and Bradfield, R. (1962). Effect of the varying leaf by defoliation and plant density on dry matter production on corn. Agronomy Journal. 54: 523 – 525.

Ikhajiagbe. B. (2016). Possible adaptive growth responses of Chromolaenaodorata during heavy metal remediation. Ife Journal of Science 18(2): 403 – 411.

Ikhajiagbe, B., Oshomoh, E.O., and Esangbedo, O. (2014). Studies of bioconcentration of heavy metals on roadside plants used in local herbal medicine preparations in Edo State. Journal of Laboratory Science, 2(1): 54 – 61.

International Institute of Tropical Agriculture (IITA). (1984). Selected methods for soil and plant analysis. IITA press, Ibadan, Nigeria. Manual Series. 1: 10-50.

Kabata-Pendias, A. and Pendias H. (2001). Trace elements in soils and plants. 3rd Edn., CRC Press, Boca Raton, Florida, USA., pp 1-413.

Kacholi D.S and Minati Sahu M. (2018). Levels and health risk assessment of heavy metals in soil, water, and vegetables of Dar es Salaam, Tanzania. Journal of Chemistry. 2018. 1402674: 1-9.

Khan A., Khan S., Khan M., Qamar Z and Waqas M. (2015). The uptake and bioaccumulation of heavy metals by food plants, their effects on plants nutrients, and associated health risk: A review. Environmental Science and Pollution Research International. 22(18): 13772–13799.

Kobayashi I., Fujiwara S., Saegusa H., Inouhe M., Matsumoto H. and Tsuzuki M. (2006). Relief of arsenate toxicity by Cd-stimulated phytochelatin synthesis in the green alga Chlamydomonas reinhardtii. Mar. Biotechnol. (NY). 8: 94 – 101.

LeDuc D.L. and Terry N. (2005). Phytoremediation of toxic trace elements in soil and water. J Ind Microbiol Biotechnol. 32(11-12): 514-20.

Linger P., Ostwald A. and Haensel J. (2005). Cannabis sativa L. growing on heavy metal contaminated soil: growth, cadmium uptake and photosynthesis. Biol Plant. 49: 567–576.

Malairajan S., Tesso M. and Wondimu L. (2015). The use of plants for detoxification of heavy metals in polluted soils. Environmental Science an Idian Journal 10(7):254-259.

Nwoko C. O., Okeke P. N., Agwu O. O. and Akpan I. E. (2007). Performance of Phaseolus vulgaris L. in a soil contaminated with spent-engine oil African Journal of Biotechnology. 6(16): 1922-1925

Ogeleka D.F., Ugwueze V.I., OkieimenF.E. (2016). Ecotoxicological Assessment of Cadmium and Lead Exposure to Terrestrial Sentinels - Snails (Archachatina marginata). International Journal of Research in Chemistry and Environment. 6(4): 1-16.

Ogeleka D.F., Edjere O., Nmai O.O., Ezeogu P. and Okieimen F.E. (2018). Consideration of contamination status of soils within the vicinity of automobile workshops in Warri, Delta State, Nigeria. Science Journal of Chemistry. 6(4): 56-65.

Ohanmu, EO, Ikhajiagbe, B, and Anoliefo, GO (2018). Growth and yield respponses of African yam bean on cadmium contaminated growth medium. 2nd Annual Conf. and stakeholder forum of the Society for Underutilized Legumes, at Covenant University, Ota. 11-12 July 2018

Ojeh, V.N. (2011). Thermal Comfort Characteristics in Warri and Environs, Delta State, Nigeria, an unpublished M.Sc Dissertation in the Department of Geography and Regional Planning, Delta State University, Abraka.

Organization for Economic Co-operation and Development, (OECD). (2003). Environment, Health and Safety Publications Series on Pesticides Persistent, Bioaccumulative, and Toxic Pesticides in OECD Member Countries Results of Survey on Data Requirements and Risk Assessment Approaches., No. 15: p 1 – 67.

Pilon-Smits E.A.H. and Freeman J.L. (2006). Environmental cleanup using plants: biotechnological advances and ecological considerations. A review. Front Ecol Environ. 4(4): 203–210.

Raskin, I. and Ensley, B. D. (2000). Recent developments for in situ treatment of metal contaminated soils. In: Phytoremediation of Toxic Metals: Using Plants to Clean up the Environment. John Wiley and Sons incorporated, New York. Available at: http//clu – n. org/techfocus.

Raskin, I., Smith, R. D. and Salt, D. E. (1997). Phytoremediation of metals: Using plants to remove pollutants from the environment. Current Opinion in Biotechnology 8: 221 – 226.

Santos E.E., Lauri D.C. and Silveira P.C.L., (2006). Assessment of daily intake of trace elements due to consumption of food stuffs by adult inhabitants of Rio de Janeiro city. Science of the Total Environment. 327: 69–79.

Sathawara N.G., Parikh D.J. and Agarwal Y.K., (2004). Essential heavy metals in environmental samples from western India. Bulletin of Environmental Contamination and Toxicology. 73: 756–761.

Spiares J.D., Kenworthy K.E., Rhykerd R.L. (2001). Emergence and height of plants seeded in crude oil contaminated soil. Tex. J. Agric. Nat. Res. 14: 37-46.

Udo, E.J. and CO. Oputa (1984). Some studies on the effect of crude oil pollution of soil on plant growth. West African Journal of Biological and Applied Chemistry.26: 3-14.

JJEES

Jordan Journal of Earth and Environmental Sciences

JJEES (2022) 13 (2): 122-129
ISSN 1995-6681

# Examining the Performance Specifications of Dunesand Reinforced with Fibers Recycled from Waste Yarn Textiles in Subgrade

Ali Mohamad Montazeri, Mohammad Mehdi Khabiri*, Zohreh Ghafori Fard

*Department of Civil Engineering, Yazd University, Yazd. Iran*

*Received 16 February 2021; Accepted 21 January 2022*

**Abstract**

In the present study, the mechanical behavior of dune sand, harvested from the central desert, and reinforced with recycled fibers, has been investigated. The recycled fibers are made of yarn twisting with an average thickness of 0.11 mm and a width of 5 mm. The purpose of this study is to evaluate the role of reinforcing fibers in California bearing ratio (CBR), soil density in terms of weight percent (Wr), and the fiber's longitudinal (L) dimensions. Besides, in the present study, the results obtained from determining CBR and density were provided and analyzed. The variables considered in this study include utilizing one type of disposable plastic fiber waste in different weight percentages in the form of random reinforcing in the granular embarkment. The present study was a small-scale laboratory, and the CBR device is used. The results show that with the use of waste fiber in sandy soil, the bearing capacity has significantly increased. The optimal weight percentages of plastic pieces relative to the sand fell in the range of 2-2.5%. Moreover, adding fibers to the soil has reduced the maximum dry density and also the samples' ductility. The CBR curve, in terms of fibers' weight percentage, shows an incremental trend. However, the slope of the resistance change curve decreases in terms of fiber weight percentage; That is, from one place to another, adding fibers does not significantly change the resistance.



**Keywords:** reinforced soil, fibers, CBR, density, dune sand, recycling.

## 1. Introduction

Generally, soil reinforcement is a technique to enhance the soil resistance using the reinforcing elements for dealing with the soil's tensile weakness; Also, to protect the environment, various types of recycled materials are used in pavement and new asphalt mixtures (Nabiun and Khabiri, 2016). In recent years, several studies have been performed on utilizing reinforced soil and the bearing capacity of the granular soils. In many studies, the attention has been only focused on the subsoil reinforced with materials including geosynthetics, metal straps and belts, and even rubber pieces and wastes and polyethylene terephthalate tapes and fibers (Hejazi et al; 2012); and the utilizing waste pieces from polyethylene plastic with 3D function has not been considered in the embarkments. In the present study, examining the effect of using plastic waste pieces on enhancing the bearing capacity of the granular soils has been addressed.

Throughout history, using the reinforcing elements in the soil has been of human interest. Using the chaff and straw for reinforcing soil (thatch mortar) has been common since ancient times, and is still used. Today, the soil reinforcement is one of the branches of geotechnics science. By using scientific principles and novel technologies, this branch uses the appropriate materials for reinforcing soil to enhance the engineering specifications and mechanical properties such as resistance, stiffness, ductility, and bearing capacity. The materials used for reinforcing the soil include metals, polymers, and plant parts(Hejaziet al; 2012). The mechanism of action and behavior of traditional reinforced soil depends on the mutual effect between soil and reinforcing materials. The friction phenomenon between soil and reinforcing elements plays a significant role in the reinforced soil(Kumar et al; 2015).

Mixing with fibers is one way for reinforcing the soil. By mixing these elements into the soil, a mixed medium is created in which the interaction of tensile components (reinforcing elements) with soil grains enhances the strength and ductility of soil in different directions (Kumar et al; 2015). Although some plants' parts have been historically used for reinforcing the soil, from about half a century ago, extensive research has been performed on the recognition and evaluation of the mechanical behavior of fiber-reinforced soil.

Natural loose soil available in the projects' sites is not always suitable as a substrate. Considerable settlement may occur in the poor soil as the load is applied. Reinforcing poor soils for use in slopes and road subgrades to create earth configuration with desired engineering properties is an essential field in civil engineering. The consolidations, compression, pre-loading, reinforcement, etc., are methods for reinforcing soils. The reinforced soil, among these methods, has attracted considerable attention in recent years.

Increased plastic waste and its extensive environmental pollution have become a significant challenge(Comăniță et al., 2016). Plastics are wastes that have high mechanical and tensile strength and rarely react with acids and bases and other chemicals; besides, plastics are completely resistant to

* Corresponding author e-mail: mkhabiri@yazd.ac.ir

micro-organisms, and as a result, they remained unchanged in nature for many years. In this regard, many works have been conducted to find an appropriate solution to eliminate wastes and or reuse them as alternative materials in civil engineering (Grad ,2021). In the reinforced soil method, given that soils do not have enough tensile strength to resist applied load, some tensile elements, including metal tapes, geosynthetics, and waste plastic, are used in the soil (Kumar et al, 2015). It should be noted that utilizing plastic wastes in soil remediation is not costly, and therefore, this type of reinforcement is economically essential.

In recent years, the economic and environmental problems have led to utilize waste resulting from Worn tires, bottles, glasses, etc. to modify and enhance the soil specifications. The soil's reinforcing and stabilizing methods are usually performed using geosynthetics, cementing agents (lime, cement, etc.), synthetic and non-synthetic fibers, or rubber crumbs (Jamshidi et al., 2018; Rezaeimalaek et al.2017; Mousavi and Karamvand, 2017; Estabragh et al. 2017; Hamidi and Hooresfand 2013; Malidarreh et al. 2018). Saberian and Khabiri (2017) investigated the effects of coal on pavement performance in mine haul roads. Their research indicated that with an increase in coal the maximum dry density, California bearing ratio before (CBR), and coefficient of permeability increased. Stabilized or reinforced soils are usually composite materials that are obtained from combining and optimizing the properties of every single ingredient. One of the pioneer methods in modifying soil specifications is utilizing plastic materials obtained from bottles.

During the last decade, many studies have been performed on utilizing reinforced soil to increase the bearing capacity of granular soils. In most cases, it has been observed that research has been limited to the embarkment reinforced with geosynthetics and metal straps and belts(Abu-Farsakh et al, 2007; Yan et al, 2010; Ferreira et al, 2015), and utilizing plastic wastes in the embarkments have not been taken into accounts. Therefore, this study investigates the effect of using plastic wastes to improve the bearing capacity of granular soils. The variables considered in this study include utilizing one type of disposable plastic fiber waste in different weight percentages in the form of random reinforcing with specified layering in the granular embarkment. In this research, the plastic parts obtained from polyethylene terephthalate bottle wastes, used for packaging and storage of beverages such as soft drinks and water, are used for improving sandy materials. The existence of plastic parts will cause considerable changes in the shear and tensile strengths of reinforced soil. The tests have been performed on the materials without/with reinforcing materials, for different irregular (random or scattered) and regular (with specified layering) weight percentages.

Various research has examined the load-displacement behavior of a kind of needle-shaped non-woven geotextile under the free and fixed conditions on the clay layer (equivalent to soft bed) from natural mines, and also beneath the sand layer (equivalent to subgrade) using the modified CBR tests with a specified mold. They concluded that geotextiles would increase the bearing capacity of the pavement, which increases as the settling increases (Garber and Rasmussen, 2010; Sudarsanan et al, 2018).

Research has investigated the strain-stress behavior of sand reinforced by scattered plastic fibers by performing three-axis compression tests. They have concluded that the plastic fiber-reinforced soil has higher tensile and shear strength compared to sandy soil. Besides, they have observed that reinforced soil will be fractured in higher strains than the sandy soil. According to their investigations, it can be concluded that the strain-stress behavior of the sand reinforced with scattered plastic fibers depends on fibers' specifications and fibers-sand friction (Lee and Barr, 2003).

In a field study, the engineering behavior of sand was reinforced by strip wastes made of polyethylene terephthalate (PET) plastic. The reinforcing material used in their investigation was fibers obtained from plastic bottles that have been used with/without quick-setting Portland cement. They performed some uniaxial and three-axial drainage tests on the samples. Their results indicate that utilizing plastic wastes, both in cemented and non-cemented cases, will increase the yield and ultimate strengths of the samples(Peddaiah et al., 2018).

In a recent study, some experimental tests have been performed to evaluate the strength and stiffness of the granular soil. The soil was stabilized chemically with cement and fly ash and mechanically with a thin cut of compressed recycled polyethylene terephthalate plastic (obtained from recycling plastic containers for water and milk). They concluded that using plastic waste strips with appropriate length and weight percentages can enhance the integrity between pavement materials, which delays and prevents the propagation of tensile cracks in the pavement. Besides, they reported that utilizing plastic waste materials will improve strength and mechanical specifications in the pavement mixture. Some researchers investigated the effect of polypropylene fibers on the mechanical specifications of the cemented and non-cemented clay soil using unconfined compression and direct shear tests. Their results indicate that an increase in plastic fibers in cemented and non-cemented fibers will lead to an increase in compression strength, shear strength, and axial strain at the fracture time and flexibility; on the other hand, it will lead to a decrease in concrete stiffness. From the electron microscopy tests, they concluded that utilizing plastic fibers increases the integrity between the materials, increases the internal friction angle, and reduces the cracking (Mishra & Gupta, 2018).

In a case study, a specific method for producing PET fibers from waste drink bottles was proposed to produce fiber-reinforced concrete. They compared specifications of different types of fibers, including polypropylene and polyvinyl alcohol, with PET fibers. According to the comparison, it was concluded that the PET fibers, among the others, have higher Alkaline resistance and are more appropriate in terms of water penetration depth test. Also, by performing bending and uniaxial tests, they concluded that by increasing the weight percentage of fibers, the compressive and tensile strengths of the reinforced concrete are increased.

In another research, the waste plastic strips and volcanic ash were used to reinforce the soil. Different amounts and sizes of these stripes have been used to investigate the effect of their sizes. It was found that by increasing the plastic strips in the saturated clay, the bearing capacity and scant modulus are increased. With an increase in the number and length of these strips, the increase in bearing capacity and scant modulus increases. The increase in the bearing capacity increases until the optimal value of 2%. However, by increasing the number of plastic strips, no changes in the bearing capacity are seen (Salimi, & Ghazavi, 2019).

Today, the soil reinforcement is one of the branches of geotechnics science. Using scientific principles and novel technologies, this branch uses the appropriate materials for reinforcing soil to improve the engineering specifications and mechanical properties. The elements used for reinforcing soil include metals, polymers, and plant parts. The mechanism of action and behavior of traditional reinforced soil depends on the mutual effect between soil and reinforcing materials. Soil-reinforcing material friction plays a significant role in reinforcing soil. One method for reinforcing soil is mixing the soil with fibers randomly and disorderly. Different studies materials such as compost, silica, bentonite, and various types of ash have been used to improve the clay specification (Firoozi, et al. 2017). In these methods, a mixed environment is created in which the interaction of tensile (reinforcing) elements with soil grains improves the strength and ductility of the soil. Although soil reinforcement has a long history, during the recent half-century, extensive research has been performed to identify and evaluate the mechanical behavior of fiber-reinforced soil.

In research, the samples are reinforced with fiber by triaxial tests, and a criterion has been provided, based on the experimental and theoretic studies, for the fracturing of sand reinforced with steel fibers and polyamide. According to their results, it was found that reinforcing soil will increase the compressive and shear strengths of the soil. On the other hand, reinforcing soil improves the response of soil mass to the dynamic loads, increases the soil's dynamic shear module, reduces the liquefaction potential, and increases the soil's ductility. According to the literature review, the present study aims to examine the qualitative specifications of the sandy soil, including density, bearing capacity, and penetration, along with different contents of recycled polymer fibers available in the packing industries' wastes.

## 2. Methodology

In this study, the dunesand prepared from the countryside of Yazd city has been used. The crushed polymer fiber particles with sizes of 5mm to 15mm and a density of 1.2kg/cm$^3$ were provided from recycled factory products to reinforce the soil. Then, the recycled polymer fibers were mixed with sandy soil with weight percentages of 0.0, 0.25, 0.5, and 1, to determine their effect on the qualitative parameter in the lab.

To prepare and reinforce soil, the Sandy soil sample was first held at a temperature of 115 °C and dried in the oven. After preparation, the particles were separated by a scissor. To prepare polymer waste fibers, first, pass the polymer fibers through a 200 sieve; so that the adhered particles separate from the polymer fibers.

## 3. Determining soil's mechanical specifications

In this study, the following tests were used to determine the subgrade's qualitative specification of primary and secondary roads before and after being reinforced with recycled fibers. It should be noted that all soil's mechanical tests have been conducted according to the American society for testing and materials (ASTM) standards.

### *3.1. Dunesand*

The soil used in this study as mentioned, the eastern deserts of Yazd were sampled at three points and since the characteristics of the sampled soils were the same, three soil samples were mixed to continue the work. Figure 1 shows the soil sampling location. This soil is of sedimentary dune sand type with uniform granulation. The unified soil classification system (USCS) falls in the SP-SM soil group, its specification is provided in Table 1.

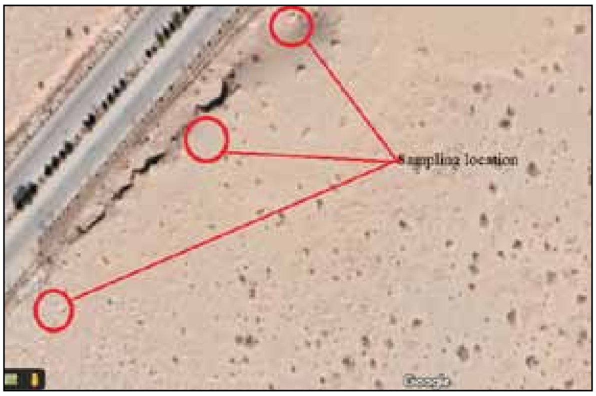


**Figure 1.** Sampling location

**Table 1.** Specifications of the soil used in this study.

| Soil type | SP-SM |
|---|---|
| $G_s$ | 2.7 |
| $D_{50}$ | 0.14 mm |
| Sand content | 93.9% |
| Silt content | 5.61% |
| Clay content | 0.49% |
| $C_u$ | 4 |
| $C_c$ | 1-3 |

Figure 2 shows the soil granulation curve. This soil has been prepared from the desert around the Yazd province located in the central desert.

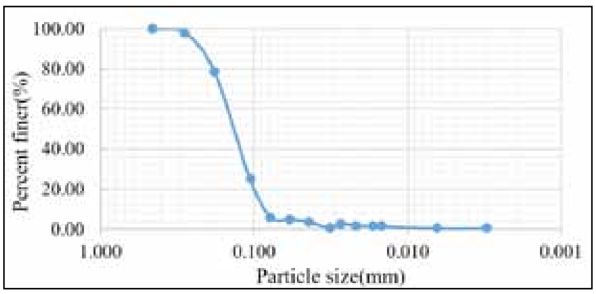


**Figure 2.** The granulation curve of the quicksand.

### *3.2. Waste textile fibers*

The element used was made of thin and short fibers provided by the waste textile after being consumed. The reinforcing elements are generally polyethylene and aluminum types, with an average thickness of 0.11mm and a width of 5mm. In the soil-fibers mixture, fibers are mixed with 0.0, 0.25%, and 0.5% by dry weight of soil and longitudinal dimensions of 1, 5, 9, and 13. The density of fibers is $G_r$ =1.18, and the maximum tensile strength and the initial elasticity module, according to the tensile tests (ASTM D4595), were 107 MPa and 9611 MPa. Figure 3 indicates these fibers and sand aggregate.

**Figure 3.** A sample of fibers with different dimensions and sand aggregate.

### *3.3. Samples preparation*

The dry soil, fibers, and water were used to prepare samples. Given the geometrical specifications, density mold, and fibers content, and for better mixing of soil and fibers, the soil, first, was moistened with about one-third of water (Optimal moisture percentage), and then the fibers were added. In the following, by gradually adding the remaining water and fully mixing the mass by hand, the sample moisture is increased to the optimal limit (14/5%) so that a homogeneous mixture is obtained. Then, the samples of CBR and compression tests were prepared using the standard method. It should be noted that 27 samples were prepared in this study; So for each percentage of fibers in a specific test, three samples were prepared and tested. The reinforced samples are shown in Figure4.

**Figure 4.** A reinforced sample

### *3.4. Compression test*

These tests have been performed according to the ASTM D1557-78 standard in a small mold on samples of primary sandy soil and reinforced soil. Details of the performed tests are shown in Figure 2. This figure indicates the variations of maximum specific gravity in terms of moisture for soil and reinforced-soil samples (Wr= 0.0%, 0.5%, 1%).

### *3.5. Permeability test*

The permeability coefficient shows that the amount of pores in the soil causes the way water moves in the soil. In this research, the permeability test of primary sandy soil reinforced with fibers according to the ASTM D 2434 standard was performed(Figure 5).

**Figure 5.** A view of the sample in the permeability test

### *3.6. California bearing capacity (CBR) test*

This experiment was performed to investigate the effect of weight percentage (Wr) and dimension ratio (LR) parameters of recycled synthetic fibers on the load-bearing capacity of primary and fiber-reinforced sandy soils. For this evaluation, CBR experiments were performed on soil and reinforced soil samples containing weight percentages (Wr) of 0, 0.25, 0.5, 0.75, 1% and dimension ratio (LR) of 13.9, 5, 1. In this study, the samples were based on ASTM D1557 compact standard and the CBR test was performed by ASTM D1883 standard method (Figure 6).

**Figure 6.** A sample of the CBR test

The samples were consolidated according to the ASTM D1557 standard, and the CBR test was performed according to ASTM D1883 standard. The details of the sampling method, how to perform tests, and the results obtained are described in the following. After preparing the mix according to clause 3, the mix was consolidated in 5 layers (by ASTM D1557 standard method) inside the specific CBR molds. As the sample was made, a loading was applied to the sample in the CBR test device with a penetration rate of 1.27 mm/min. The load applied was continued until the approximate penetration of 12.7 mm of the mandrel in the sample, then the results were recorded. In the next step, the samples were consolidated again using the same method mentioned above, and then the required overhead weights grid was placed on the mold containing soil, and the samples were immersed in the water reservoir. After 24h, the samples were removed, and after drainage of the additional water from the sample (about 15 min), the sample undergoes a loading according to case A.

## 4. Results

### 4.1. Analysis of compression tests results

By examining Figure 7, it can be found that in constant compression energy, by adding fibers to the soil, the maximum dry specific gravity of the samples reduces. This may be attributed to the lower density of reinforcing elements compared to the soil particles. On the other hand, the placement of these elements between the soil particles prevents the particles from getting closer to each other. As a result, these factors will reduce maximum dry specific gravity in the reinforced samples.

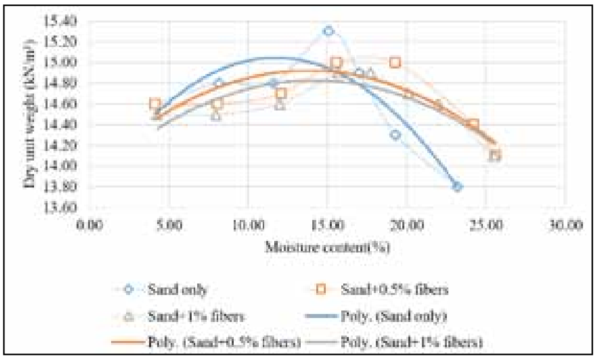


**Figure 7.** Plot showing the compression curves of soil and reinforced soil.

According to Figure 6, it can be seen that with an increase in the weight percentage of reinforcing elements, the sample's optimal moisture percentage increases. The reason for this increase may be attributed to the increased porosity of the samples.

Some other researchers, in a part of their studies, investigated the behavior of the sand reinforced with artificial fibers in the compression test (Claria and Vettorelo; 2016). Their results suggest that fibers have no significant effect on reducing dry specific gravity and an increase in the moisture percentage. Similar results were reported by studying the laminated sand with polyester synthetic fibers. In sum, it can be concluded that the addition of a reinforcing element with a specific gravity less than that of soil will reduce the maximum dry specific gravity and increases the optimal moisture in the samples.

### 4.2. Analysis of permeability tests results

Drainage of surface waters, which is penetrated pavement structure through cracks, is essential. Entering these waters into subgrades and the layers without cohesive material and remaining in these layers will reduce the strength and increases the damage. Impermeability of the substrate or foundation prevents the surface water from penetrating the subgrade and reducing its strength, which effectively reduces failures due to cracking and rutting of the pavement. The permeability test of recycled fibers-reinforced samples in different content was performed according to the ASTM D2434-87 standard. Figure 8 is depicted to show the results of permeability tests on three different mixtures that have been stabilized with different contents of additives. As can be seen from the figure, by adding the additives, the permeability rate has considerably reduced, and the permeability of three types of soil with additive content of 0.75% has reached zero.

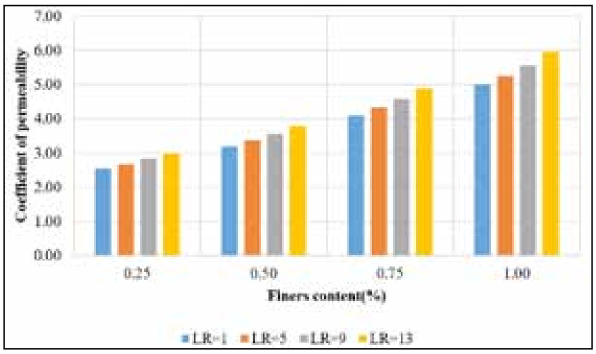


**Figure 8.** Results of the permeability test.

### 4.3. Analysis of CBR tests results

The permeability-stress curves obtained from CBR tests that are performed on the reinforced and non-reinforced sands with 0, 0.5%, and 1% by dry weight of soil and L of 1, 5, 9, and 13 in the moisture and submerged conditions are shown in Figure 9 to Figure 16. These plots indicate the behavior of brittle materials (such as dense sands of stiff clays) for non-reinforced samples in both optimal moisture and submerge conditions. by adding fibers to the soil, a turning point appears in the permeability-stress curve, so that in low penetration, the strength in reinforced soil is less than that of non-reinforced soil. This trend will increase as the content and L of the fibers is increased. It should be noted that the CBR plots for different soils usually have one turning point that is due to the non-uniformity of the sample surface and its complete contact with the loading piston at the test start. In this case, the plots must be modified according to the standard method. However, since no turning point is seen in the non-reinforced soil plot, these plots have not been modified. In other words, the creation of a turning point is usually due to the effect of the fiber.

Besides, adding fibers to soil increases the soil strength and permeability at maximum strength, and also reduced the distance between peak strength and post-peak strength. This means that by adding the fibers, the samples become more ductile.

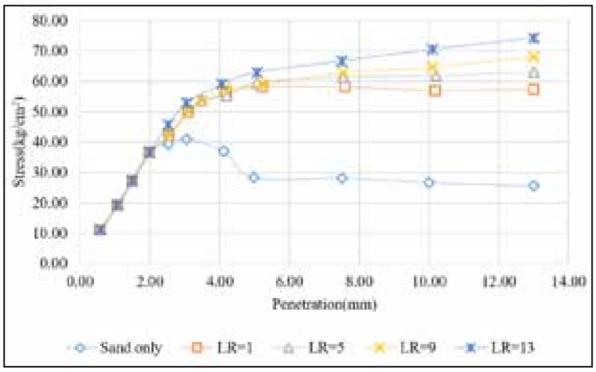


**Figure 9.** The variation of stress in terms of mandrel penetration for samples with optimal weight percentage and L in CBR test.

Examining these plots show that the increase in CBR (about 3%) is for submersion and optimal moisture occurs at LR=1. While, for LR=13 in the submersion and the optimal moisture cases, this increase is 22% and 17%, respectively. In the constant fibers content, the number of fibers in the longitudinal direction is more, which can indicate the higher effect of fibers length against their numbers in the reinforced soil mass. This behavior may be due to the increased lap-length of the reinforcing element as the L increases; this will improve the mutual effects of the soil and reinforcing materials.

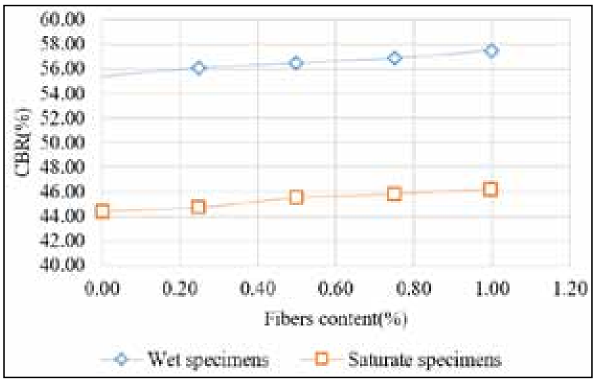


**Figure 10.** The CBR variations in terms of fibers' weight percentage for samples with optimal moisture and submersion with L=1.

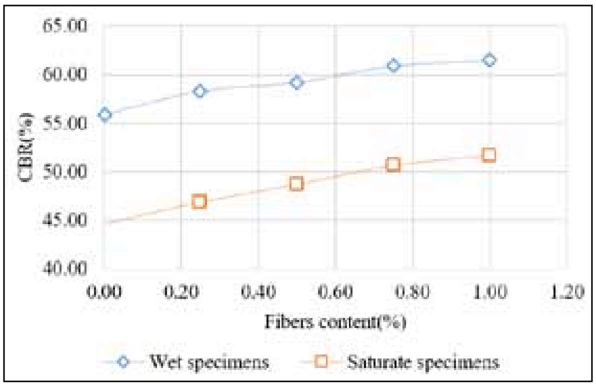


**Figure 11.** The CBR variations in terms of fibers' weight percentage for samples with optimal moisture and submersion with L=5.

Figures 9-11 show the CBR variations of samples with optimal moisture and submersion against fibers' weight percentage. The plots show a reduction of about 11 units for CBR of the submersion case compared to the case with optimal moisture. The reason for this reduced strength can be attributed to the uniform granulation of soil due to the loss of capillary force in submerged cases relative to optimal moisture conditions. Besides, increased pore pressure and reduced friction force between the soil particles are the other reasons.

Figures 13 and 14 show that by increasing the weight percentage of the elements, the CBR increases; however, this increase has a decreasing rate, which indicates the existence of an ultimate limit for the addition of reinforcing elements. This is because of the replacement of fibers with soil grains. In fact, by adding fibers, they gradually change the nature of composite mass.

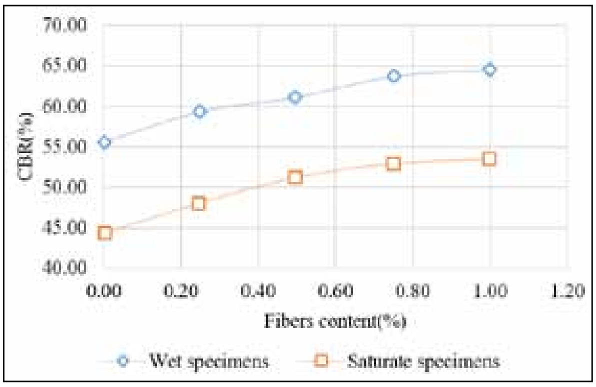


**Figure 12.** The CBR variations in terms of fibers' weight percentage for samples with optimal moisture and submersion with L=9.

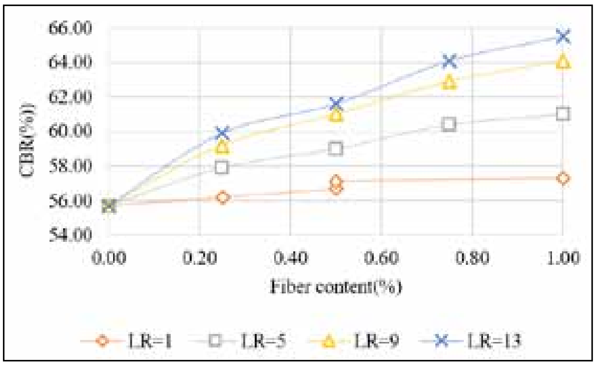


**Figure 13.** The CBR variations in terms of fibers' weight percentage for samples with optimal moisture.

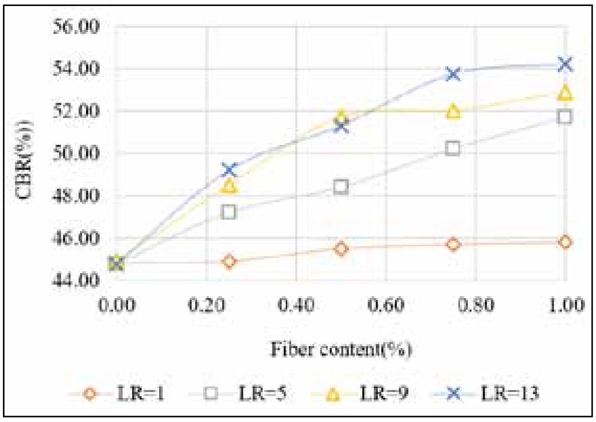


**Figure 14.** The CBR variations in terms of fibers' weight percentage for submerged samples.

On the other hand, from Figures 15 and 16, it is evident that by increasing the L of reinforcing elements, the slope of the plots decreases. This suggests that the increased rate of CBR against the fibers' length is decremental. This may be attributed to the increase in reinforcing materials' deformation as their length increases, such that by increasing the elements' length, the possibility of bending and thus reducing their length increases during sampling. This effect of reinforcing elements on the CBR strength is also reported by other researchers (Patel, & Singh, 2019).

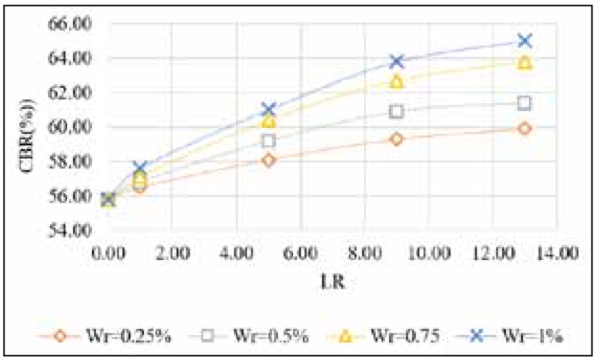


**Figure 15.** The CBR variations in terms of L of reinforcing elements for samples with optimal moisture.

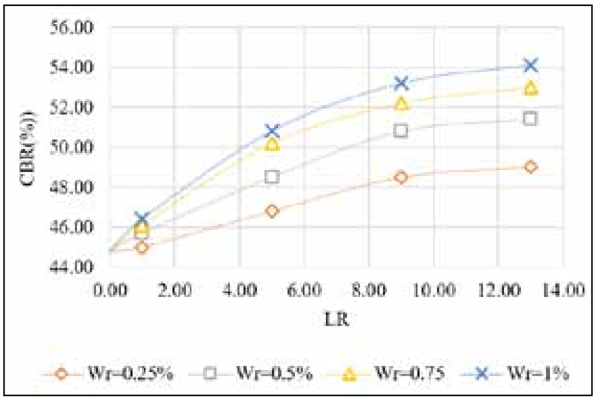


**Figure 16.** The CBR variations in terms of L of reinforcing elements for submerged samples.

## 5. Conclusions

The results of this study regarding the use of waste fibers can be summarized as follow:

Results show that adding fibers to the soil reduces the maximum dry density and increases the CBR and deformability of the samples. The variations of CBR curves in terms of fibers' weight percentage have an increased rate. However, the rate of the slope of the strength curve in terms of fibers' weight percentage has a decreasing trend. The effect of an increase in L on the CBR of samples is also similar to the Wr effect.

With the addition of reinforcing elements to the soil, the specific gravity of the set is reduced. On the other hand, it is expected that by increasing the fibers' weight percentages in the soil, the porosity increases enough which reduces the soil strength. By the examining results of CBR tests with constant weight percentages of fibers and different LR, it was found that the elements' length plays a more significant role than their number. This result indicates the effect of a minimum value for the lap-length of reinforcing elements.

An increase in the reinforcing elements in the sample will increase the optimal moisture compared to the non-reinforced sample. This may be attributed to the increase in the porosity of the sample due to the addition of fibers. Adding reinforcing fibers to the soil increases the CBR and reduces the stiffness, and improves the ductility of the sample. However, the increasing trend of the strength has a decreasing rate, indicating the existence of an ultimate limit for using fibers in both weighted and longitudinal cases. This means that, after a certain weight percentage and L, the addition of fibers has no positive effect on the soil bearing capacity.

Submerging samples will decrease their CBR values compared to samples with optimal moisture. The reason behind this can give the uniform granulation of soil due to the loss of capillary force in submerged cases relative to optimal moisture conditions. Besides, increased pore pressure and reduced friction force between the soil particles are the other reasons.

Using reinforcing fibers of the soil must be examined in terms of durability; however, due to the very low permeability of the soil reinforced with this material, it is expected that the repetition of frost and thawing has no significant effect on its performance.

## References

Abu-Farsakh, M., Coronel, J., & Tao, M. (2007). Effect of soil moisture content and dry density on cohesive soil–geosynthetic interactions using large direct shear tests. Journal of Materials in Civil Engineering,19(7):540-549.

https://doi.or10.1061/(ASCE)0899-1561(2007)19:7(540)

Claria, J. J., & Vettorelo, P. V. (2016). Mechanical behavior of loose sand reinforced with synthetic fibers. Soil Mechanics and Foundation Engineering, 53(1), 12-18.

https://doi.org/10.1007/s11204-016-9357-9

Comăniță, E. D., Hlihor, R. M., Ghinea, C., & Gavrilescu, M. (2016). Occurrence Of Plastic Waste In The Environment: Ecological And Health Risks. Environmental Engineering & Management Journal (EEMJ), 15(3)

Estabragh, A., Ranjbari, S., & Javadi, A. (2017). Properties of clay soil and soil cement reinforced with polypropylene fibers. ACI Materials Journal.

https://doi.org/10.14359/51689469

Ferreira, F., Vieira, CS., & Lopes, M. (2015). Direct shear behavior of residual soil–geosynthetic interfaces–influence soil moisture content, soil density, and geosynthetic type. Geosynthetics International,22(3):257-272.

https://doi.org/10.1680/gein.15.00011

Firoozi, A. A., Olgun, C. G., Firoozi, A. A., & Baghini, M. S. (2017). Fundamentals of soil stabilization. International Journal of Geo-Engineering, 8(1), 1-16.

https://doi.org/10.1186/s40703-017-0064-9

Garber, S., & Rasmussen, R. O. (2010). Nonwoven geotextile interlayers in concrete pavements. Transportation research record, 2152(1), 11-15.

https://doi.org/10.3141/2152-02

Hamidi, A., & Hooresfand, M. (2013). Effect of fiber reinforcement on triaxial shear behavior of cement treated sand. Geotextiles and Geomembranes, 36, 1-9.

https://doi.org/10.1016/j.geotexmem.2012.10.005

Hejazi, S. M., Sheikhzadeh, M., Abtahi, S. M., & Zadhoush, A. (2012). A simple review of soil reinforcement by using natural and synthetic fibers. Construction and building materials, 30, 100-116.

https://doi.org/10.1016/j.conbuildmat.2011.11.045

Jamshidi Chenari, R., Fatahi, B., Ghorbani, A., & Alamoti, M. N. (2018). Evaluation of strength properties of cement stabilized sand mixed with EPS beads and fly ash. Geomechanics and Engineering, 14(6), 533-544.

https://opus.lib.uts.edu.au/bitstream/10453/125410/1/3.GAE77781C%28ok%29.pdf

Kumar, D., Dhane, G., & Priyadarshee, A. (2015). Performance of different form of soil reinforcement: a review. Int. J. Sci. Technol. Manage, 4(1), 667-677.

http://www.ijstm.com/images/short_pdf/1422589766_455.pdf

Lee, M. K., & Barr, B. I. G. (2003). Strength and fracture properties of industrially prepared steel fibre reinforced concrete. Cement and Concrete Composites, 25(3), 321-332.

https://doi.org/10.1016/S0958-9465(02)00060-4

Malidarreh, N., Shooshpasha, I., Mirhosseini, S., & Dehestani, M. (2018). Effects of reinforcement on mechanical behaviour of cement treated sand using direct shear and triaxial tests. International Journal of Geotechnical Engineering, 12(5), 491-499.

https://doi.org/10.1080/19386362.2017.1298300

Mishra, B., & Gupta, M. K. (2018). Use of randomly oriented polyethylene terephthalate (PET) fiber in combination with fly ash in subgrade of flexible pavement. Construction and Building Materials, 190, 95-107.

https://doi.org/10.1016/j.conbuildmat.2018.09.074

Mousavi, S. E., & Karamvand, A. (2017). Assessment of strength development in stabilized soil with CBR PLUS and silica sand. Journal of Traffic and Transportation Engineering (English Edition), 4(4), 412-421.

https://doi.org/10.1016/j.jtte.2017.02.002

Nabiun, N., & Khabiri, M. M. (2016). Mechanical and moisture susceptibility properties of HMA containing ferrite for their use in magnetic asphalt. Construction and Building Materials, 113, 691-697.

https://doi.org/10.1016/j.conbuildmat.2016.03.058

Patel, S. K., & Singh, B. (2019). Investigation of glass fiber reinforcement effect on the CBR strength of cohesive soil. In Ground Improvement Techniques and Geosynthetics (pp. 67-75). Springer, Singapore.

https://doi.org/10.1007/978-981-13-0559-7_8

Peddaiah, S., Burman, A., & Sreedeep, S. (2018). Experimental study on effect of waste plastic bottle strips in soil improvement. Geotechnical and Geological Engineering, 36(5), 2907-2920.

https://doi.org/10.1007/s10706-018-0512-0

Rezaeimalek, S., Nasouri, A., Huang, J., Bin-Shafique, S., & Gilazghi, S. T. (2017). Comparison of short-term and long-term performances for polymer-stabilized sand and clay. Journal of traffic and transportation engineering (English edition), 4(2), 145-155.

https://doi.org/10.1016/j.jtte.2017.01.003

Saberian, M., & Khabiri, M. M. (2017). Experimental and numerical study of the effects of coal on pavement performance in mine haul road. Geotechnical and Geological Engineering, 35(5), 2467-2478.

https://doi.org/10.1007/s10706-017-0235-7

Salimi, K., & Ghazavi, M. (2019). Soil reinforcement and slope stabilisation using recycled waste plastic sheets. Geomechanics and Geoengineering, 1-12.

https://doi.org/10.1080/17486025.2019.1683620

Sudarsanan, N., Mohapatra, S. R., Karpurapu, R., & Amirthalingam, V. (2018). Use of natural geotextiles to retard reflection cracking in highway pavements. Journal of Materials in Civil Engineering, 30(4), 04018036.

https://orcid.org/0000-0002-5315-6928.

Yan Q., Li, C., Mei, Y., & Deng, W. (2010). Study on the characteristics of geogrids/soil interface. Mechanic Automation and Control Engineering (MACE), IEEE, 1241-1248.

10.1109/MACE.2010.5536373

JJEES

JJEES (2022) 13 (2): 130-145
ISSN 1995-6681

Jordan Journal of Earth and Environmental Sciences

# Anthropogenic Influence on Soil Quality Dynamics and Potential Ecological Risk in Agricultural Soils of the Nworie River Watershed, Nigeria

Ubuoh Emmanue Attah[1*], Ofoegbu Clara Chinwendu[2], Boise Ekene[3]

*Michael Okpara University of Agriculture, College of Natural Resources and Environmental Management, 1&2Department of Environmental Management and Toxicology, Nigeria.*
*3University of Benin, Benin City, Faculty of Life Sciences, 3Department of Environmental Management and Toxicology, Nigeria.*

*Received 17 February 2021; Accepted 28 January 2022*

**Abstract**

The study assessed soil nutrients and heavy metals in agricultural soils along Nworie River watershed at three depths: 0 – 15, 15 – 30, and 30 - 45cm. The results indicated that the soil was predominantly sandy with a moderate acidity of 5.2. Except for base saturation, other physicochemical parameters were below the WHO/FAO critical limits. Ratings of soil nutrients in agricultural soils recorded low nitrogen, moderate available P, very low to low exchangeable $K^{+,}$ and low to moderate exchangeable $Ca^{+}$. Positive and negative correlations exist between physicochemical characteristics and heavy metals. Geo-accumulation ($I_{-geo}$) ranges from uncontaminated to moderately contaminated. The pollution load index (PLI) recorded ≤ 1 signifying no pollution. The potential risk factors (prf) ranged from low potential to considerably potential risks in order of Cd ≥ Pb ≥ Cu ≥ Zn ≥ Cr. The potential ecological risk index and risk assessment code examined indicated that of the metals sampled, Cd posed the most significant environmental risk associated with complex human activities like indiscriminate application of inorganic fertilizer, waste disposal, and ill-farming practices along the slopes of the watershed. Therefore, anthropogenic sources that degraded agricultural soils within the watershed should be avoided through enforcement of the existing environmental laws.



**Keywords:** Anthropogenic pollution, Agricultural soils, Toxic elements, Ecological risk, Nworie watershed

## 1. Introduction

Soil is an important resource for life that provides a variety of goods and services to meet human needs on earth (Garcia-Ruiz et al., 2015; Anache et al., 2017), and is a key factor for sustainable development in the terrestrial world (Ubuoh and Ogbonna, 2018). The improper practices of agriculture could result in anthropogenic impacts on existing natural resources (Zawadzka and Łukowski, 2010), and have become a global environmental issue and concern (Chen et al., 2017; Shao et al., 2018).

The existence of these heavy metals in soil is of great problem due to their potential toxicity (Khan et al., 2015). These metals are indestructible and most of them are categorized as of high toxicity to plants, animals, and humans even at low concentrations (Khan et al., 2015). Environmental factors that govern the transfer mechanism such as soil characteristics have to regulate heavy metal accumulation levels in plants (Velickovic et al., 2016). Noticeably, soil physicochemical characteristics, including pH (Ubuoh et. al., 2019, Ubuoh et al., 2020a), electrical conductivity (EC), organic matter content, and cation exchange capacity (CEC) have been found to affect the absorption of metals in plants (Yu et al., 2014). However, the same soil property can have multiple variant effects on different heavy metal plant systems (Yu et al., 2014). For instance, a study reported that the soil CEC and exchangeable calcium (Ca) are important indices for predicting the critical value of nickel (Ni) in barley and tomato (Rooney et al., 2007), whereas two other reports found that soil pH rather than soil CEC significantly affects the critical value of Ni toxicity in barley or tomato (Zhang et al., 2009; Li et al., 2011). On the other hand, the control of pollution sources is required to minimize their impact, where soils are generally described as geochemical sinks that are normally associated with heavy metals; and also sources for the movement or migration of the metals to other ecological systems (Abbas et al., 2011).

The accumulation effects of heavy metals in drainage basins have been previously investigated at the Pearl River Delta (Zhang et al., 2015), the Luan River (Liu et al., 2009), and the Yangtze River (Yi et al., 2011). However, analyzing soil properties in agricultural soil within Nworie is of great importance in evaluating the safety risks of farmlands for crops safety and farmers' survival void of toxic elements. Its watershed is used for intensive human and industrial discharge of the various pollutants both organic and inorganic in nature (Acholonu et al., 2008), from solid waste dumpsites (Ubuoh et al., 2014). Other activities include emission of automobile exhaust, automobile workshops, building constructions, road construction, destroyed vegetation mostly grasses, and polluted water and sand mining. Recent studies have also shown that the flood plain serves as a waste dumpsite that polluted soils (Ibe et al., 2017).

Meanwhile, regular monitoring and assessment of agricultural soil on Nworie valley slopes are necessary to

* Corresponding author e-mail: ubuohemmanuel@yahoo.com

assess the impact of human activities on soil quality and the pollution/contamination status (Gotelli and Ellison, 2004). To assess the severity of soil contamination and to distinguish between natural and anthropogenic inputs in the soil, several approaches like Geo-accumulation Index ($I_{-geo}$), contamination factors (CF), and Pollution Load Index (PLI) have been applied (Manoj et al., 2012; Mohsen and Alireza, 2014).

The study focused on the assessment of the dynamics of soil quality in agricultural and heavy metals in an area prone to human-induced activities using different multivariate approaches and assesses the degree of soil pollution, potential ecological risk, and identifying the local sources of contamination and pollution respectively.

## 2. Materials and Methods

### *2.1 Study Area:*

Nworie river is about 5km long and it lies between latitudes $5^0$ 4' and $6^0$ 3' N and longitude $6^0$ 15'and $7^0$ 34' E. It falls within the rainforest zone with an annual rainfall of 2290 mm, relative humidity of 55-85%, and temperature of $27^0$C. The river course, however, covers an area of about 5km$^2$ from its source to the point where it empties into the Otamiri River to form a confluence (Duru and Nwanekwu, 2012). Currently, human activities exist in the watershed including sand mining, waste disposal, fishing, mechanic workshop, effluent from residential areas and hospitals, and agricultural activities.

### *2.2 Soil Sampling and preparation*

A reconnaissance survey was undertaken to identify the soil sampling sites and indeed familiarize them with human activities within the Nworie River catchment. **The samples were collected during the dry season event.** Soil samples were collected in a randomized method along the valley slope of Nworie River (Figure 1), where human activities were pronounced using an auger-boring instrument at the depths of 0 – 15cm depth (topsoil) and subsoils 15 – 30cm and 30 -45cm according to coordinates (Table 1). The collected soil samples were poured into polythene bags, labeled adequately, and transported to the laboratory immediately for analyses. The soils sampled were air dried at room temperature for sieving. The sampled soil was grounded and sieved with a 2 mm mesh sieve according to standard protocol by the Food and Agricultural Organization (FAO) (2006) and kept for further analysis.

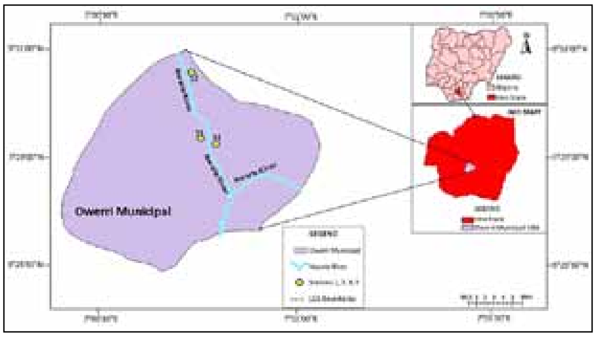


**Figure 1.** Location map of the study area

**Table 1.** Soil Sampling Points and Coordinates

| Locations | Coordinates | Human activities |
|---|---|---|
| Egbeada : $SSP_1$ | N05°29' 10.9" , E 007° 01'43.5" | Sand mining, Waste dump, erosion, farming, mechanic workshop |
| Amakohia :$SSP_2$ | N 05°30'56.6" , E 007° 00'59.2" | Sand mining, Waste dump, farming, runoff |
| Umezuruike Hospital :$SSP_3$ | N 05°29'16.1" , E 007° 01'30.0" | Waste dump, hospital effluent discharge, road construction, urban runoff |

### *2.3 Soil physical characteristics:*

Particle size distribution expressed in percentage (sand, silt, and clay) was measured by the hydrometer method (Gee and Or, 2002). The soil texture was determined using the soil textural triangle based on the percentages of the different soil particle sizes (Sutherland and Dejong, 1990).

### *2.4 Soil chemical characteristics:*

The soil pH was determined using procedures by Min Liu et al. (2004). The percentage of soil organic carbon was measured using the method by Walkley and Blacks (1965). Percentage soil organic matter is considered the total carbon multiplied by a conversion factor of 1.72 (Chikwendu et al., 2019). Soil Nitrogen was determined using the method by Dhyan et al. (1999). Available phosphorus was determined using the Bray No. 1 extraction method (Bray and Kurtz, 1945). Potassium and Sodium were determined by the flame emission photometer (Pinta, 1970). Calcium and magnesium were determined using the ethylene-diamine–tetracettic-acid (EDTA) method (Allison, 1973). The exchangeable acidity and the exchangeable aluminum were determined by titration as described by Juo (1975). Effective Cation Exchange Capacity (ECEC) was obtained as the summation of exchangeable cations and exchangeable acidity. To calculate the percent base saturation, the sum of the Potassium (K), Magnesium (Mg), Calcium (Ca), and Sodium (Na) (the bases) in Meli equivalent per 100g of soil (Meg/100mg soil) was divided by the CEC and result was multiplied with 100%. Thereafter, the result was compared with the acceptable nutrient standards for soil quality for agriculture by FAO/WHO, and other important environmental standards respectively.

### *2.5 Soil heavy metals digestion:*

Aqua-regia wet digestion was used for the estimation of the selected heavy metals. The extractants were prepared using mixed concentrated HCl with concentrated $HNO_3$ in 3:1 and the mixture was allowed to mix properly for 5 hours; 10 g of soil samples were taken in acid-washed beakers and 30 ml of aqua-regia was introduced. The mixture was reduced to 10–20 mL by heating at 9°C on a hot plate according to Enyoh and Isiuku (2020). Accordingly; the mixture reduced was allowed to cool and made to a final volume of 50 mL by addition of de-ionized water, followed by filtration resulting in the filtrate.

### *2.6 Soil heavy metal determination:*

The digested filtrates were used for the total metal quantification using Atomic Absorption Spectrophotometer (Perkin Elmer A Analyst 400). The characteristic wavelengths of metals determined were first set using the hollow cathode lamp, and the digested filtrate samples were aspirated directly into the flame.

***2.7 Quality Control and Quality Assurance (QC/QA):***

Quality control and quality assurance (QC/QA), accuracy, and precision (A/P) were verified using reference materials sediment-certified samples "GBW07311 (GSD-11) and GBW07366 (GSD-23) of the National Center of China". Equipment for soil analysis was calibrated before soil analysis. The blanks in every set were tested in duplicates using Standard reference material GBW07405 (National Research Center for Standards in China) was used to verify analytical accuracy, and results were presented in mean values of duplicated analysis. For repeat tests, soil samples were picked randomly. All glasses, plastics, and quartz were cleaned and rinsed using 10% $HNO_3$, and ultrapure water (18.25 Mohmcm$^{-1}$) was used to rinse every time

## 3. Three Assessments of contamination in agricultural soils

In this study, geo-accumulation index ($I$-$_{geo}$), contamination factor (), degree of contamination (Cd), ecological risk factor (), and pollution load index (PLI) were calculated to assess the heavy metal contamination levels and associated risk in agricultural soils understudies.

***3.1 Geo-accumulation index (I-geo):***

Index of Geo-accumulation ($I_{-geo}$) was introduced to assess metal pollution in sediments and has been applied in recent pollution studies to enable the qualitative assessment of soil contamination by heavy metals (Yaylali-Abanuz, 2011; Bentum et al., 2017). $I$-$_{geo}$ is computed by:

$$I_{-geo} = log_2\left(\frac{Cn}{1.5Bn}\right) \quad (1)$$

Where;

$C_n$ is the concentration of the element in the tested soil, $B_n$ is the geochemical background value in the average shale of element (Loska et al., 2004), and the constant 1.5 compensates for natural fluctuations of given metal and minor anthropogenic impacts (Taylor and McLennan, 1995). The seven classes of $I_{-geo}$ as proposed by Müller are as follows: $I_{-geo} \leq 0$, uncontaminated (UC) (Class 0); $0 < I_{-geo} \leq 1$, uncontaminated to moderately contaminated (UNC) (Class 1); $1 < I_{-geo} \leq 2$, moderately contaminated (Class 2); $2 < I_{-geo} \leq 3$, moderately to heavily contaminated (MHC)(Class 3); $3 < I_{-geo} \leq 4$,heavily contaminated (HC) (Class 4); $4 < I_{-geo} \leq 5$, heavily to extremely contaminated(HEC) (Class 5); $I_{-geo} > 5$, extremely contaminated (EC) (Class 6).

***3.2 Contamination factor ($C_f^i$) and Contamination degree (Cd):***

Contamination factor (CF) is expressed as a ratio of every metal in the present sample to the background values in the same metal. Assessment of soil contamination is performed by the contamination factor ($C_f^i$) and degree of contamination (Cd) (Table 2):

$$C_f^i = \frac{c_0^i}{c_n^i},\ \text{Cd} = \sum_i^m C_f^i \quad (2)$$

Where,

SI is the content of metal I, and is the reference value, baseline level, or national criteria of metal i. The contamination factor can be categorized according to their values from 1 to 6 "if CF ≤ 1,low contamination (LC); 1 ≥ CF ≤ 3, moderate contamination ; 3 ≤ CF ≤ 6, considerable contamination ; CF ≥ 6, very high contamination (VHC) (Hakanson, 1979).

**Table 2.** Classification of Degree of contamination

| Classes | Indications | Acronym |
|---|---|---|
| Cd<8 | Low degree of contamination | LDC |
| 8≤cd<16 | A moderate degree of contamination | MDC |
| 16≤cd<32 | A considerable degree of contamination | CDC |
| 32≤cd | A very high degree of contaminated | VHDC |

***3.3 Potential Ecological Risk Index***

The Potential Ecological Risk Index, advanced by Hakanson (1980), which represents the toxicity of heavy metals and the extent of pollution of the environment, is defined as:

$$\boldsymbol{R1 = Er^i = \sum(T_i \times C_i/B_i)} \quad (3)$$

Where,

R1 is the risk index and calculated as the sum of all six risk factors for heavy metals in soils, *Eri* is the single potential ecological risk factor, $T_i$ is the developed metal toxicity factor. $C_i$ /$B_i$ is the metal pollution factor, $C_i$ is the practical concentration of metals in soil, and $B_i$ is the background value for metals.

***3.4 The ecological risk factor ($E_r^i$)***

The ecological risk factor ($E_r^i$) (Table 3), to quantitatively express the potential ecological risk of a given contaminant also suggested by Hakanson (1980), and expressed mathematically:

$$\boldsymbol{E_r^i = T_r^i C_f^r}\quad ,\left(\boldsymbol{C_f^r} = \frac{c_0^i}{c_n^i}\right) \quad (4)$$

Where, the single potential ecological risk factor, is the toxic response factor for a given metal, is the contamination factor, the concentration of metals in agricultural soil, and is the reference value for metals.

**Table 3.** Descriptive Ecological Risk factor (Eri)

| Classes | Indicators | Acronym |
|---|---|---|
| Eri≤40 | Low potential ecological risk | LPER |
| 40≤ Eri<80 | Moderate potential ecological risk | MPER |
| 80≤ Eri<160 | Considerable potential ecological risk | CPER |
| 160≤ Eri<320 | High potential ecological risk | HPER |
| Eri≥320 | very high ecological risk | |

*Hakanson (1980),*

***3.5 Ecological risk index (Ir)***

$$I_r = \sum_i^n E_r^i = \sum_i^n T_r^i C_f^i = \sum_i^n T_r^i C_f^i / C_n^i \quad (5)$$

Where the symbols are as described above, Table 4 lists the classes.

**Table 4.** Descriptive Table for Ecological Risk index (Ir)

| Classes | Indications | Acronym |
|---|---|---|
| Ir<150, | low ecological risk | LER |
| 150≤ Ir<300 | moderate ecological risk | MER |
| 300≤ Ir<600 | considerable ecological risk | CER |
| Ir>600 | very high ecological risk | VHER |

### *3.6 Pollution Load Index (PLI)*

The pollution load index (PLI) has been used in this study to measure the pollution load of metals from agricultural soils (HIS, 1998). The pollution load index is expressed as the ratio of the metal concentration in the study to the background content of the abundance of chemical elements in the continental crust (Dos Anjos et al., 2000). PLI for the soil samples was determined by the equation below, as proposed by Tomlinson et al. (1980). The PI of each element is classified as either low (PLI ≤ 1), middle (1 < PLI ≤ 3), or high (PLI ≥ 3) (Chen et al., 2005), and mathematically expressed as:

$$PLI = (CF_n \times CF_n \times CF_n \times CF_n \times CF_n \times CF_n)^{\frac{1}{n}} \quad \text{............ (6)}$$

Where,

PLI, pollution load index, contaminant factor, n is the observed metal,

### *3.7 Statistical analytical technique*

Analysis of Variance (ANOVA) was used to test for differences between means at a 5%level of significance. Duncan's multiple post hoc test was used to obtain the specific significant differences among the sampling intervals using the GenStat Release 9.2 (PC/Windows), with the inference drawn at a P≤0.05 significant level. Person's correlation analysis was used to establish a relationship between soil quality parameters, while principal component analysis (PCA) was used to determine precise contamination sources (Verla et al., 2020). The factor loadings for heavy metals in the soils were extracted based on Eigen value >1 (Ubuoh et al., 2019).

## 4. Results and Discussion

The results represented the mean ± standard deviation of the soil physicochemical characteristics of the agricultural land in Tables 5 and 6.

**Table 5.** Mean ±SD of physical properties of soil in Nworie River watershed.

| Sample location | Soil depth (cm) | Sand % | Silt % | Clay % | Textural Class* |
|---|---|---|---|---|---|
| Soil sample point ($SSP_1$) | 0-15 | 82.78 ±1.501[a] | 7.673 ±1.276[a] | 9.543±0.229[a] | Loamy sand (LS) |
| Upper course (UC) | 15-30 | 82.89 ±1.529[a] | 7.580±1.251[a] | 9.530±0.279[a] | Loamy sand (LS) |
| Catchment | 30-45 | 82.55 ±1.297[a] | 9.017±1.025[a] | 8.433±0.843[b] | Loamy sand (LS) |
| | Mean | 82.74 | 8.090 | 9.169 | |
| | %Cv | 1.9 | 15.9 | 5.8 | |
| | Se | 1.550 | 1.283 | 0.535 | |
| Soil sample point ($SSP_2$) | 0-15 | 85.12±1.633[b] | 5.280±0.658[b] | 9.597±1.032[a] | Loamy sand (LS) |
| Middle course (MC) | 15-30 | 89.28±1.502[a] | 3.200±1.276[a] | 7.517±0.229[b] | Loamy sand (LS) |
| Catchment | 30-45 | 87.63±1.160[a] | 3.470±0.506[a] | 8.958±0.826[a] | Loamy sand (LS) |
| | Mean | 87.35 | 3.966 | 8.689 | |
| | %Cv | 1.0 | 13.5 | 6.6 | |
| | Se | 0.872 | 0.535 | 0.076 | |
| Soil sample point ($SSP_3$) | 0-15 | 82.78±1.786[a] | 7.673±1.523[a] | 9.543±0.266[a] | Loamy sand (LS) |
| Lower course (LC) | 15-30 | 82.55±1.297[a] | 8.983±0.980[a] | 8.467±0.809[b] | Loamy sand (LS) |
| Catchment | 30-45 | 82.78±1.786[a] | 7.673±1.523[a] | 9.544±0.266[a] | Loamy sand (LS) |
| | Mean | 82.71 | 8.110 | 9.184 | |
| | %Cv | 2.0 | 16.8 | 5.6 | |
| | Se | 1.640 | 1.366 | 0.515 | |
| | Overall CV (%) | 1.6 | 10.4 | 6 | |
| | Overall mean | 84.3 | 6.7 | 9.0 | |

*Different letters refer to significant differences between mean + standard deviation of different depths, similar letters refer to the insignificant difference between mean+ standard deviation of different depths Se= standard error, %CV = coefficients of variation.*

### *4.1 Physical Characteristics*

Particle size distribution recorded the mean values of 82.74% at the upper river catchment, 87.35% middle river, and Lower River at 82.71% with the overall mean value of 84.3% (Table 5). Except for the soil depth of 0-15cm that recorded a significant difference, other soil depths at the $SSP_{1-3}$ were significantly the same at *P*≤ 0.05 level. The sand abundance was in the order of UC ≥ MC ≥ LC. The overall mean value of sand being 84.3% in the study is greater than the76.29 % (Challawa,), 75.7% (Eyong and Akpa, 2019) in forested soil in Agoi-Ibami, Cross River State, Nigeria, 80.48% (Jakarta), and 73.41% (Watari) agricultural land in Kano, Nigeria respectively (Dawaki et al., 2013), suspected to be influenced by parent material. Silt recorded the mean values of 8.090 % for the upper course, 3.966% middle course, and 8.110% for the lower course with the overall mean value of 6.7%, with 0.15cm of the middle course ($SSP_2$) being significantly different from others at p ≥ 0.05 level. The silt was in decreased abundance order: UC ≥ MC ≥ LC. The overall mean value of silt is far less than 25.28±11.96 % of silt from anthropogenic sites in Abeokuta, Nigeria (Olayinka et al., 2017), and far below the 30% silt critical value for agriculture (FAO, 2014). Clay recorded mean values of 9.169% in the upper course, 8.689% middle course, and lower course 9.184% with an overall mean value of 9.0%. Clay content at soil depths 30-45cmUC, MC and 15-30cm (LC) were significantly the same and significantly different from others at P ≥ 0.05 levels. The mean clay contents recorded were higher than clays (6–10 Cmol/kg) in the soils of colluvial deposits in Akamkpa, Nigeria ( Aki and Ediene, 2018). Kingsley et al. (2020) reported a low CEC to low activity of clay. Clay was in decreased trend of LC ≥ UC ≥ MC. The overall mean value of soil fractions was in decreased trend: Sand ≥ Clay and Silt, with sand dominating, indicating typical soils of the coastal plain sands (Osakwe and Okolie, 2015). The result agreed with the findings of Onweremadu et al. (2011), Osujieke et al. (2016) who reported high sand and low clay in Southern Nigeria. The result is in agreement with World Reference Base (FAO, 2014), which reported sandy clay loamy content as a dominant fraction in agricultural soil, influenced by parent material (Osujieke et al., 2016).

**Table 6.** Mean ± SD of chemical properties of agricultural soil in Nworie River watershed

| Study location/ Soil depth | pH | P (mglkg) | N% | OC% | OM% | Exchangeable bases (cmol/kg) | | | | EA | ECEG | %BS |
|---|---|---|---|---|---|---|---|---|---|---|---|---|
| | | | | | | Ca (cmol/kg) | $Mg^{2+}$ (cmol/kg) | K (cmol/kg) | Na (cmol/kg) | | | |
| $SSP_1$ | Upper course | | | | | | | | | | | |
| 0-15 cm | 5.2±0.265$^{a}$ | 17.3±0.351$^{a}$ | 0.1±0.404$^{a}$ | 0.9±0.100$^{a}$ | 1.5±0.173$^{a}$ | 2.7±0.503$^{a}$ | 1.7±0.265$^{a}$ | 0.2±0.022$^{a}$ | 0.1±0.015$^{a}$ | 0.9±0.202$^{a}$ | 5.6±0.421$^{a}$ | 83.1±2.403$^{a}$ |
| 15-30 cm | 4.5±0.557$^{a}$ | 13.3±0.818$^{b}$ | 0.6±0.012$^{b}$ | 0.4±0.091$^{b}$ | 0.7±0.157$^{b}$ | 2.7±0.321$^{a}$ | 1.1±0.115$^{b}$ | 0.1±0.022$^{b}$ | 0.1±0.005$^{b}$ | 1.1±0.129$^{a}$ | 5.0±0.315$^{a}$ | 78.5±1.263$^{a}$ |
| 30-45cm | 4.9±0.321$^{a}$ | 8.9±0.404$^{c}$ | 0.05±0.010$^{b}$ | 0.5±0.126$^{c}$ | 0.8±0.183$^{b}$ | 2.6±1.155$^{a}$ | 1.2±0.152$^{b}$ | 0.1±0.010$^{c}$ | 0.1±0.003 $^{b}$ | 1.1±0.092$^{a}$ | 5.1±0.978$^{a}$ | 78.1±4.660$^{a}$ |
| Mean | 4.869 | 13.19 | 0.068 | 0.592 | 1.021 | 2.7 | 1.333 | 0.1 | 0.114 | 1.038 | 5.3 | 79.92 |
| Cv% | 8.5 | 4.8 | 21.1 | 17.3 | 17.4 | 27.1 | 14.1 | 13.7 | 10.3 | 9.5 | 13.5 | 3.6 |
| Se | 0.414 | 0.627 | 0.015 | 0.103 | 0.177 | 0.723 | 0.187 | 0.017 | 0.012 | 0.099 | 0.714 | 2.871 |
| $SSP_2$ | Middle course | | | | | | | | | | | |
| 0-15 cm | 5.6±0.127$^{a}$ | 21.6±1.273$^{a}$ | 0.3±0.021$^{a}$ | 0.9±0.035$^{a}$ | 1.6±0.037$^{a}$ | 3.5±1.273$^{a}$ | 1.7±0.707$^{b}$ | 0.1±0.032$^{a}$ | 0.1±0.017$^{a}$ | 1.0±0.778$^{a}$ | 6.6±0.261$^{ab}$ | 84.6±8.860$^{a}$ |
| 15-30 cm | 5.0±0.177$^{a}$ | 9.9±0.212$^{b}$ | 0.05±0.010$^{a}$ | 0.4±0.033$^{b}$ | 0.8±0.064$^{b}$ | 4.6±0.728$^{b}$ | 1.7±2.05$^{b}$ | 0.2±0.019$^{ab}$ | 0.1±0.006$^{a}$ | 0.9±0.707$^{a}$ | 7.4±2.085$^{a}$ | 88.1±12.49$^{a}$ |
| 30-45cm | 5.4±0.247$^{a}$ | 9.2±0.884$^{b}$ | 0.04±0.020$^{a}$ | 0.5 ±0.042$^{b}$ | 0.8±0.078$^{b}$ | 1.3±0.707$^{c}$ | 3.4±0.778$^{a}$ | 0.1±0.014$^{c}$ | 0.1±0.049$^{b}$ | 0.9±0.212$^{a}$ | 5.8±1.336$^{c}$ | 83.7±3.189$^{a}$ |
| Mean | 5.3 | 13.60 | 0.1 | 0.6 | 1.0 | 3.1 | 2.3 | 0.2 | 0.1 | 0.938 | 6.6 | 85.4 |
| Cv% | 8.0 | 7.7 | 164.5 | 15.0 | 14.9 | 14.9 | 17.6 | 14.6 | 11.7 | 21.7 | 8.9 | 3.8 |
| Se | 0.500 | 1.051 | 0.232 | 0.091 | 0.156 | 0.468 | 0.400 | 0.022 | 0.014 | 0.204 | 0.588 | 3.27 |
| $SSP_3$ | Lower course | | | | | | | | | | | |
| 0-15 cm | 5.0±0.085$^{a}$ | 23.7±1.473$^{b}$ | 0.1±0.016$^{b}$ | 1.3±0.625$^{a}$ | 2.2±1.078$^{a}$ | 3.6±0.451$^{a}$ | 1.3±0.503$^{a}$ | 0.1±0.018$^{b}$ | 0.1±0.012$^{b}$ | 0.8±0.132$^{a}$ | 5.9±0.411$^{b}$ | 86.8±1.348$^{b}$ |
| 15-30 cm | 5.2±0.200$^{a}$ | 27.2±2.002$^{a}$ | 0.2±0.025$^{a}$ | 2.3±0.626$^{a}$ | 4±1.079$^{a}$ | 4.2±0.764$^{a}$ | 2.5±0.473$^{a}$ | 0.2±0.013$^{a}$ | 0.2±0.022$^{a}$ | 0.8±0.127$^{a}$ | 7.8±1.009$^{a}$ | 90.03±0.88$^{a}$ |
| 30-45cm | 5.5±0.500$^{a}$ | 7.4±0.557$^{c}$ | 0.03±0.006$^{c}$ | 0.2±0.081$^{b}$ | 0.4 ±0.141$^{b}$ | 5±0.917$^{a}$ | 2.5±0.503$^{a}$ | 0.1 ±0.015$^{c}$ | 0.1±0.008$^{b}$ | 0.8± 0.136$^{a}$ | 8.5±1.080$^{a}$ | 90.8±0.710$^{a}$ |
| Mean | 5.2 | 19.4 | 0.1 | 1.3 | 2.2 | 6.0 | 2.1 | 0.1 | 0.1 | 0.8 | 7.4 | 89.2 |
| Cv% | 6.0 | 7.6 | 17.5 | 40.6 | 40.7 | 17.3 | 23.4 | 10.6 | 11.9 | 16.8 | 11.9 | 11.1 |
| Se | 0.315 | 1.479 | 0.018 | 0.513 | 0.885 | 0.736 | 0.493 | 0.015 | 0.015 | 0.132 | 0.886 | 1.017 |
| Overall mean | 5.15 | 15.4 | 0.1 | 0.82 | 1.41 | 3.9 | 1.9 | 0.14 | 0.12 | 0.92 | 14.4 | 86.2 |
| Overall CV | 7.5 | 6.7 | 17.9 | 24.3 | 24.3 | 19.7 | 18.3 | 13 | 11.3 | 15.9 | 11.4 | 6.2 |

*Different letters refers to significant differences between mean + standard deviation of different depth, similar letters refers to insignificant difference between mean+ standard deviation of different depths Se= standard error, CV% = coefficients of variation, P= phosphorous, N= nitrogen, OC= organic matter, OM= organic matter, Ca= calcium , Mg= magnesium, K= potassium, Na= sodium, EA= exchangeable acidity, ECEC= cation exchangeable capacity, BS=base saturation.*

***4.2 Chemical properties of soils***

The Soil pH ranged from 4.5 (strongly acidic) at $SSP_1$ to 5.6 at SSP $_3$ (moderately acidic) across the stations and depths, indicating no significant difference at P≥ 0.05 (Table 6). The result is consistent with the finding of Hazelton and Murphy (2007) who reported moderately acidic soils in Wouri River due to human activities (Tening et al., 2013), and high amounts of rainfall on soils dominated by acidic cations in parent material from which the soils are derived (Ahukaemere et al., 2015; Ubuoh and Ogbonna, 2018; Osujieke et al*.,* 2016; Ubuoh et al*.,* 2020[a]).

The mean values of available phosphorus ranged between 13.2-19.4 mg/kg$^{-1}$, with the overall mean value of 15.4 mg/kg and Cʋ of 6.7%, with $SSP_1$ recording the lowest value and the highest being $SSP_3$ followed by $SSP_2$, with significant different at P>0.05 level, at various soil depths and locations. However, the overall mean available phosphorus was <20 critical limits (Landon, 1991). The available phosphorus significantly varied across the depths at p<0.05 level, suspected to be due to excessive rainfall through the leaching of sandy soil (Ubuoh et al., 2013; Ubuoh and Ogbonna, 2018; Ubuoh et al., 2020b).

The mean nitrogen of the soils varied from 0.07-0.14%, with the overall mean value of 0.1% and Cʋ 17.9% respectively, with $SSP_1$ being the lowest and $SSP_2$ recording the highest followed by $SSP_3$, < 1.5 critical limit of N described as low in content (Esu, 1991), and ≤ 2.0 critical levels of N for soils of the humid tropics (Adeoye and Agboola, 1984), due to high rainfall (Brady and Weil, 2008). The total nitrogen significantly decreased down the soil depths at all the sample locations at p>0.05 level, which may be due to leaching. However, the total nitrogen of all sites recorded a low value compared to the rating of soils of southeastern Nigeria (Ubuoh et al*.,* 2010). Organic matter ranged from 1.0 -2.1%, with a mean value of 1.4% and Cʋ of 24%, with $SSP_1 \leq SSP_3 \geq SSP_2$. The organic matter content significantly varied across the depths at p ≥ 0.05. The result of OM in the study is within 0 to 3.9%, which was rated low (Enwezor et al*.,* 1989). Organic carbon ranged from 0.6-1.3%, having an overall mean value of 0.82% and overall Cʋ of 24.3%, with OC in order: $SSP_1 \leq SSP_3 \geq SSP_2$. The result of OC is less than (≤ 10%) critical value for agricultural soil (Esu, 1991). The low OC is suspected to be caused by poor soil management in the area and the sloppy land toward the River (Lal, 2018), and unsustainable farming activities along the slopes (Omuto and Vargas, 2018).

Exchangeable bases are $Ca^+$, $Mg^+$, $Na^+$ and $K^+$ (Ubuoh et al*.,* 2020[a]; Ubuoh et al*.,* 2020[b]). The mean result of calcium varied from 2.6 - 6 cmolkg$^{-1}$, having an overall mean of 3.9 cmolkg$^{-1}$ and an overall means Cʋ of 19.7%, with $SSP_1 \geq SSP_3 \geq SSP_2$. The overall mean value of Ca is within 2-5 soil critical limit (Esau, 1991), which may be due to organic materials from solid wastes (Tanimu et al., 2013). The result is against the findings of Edosomwan et al. (2001), Emmanuel et al. (2018) who reported low levels of Ca in most Nigerian soils, due to low decomposition of organic matter and slow release of chemical elements into the soil (Brady and Weil, 2008).

The mean of magnesium ranged from 1.3-2.3, with an overall mean of 1.9 and 18.3% Cʋ, with $SSP_1$ having the lowest value and the $SSP_2$ with the highest value ≥ $SSP_3$. The magnesium of the $SSP_2$ and $SSP_3$ showed a significant increase with depths while $SSP_1$ recorded a significant decrease. Generally, the $Mg^{2+}$ was higher than the critical level of 0.5cmolkg$^{-1}$ soil across the sample points (Landon, 1991), suspected from organic wastes (Tanimu et al., 2013), and against the finding of Emmanuel et al. (2018) who reported low $Mg^{2+}$ in Nigerian soils.

The mean value of potassium varied from 0.12-0.2 cmolkg$^{-1}$, with the overall mean of 0.14 cmolkg$^{-1}$, having 13% Cʋ respectively, with the mean order: $SSP_1 \leq SSP_2 \geq SSP_3$. The exchangeable potassium ($K^+$) significantly varied across the soil depths at *P*≥0.05, with the overall mean of $K^+$ less than ≥0.6 cmol/kg critical limit (Landon,1991). The result is a variant of the findings of Edosomwan et al. (2001), Emmanuel et al. (2018) that reported low $K^+$ in the tropical soil due to the high tropical rainfall and low decomposition of organic matter soil. The mean sodium varied from 0.114-0.126 cmolkg$^{-1}$ having the mean value of 0.12 cmolkg$^{-1}$ less than 1cmolkg$^{-1}$ soil critical limit (Landon, 1991), having 11.3%Cʋ, with location order: $SSP_1 \leq SSP_3 \geq SSP_2$. The exchangeable sodium content varied significantly across the soil depths at P≥0.05.

The mean Exchangeable acidity as acid cation ($H^+$ $AL^{3+}$ ) varied from 0.8-1.0 cmolkg$^{-1}$, with the overall mean value of 0.9 cmolkg$^{-1}$, less than 1.1 cmolkg$^{-1}$ obtained from farmland in Kano (Adamu *et al.*,2014), with 15.9% Cʋ with the mean order: $SSP_3 \leq SSP_1 \leq SSP_2$, having no significant differences across the soil depths and locations at *P*≥0.05. Low EA may result in an increase in soil acidity that results in toxicity in soil (George, 2009).

The effective cation exchange capacity (ECEC) of the soils ranged from 5.1-8.5 cmolkg$^{-1}$ across the three stations and soil depths, greater than 3.7-4.9 cmol/kg ECEC rated low (Benton, 1999), 4.31 cmolkg$^{-1}$ ECEC in soils around River Wouri in Cameroun (Norbert et al., 2018). However, the cation exchange capacity values obtained in this study were below the value of 20 cmol/kg-$^1$ reported as being suitable for crop production (FAO, 1995). Meanwhile, where the cation exchange capacity of the soil is ≤ 5, such soil is inherently infertile (Christian and Beniah, 2020), due to leaching through excessive rainfall (Njoku, 2017).

The base saturation of the soils ranged from 78.1–to 90.8% across the three-course streams and depths. Base saturation had mean values of 86.2% for the study catchment was greater than the FMEnv/WHO limits of 80% at some stations (FMEnv, 1991). Generally, the base saturation is relatively high in moderately weathered soils that formed from the basement complex (Draft Report, 2016). Based on the classification of Cʋ variations by Lian et al. (2019), pH, phosphate, potassium, ECEC, and base saturation Cʋ were below Cʋ ≤ 15%, an indication of low, nitrate, organic matter and carbon, calcium, manganese, sodium, and EA fall within 15% ≤ Cʋ ≤ 36% that indicate medium variation in soil respectively.

**Table 7.** Comparison of soil nutrients with agricultural soil in Nworie River Catchment.

| Soil nutrients | Ratings of soil nutrients: Loganathan, 1987 | | | | | The study: Nworie River | Remark |
|---|---|---|---|---|---|---|---|
| | Very low | Low | Moderate | High | Very high | | |
| (Total N, %) | <0.05 | 0.05–0.15 | 0.15–0.20 | 0.20–0.30 | >0.30 | 0.068 - 0.140 | Very low –low |
| (available P, Bray and Kurtz No.1, ppm) | <3 | 3 – 10 | 10 – 20 | 20 – 30 | > 30 | 13.19 - 19.42 | Moderate |
| (exchangeable K, meq/100g) | <0.2 | 0.2–0.3 | 0.3–0.6 | 0.6–1.0 | > 1.0 | 0.124 - 0.150 | Very low |
| (exchangeable Ca meq/100g) | <2 | 2 – 5 | 5 – 10 | 10 – 20 | > 20 | 2.667 - 6.000 | Low- moderate |
| (exchangeable Mg, meq/100g) | <0.3 | 0.3–1 | 1 – 3 | 3 – 8 | > 8 | 1.333 - 2.26 | Moderate |

From the comparison of rating of the selected soil nutrient values in agricultural soils by Loganathan (1987) to Nworie River catchment agricultural, soil (Table 7). The total N of the study was recorded low, which is in tandem with the finding of Enwezor et al. (1988) who reported low to medium total nitrogen (0.15 – > 0.20%) in Nworie River agricultural soil, available P (moderate), as Enwezor et al. (1988) reported low, moderate and high available P in Nworie soil. Exchangeable K (very low), exchangeable Ca (low - moderate), and exchangeable Mg (moderate) agreed with the finding of Isirimah et al. (2003). Low to moderate nutrient values in agricultural soil in Nworie River catchment were recorded along the slopes toward the river course, reflecting the impact of human activities on soil nutrients.

**Table 8.** Mean ±SD of heavy metals of soil in Nworie River Catchment.

| Location | Depth(cm) | Heavy metals (mg/kg$^{-1}$) | | | | | |
|---|---|---|---|---|---|---|---|
| | | Cd | Cr | Cu | Fe | Pb | Zn |
| $SSP_1$ | 0 – 15 | 0.25± 0.067$^a$ | 0.012± 0.012$^a$ | 0.37± 0.038$^c$ | 16.67 ± 0.332$^a$ | 0.95± 0.067$^a$ | 8.83± 0.216$^a$ |
| Upper course | 15 – 30 | 0.04± 0.210$^b$ | 0.03± 0.102$^a$ | 0.68± 0.167$^b$ | 13.85 ± 0.225$^b$ | 0.76± 0.104$^b$ | 6.33± 0.276$^b$ |
| | 30 – 45 | 0.09± 0.032$^b$ | 0.08± 0.022$^a$ | 1.31± 0.169$^a$ | 12.80 ± 0.166$^c$ | 0.92± 0.090$^{ab}$ | 4.89± 0.020$^c$ |
| | Mean | 0.125 | 0.044 | 0.786 | 14.44 | 0.878 | 6.683 |
| | %Cυ | 34.5 | 139.0 | 17.7 | 1.7 | 9.9 | 10.6 |
| | Se | 0.043 | 0.061 | 0.139 | 0.239 | 0.087 | 0.700 |
| $SSP_2$ | 0 – 15 | 0.04± 0.012$^b$ | 0.02± 0.014$^a$ | 0.61± 0.125$^a$ | 12.47± 0.053$^{ab}$ | 2.25± 0.210$^a$ | 3.96± 0.078$^c$ |
| Middle course | 15 – 30 | 0.14± 0.067$^a$ | 0.02±0.010$^a$ | 0.4± 0.163$^{ab}$ | 8.83± 0.237$^c$ | 0.78± 0.151$^b$ | 5.83± 0.216$^b$ |
| | 30 – 45 | 0.04± 0.006$^b$ | 0.03± 0.016$^a$ | 0.47± 0.065$^c$ | 14.93± 0.117$^a$ | 1.09± 0.185$^a$ | 8.02± 0.306$^a$ |
| | Mean | 0.072 | 0,021 | 0,462 | 12.08 | 1.373 | 5,937 |
| | %Cυ | 54.0 | 61.8 | 26.9 | 1.3 | 13.4 | 3.7 |
| | Se | 0.039 | 0.013 | 0.124 | 0.155 | 0.183 | 0.220 |
| $SSP_3$ | 0 – 15 | 0.05± 0.006$^b$ | 0.05± 0.035$^a$ | 0.22± 0.120$^b$ | 11.43 ± 0.147$^c$ | 0.94± 0.080$^b$ | 6.35± 0.150$^b$ |
| Lower course | 15 – 30 | 0.23± 0.074$^a$ | 0.02± 0.002$^a$ | 1.04± 0.173$^a$ | 17.64 ± 0.195$^a$ | 1.41± 0.137$^a$ | 9.58± 0.204$^a$ |
| | 30 – 45 | 0.03± 0.013$^b$ | 0.01± 0.013$^a$ | 0.23± 0.083$^b$ | 14.95 ± 0.127$^b$ | 0.717 ± 0.273$^b$ | 9.35± 0.575$^a$ |
| | Mean | 0.10 | 0.03 | 0.50 | 14.7 | 1.02 | 8.42 |
| | %Cυ | 42.9 | 84.9 | 26.4 | 1.1 | 17.8 | 4.3 |
| | Se | 0.043 | 0.021 | 0.130 | 0.159 | 0.182 | 0.363 |
| OCV | | 43.8 | 95.2 | 23.7 | 1.4 | 13.7 | 6.2 |
| Omv | | 0.10 | 0.03 | 0.6 | 13.7 | 1.1 | 7.0 |

*Different letters refer to significant differences between mean + standard deviation of different depths, similar letters refer to the insignificant difference between mean+ standard deviation of different depths.SSP- Soil sampling point, OCV- Overall coefficient value, OMV-Overall mean value*

### *4.3 Heavy metal concentration in soil*

Table 8 presents the summary of the heavy metals in agricultural soil samples from the study locations. The mean cadmium (Cd) ranged from 0.07–0.125 mgkg$^{-1}$, $SSP_2$ recording the lowest value and $SSP_1$ with the highest value ≥ $SSP_3$, less than cadmium concentrations in soil that ranged between 0.25 - 1.64 mg/kg-$^{1}$ in Accra (Fosu-Mensah et al., 2017). The overall mean of Cd (0.10) in all agricultural soil falls below the WHO/FAO (2001) permissible limit of 3 mg/kg for soils. The level of cadmium concentration decreased with depth and varied significantly across the soil depths and study locations at $P \geq 0.05$ level. The level of Cd in this study was found to be lower than values obtained in soils of Malaysia (Yap et al., 2003), and within the range of results obtained in Lagos, Nigeria (Okereke et al., 2019), less than 1.8 mgkg$^{-1}$ in agricultural soils near a dumpsite in Umuahia, Abia State, Nigeria (Ubuoh et al, 2019).

The mean chromium (Cr) ranged from 0.02 -0.04 mgkg$^{-1}$, with $SSP_2 \leq SSP_1 \geq SSP_3$, with the overall mean value of 0.03 mg kg$^{-1}$ less than the range of 22.4-102.04 mg kg$^{-1}$ by Mohammed et al. (2015). The result of Cr is far less than Cr ranging from 2.28 mg/kg at $S_3$ to 56.00 mg/kg at $S_1$ with a mean value of 11.55 mg/kg-$^{1}$ in e-waste dumpsite in Accra (Fosu-Mensah et al., 2017), and the high contents of Cr recorded may come from solid wastes deposition

(Fosu-Mensah et al., 2017). The Cr recorded no significant difference between the study locations and soil depths at $P \geq 0.05$. The overall mean of Copper (Cu) in soil samples was recorded at 0.6 mg/kg$^{-1}$ and ranges from 0.462 - 0.495 mgkg$^{-1}$, with $SSP_1$ being the lowest and $SSP_3$ being the highest $>SSP_2$, and far above the Cu (202.99 mg/kg) in soils at Korle Lagoon area in Accra, Ghana (Fosu-Mensah et al., 2017), with the overall mean value of Cu in the soil below the WHO/FAO (2001) permissible limit of 100 mg/kg$^{-1}$ for soils, but above 0.2 (Esu, 1991). The copper concentration increased significantly with soil depths and locations at $P \geq 0.05$. The variations in the concentration of Cu in the stations may be due to vehicle flow, household and medical waste materials as copper is commonly found in electrical wirings, engine wear, brake linings, and some medical materials (Manno et al., 2006).

The iron (Fe) content varied from 12.08 - 14.67 mg kg$^{-1}$ with $SSP_2 \leq SSP_3 \leq SSP_1$, having an overall mean value of 13.7 mg kg$^{-1}$, less than Fe mean of 29.1 mg kg$^{-1}$ in agricultural soils in Northern China (Yushu et al., 2013), and far below the average Fe (10351.83 mg kg$^{-1}$ in agricultural soils of Siling Reservoir Watershed in Zhejiang Province, China (Naveedullah et al., 2013). The Fe concentration decreased significantly with depths and locations at $P \geq 0.05$ level. It is reported that Fe between 0.1 to 50–100 µg/g in soil within a few weeks, can a be a problem in lowland acid soils suffering from weathering (FAO, 2006), and in toxicity is mostly associated with highly acidic soil leading to nutrient deficiencies like SOM, N, P and K (FAO, 2006). Lead (Pb) concentration varied from 0.9 - 1.4 mg kg$^{-1}$, in order of $SSP_1 < SSP_2 > SSP_3$ with the mean value of 1.1 mg kg$^{-1}$greater than Pb in soils 0.0001-1.41mg/kg (Mohammed and Folorunsho, 2015), and less than 25.76 mg/kg in agricultural soil in Buriganga riverbank (Rahaman et al., 2016). Significant variations of Pb were observed across the depths and locations at $P > 0.05$ level. The mean value of Zinc (Zn) ranged from 5,937 - 8.424 mg kg$^{-1}$, in order: $SSP_2 < SSP_3 > SSP_1$, with the overall mean value of 7.0 mg kg$^{-1}$, less than the mean value of 8.68 mg/kg in agricultural soil (Fosu-Mensah et al., 2017), 75.6 mg kg$^{-1}$ Beijing (Wu et al., 2010) respectively. The mean value of Zn of the study was below the WHO/FAO (2001) permissible limit of 300.00 mg/kg for soils. The presence of zinc in soil could be attributed to municipal wastes (Bai et al., 2011; Ubuoh et al., 2014).

**Table 9.** Comparison of heavy metals in agricultural soil with existing standards (mg/kg) globally

| Standard | Cr | Cu | Zn | Cd | Pb | Fe |
|---|---|---|---|---|---|---|
| CCME[a] | 64 | 63 | 200 | 1.4 | 70 | - |
| Dutch intervention value[b] | 180 | 190 | 720 | 13 | 530 | - |
| USEPA[c] | - | 30 | - | - | 10 | - |
| WHO | - | 4 | 50 | 0.3 | 20 | 47,200 |
| FAO | - | 0.2 | 2.0 | 0.01 | 5 | - |
| Present study | 0.1.0 | 0.03 | 0.6 | 13.7 | 1.1 | 7.0 |
| [a] Canadian soil quality guidelines for the Protection of Environment and Human Health, 2007 | | | | | | |
| [b]VROM 2009 | | | | | | |
| United State Environmental Protection Agency | | | | | | |
| WHO World Health Organization, FAO Food, and Agriculture Organization (United Nations) | | | | | | |

To understand the status of heavy metal concentrations in agricultural soils in the Nworie River catchment, a comparison of the results obtained in the study with other studies in agricultural soils from different regions of the world was made (Table 9). The mean concentration of Cr, Cu, Zn, Pb, and Fe (WHO/FAO) only in soil samples are under the Dutch intervention value (180, 190, 720, 13, and 530 mg/kg respectively). These values were below the standard of the world guidelines recognized by World Health Organization (WHO/FAO) limits. Accordingly, the concentrations of Cr, Cu, Zn, and Pb in samples are lower than the Canadian quality guidelines for agricultural soils (CCME) (Table 9). Meanwhile, the obtained value of Cd exceeds the standard value (1.4 mg/kg) recommended by the Canadian soil contamination, CCME, and WHO/FAO guidelines, suspected to be from industrial and domestic wastes (Bohn et al., 1985). The result is in consonant with the finding of Oumenskou et al. (2018) who reported the exceedance of Cd in agricultural soils from Beni Amir in Tadla plain, Morocco. It is reported that Cd is toxic even in small concentrations in soil (Oumenskou et al., 2018), resulting in changes in the size, composition, and activity of soil microbial community ( Liao et al., 2005).

**Table 10.** Correlation coefficients between different heavy metals in the soil around Nworie River catchment

| Soil sample point | | Cd | Cr | Cu | Fe | Pb | Zn |
|---|---|---|---|---|---|---|---|
| $SSP_1$ | Cd | 1.000 | | | | | |
| (Upper course) | Cr | -0.309 | 1.000 | | | | |
| | Cu | -0.515 | 0.013 | 1.000 | | | |
| | Fe | 0.816 | -0.162 | -0.856 | 1.000 | | |
| | Pb | 0.603 | 0.005 | 0.185 | 0.319 | 1.000 | |
| | Zn | 0.681 | -0.236 | -0.916 | 0.940 | 0.062 | 1.000 |
| | | | | | | | |
| $SSP_2$ | Cd | 1.000 | | | | | |
| (Middle course) | Cr | 0.208 | 1.000 | | | | |
| | Cu | 0.139 | 0.039 | 1.000 | | | |
| | Fe | -0.789 | 0.237 | -0.172 | 1.000 | | |
| | Pb | -0.508 | -0.132 | 0.716 | 0.298 | 1.000 | |
| | Zn | -0.028 | 0.459 | -0.672 | 0.442 | -0.675 | 1.000 |
| | | | | | | | |
| $SSP_3$ | Cd | 1.000 | | | | | |
| Lower course | Cr | -0.280 | 1.000 | | | | |
| | Cu | 0.968 | -0.350 | 1.000 | | | |
| | Fe | 0.742 | -0.603 | 0.804 | 1000 | | |
| | Pb | 0.860 | -0.091 | 0.832 | 0.547 | 1.000 | |
| | Zn | 0.458 | -0.682 | 0.545 | 0.913 | 0.207 | 1.000 |

*SSP-Soil sample point. Correlation is significant at the 0.01 level (two-tailed).*

### *4.4 Correlation Matrix of Heavy Metals in the Soil*

To obtain more reliable information about the relationships among the variables, factor analysis was applied (Bartolomeo et al., 2004). Regression values for the relationship were characterized as negative when $-1 \leq 0$ and positive when $\geq 0 \leq 1$ (Verla et al., 2020). The correlation identifies the source and movement of metals among heavy metals (Wang et al., 2017). Pearson's correlation coefficients among heavy metals in the studied agricultural soil along the valley slopes of Nworie River are presented in Table 10. Many metal pairs had positive correlations ($P<0.01$) in soils along Nworie River catchments. The correlation relationship in $SSP_1$ indicates that Cd is negatively correlated with Cu ($r^2$: -0.515), and positively associated with Fe ($r^2$: 0.816), Pb ($r^2$: 0.603), Zn ($r^2$: 0.681) respectively. Cu is negatively associated with Fe ($r^2$: -0.856), Zn ($r^2$: -0.916) respectively and Fe is positively associated with Zn ($r^2$: 0.940). At $SSP_2$, Cd is negatively associated with Fe ($r^2$: -0.789) and Pb (r: -0.508). The Cu is positive with Pb ($r^2$: 0.716) and negative with Zn ($r^2$: -0.672). At $SSP_3$, Cd is positively associated with Cu ($r^2$: 0.968), Fe ($r^2$: 0.742), Pb ($r^2$: 0.860) respectively, Cr negative with Fe, Zn ($r^2$: -0.603; -0.682) respectively. Copper was positively correlated with Fe ($r^2$: 0.804), Pb ($r^2$: 0.832), Zn ($r^2$: 0.545). Fe indicates a positive association with Pb ($r^2$: 0.547) and Zn ($r^2$: 0.913) at $p< 0.01$, in soil within the Nworie River catchment. This observation is in line with the finding of Lian et al. (2019), who reported a highly positive correlation among metals from the same source. The sources of metals in agricultural soils of the study are in agreement with the findings of Enyoh and Isiuku (2020), and Ubuoh et al. (2020[c]) who observed that the mixed sources like artisanal activities, metal processing works, surface run-off, vehicle emissions, and agricultural activities may be responsible for soil pollution in flood basin in Amakohia, Owerri, Nigeria. Previous studies have also shown that these sources play a major role in introducing metals into the environment (Verla et al., 2017; Verla et al., 2020; Isiuku and Enyoh, 2020).

**Table 10.** Comparison of heavy metal concentrations in the soils from other regions of the world with this study

| Author | Cr | Cu | Zn | Cd | Pb | Fe | Location |
|---|---|---|---|---|---|---|---|
| This study | 0.03 | 0.6 | 7.0 | 0.19 | 1.1 | 13.7 | Nworie River (agric. Soil)Nigeria |
| Rodríguez Martín et al. (2013) | 29.6 | 25.7 | 65.7 | 0.4 | 25.6 | - | Almería (Spain) |
| Sun et al. (2013) | 49.7 | 18.9 | 58.9 | - | 35.4 | - | Dehui (China) |
| Cai et al. (2012) | 27.61 | 16.74 | 57.21 | 0.10 | 44.66 | - | Huizhou (China) |
| Nanos and Martin (2012) | 20.53 | 11.01 | 42.42 | 0.159 | 14.06 | - | Duero basin (Spain) |
| Acosta et al. (2011) | 17.6 | 11 | 18.4 | 0.22 | 48.9 | - | Murcia (Spain) medians |
| Parizanganeh et al. (2012) | - | 67.68 | 299.31 | 1 .4 | 58.18 | - | Zanjan Province (Iran) |
| Huang et al. (2007) | 77.2 | 33.9 | 98.1 | 0.3 | 35.7 | - | Yangzhong District (China) |
| Zhao et al. (2007 | 58.6 | 40.4 | 112.9 | 0.14 | 46.7 | - | Wuxi (China) |
| Li et al. (2009) | 64.65 | 24.0 | 162.6 | 0.28 | 58.0 | - | Guangzhou (China) |
| Benlkhoubi et al. (2015) | 7.81 | 37.61 | 105.56 | 7.81 | 26.71 | - | Sebou basin-Kenitra (Morocco) |
| Tomgouani et al. (2007) | 5.25 | 10.91 | 20.12 | 0.21 | 29.66 | - | Settat (Morocco) |
| Oumenskou et al. (2018) | 57.0 | 25.9 | 294.7 | 1.8 | 33.3 | - | Beni Amir perimeter (Morocco) |

Table 11 lists the contents of heavy metals sampled in soil within Nworie River catchment were lower than areas compared with, except Cadmium (Cd) and Fe in some cases. The Cd (0.19 mg kg$^{-1}$) in soil within Nworie River catchment was slightly higher than 0.10 mg kg$^{-1}$ Huizhou (China) (Cai et al., 2012), 0.159 mg kg$^{-1}$ Duero basin (Spain) (Nanos and Martin, 2012). Iron (Fe) with 13.7 mg kg$^{-1}$ recorded the highest, while compared locations recorded none. The factor that might influence the higher concentration of Cu, Cd, and Mn in agricultural soil in Nworie River catchment is an anthropogenic activity from the surrounding area (Owanda et al., 2018). The mean result of Cr, Cu, Zn, and Pb in the agricultural soil of Nworie River catchment are far less than soils from different regions of the world indicated in Table 11.

**Table 12.** Rotated Loading Matrix of the physicochemical characteristics and heavy metals in agricultural soil

| Principal component (PC) as factorial loading | | | | | | |
|---|---|---|---|---|---|---|
| Soil Quality as Item | $PC_1$ | $PC_2$ | $PC_3$ | $PC_4$ | $PC_5$ | $PC_6$ |
| Physical soil tracer | | | | | | |
| Sand | -0.118 | -0.977 | 0.037 | 0.129 | -0.004 | -0.015 |
| Silt | 0.212 | 0.916 | 0.053 | -0.147 | -0.112 | 0.207 |
| Clay | -0.208 | 0.611 | -0.264 | -0.01 | 0.323 | -0.526 |
| Chemical soil tracer | | | | | | |
| pH ($H_2O$) | -0.053 | -0.166 | 0.184 | 0.64 | 0.496 | -0.086 |
| Phosphorous (Avail. P) | 0.818 | 0.22 | 0.026 | -0.129 | 0.414 | -0.183 |
| Nitrogen (avail. N) | 0.211 | 0.053 | 0 | 0.023 | 0.74 | 0.067 |
| Org. C. (OC) | 0.889 | 0.24 | 0.079 | 0.093 | 0.139 | 0.008 |
| OrgM (OM) | 0.889 | 0.24 | 0.079 | 0.092 | 0.139 | 0.008 |
| Calcium ( Ca) | 0.079 | 0.038 | 0.97 | -0.124 | 0.015 | -0.023 |
| Magnesium (Mg) | 0.036 | -0.197 | 0.016 | 0.823 | -0.044 | -0.227 |
| Potassium (K) | 0.779 | -0.24 | 0.155 | -0.044 | 0.37 | -0.114 |
| Sodium (NA) | 0.828 | -0.077 | 0.245 | 0.195 | 0.169 | 0.202 |
| Exch A (EA) | -0.2 | -0.027 | -0.388 | -0.118 | 0.242 | 0.682 |
| Exch C | 0.107 | -0.093 | 0.869 | 0.356 | 0.032 | -0.079 |
| Base saturation (BS) | 0.263 | -0.098 | 0.771 | 0.22 | -0.045 | -0.486 |
| Heavy metals | | | | | | |
| Iron | 0.337 | 0.557 | -0.199 | 0.642 | -0.101 | -0.011 |
| Zinc | 0.27 | 0.254 | 0.148 | 0.676 | -0.428 | -0.345 |
| Lead | 0.339 | -0.049 | -0.022 | 0.053 | 0.847 | 0.077 |
| Copper | 0.268 | 0.178 | -0.093 | -0.12 | 0.007 | 0.832 |
| Cadmium | 0.735 | 0.062 | 0.002 | 0.151 | -0.32 | 0.228 |
| Chromium | -0.053 | 0.164 | -0.267 | -0.554 | -0.173 | -0.186 |
| Total Eigenvector | 4.737 | 2.922 | 2.788 | 2.62 | 2.394 | 2.082 |
| % of Variance | 22.6 | 13.914 | 13.276 | 12.478 | 11.399 | 9.916 |
| Cumulative % | 22.556 | 36.47 | 49.746 | 62.224 | 73.623 | 83.539 |

*P(0.05)*

### *4.5 Principal Component Analysis (PCA)*

Principal component analysis (PCA) has been used to infer the hypothetical source of heavy metals (natural or anthropogenic) (Li et al. 2009; Yi et al. 2011). In this study, heavy metals were grouped into a six-component model, which accounted for 83.5 % of all the data variation (Table 12). The initial component matrix indicated that the first PC ($PC_1$, variance of 22.6 %) included 25 variables. Meanwhile, out of twenty-five variables, Phosphorous, organic carbon, organic matter, magnesium, sodium, and cadmium were positively loaded as anthropogenic components and may originate from similar pollution sources (Ghrefat and Nigem, 2006; Shan et al., 2013; Lian et al., 2019). The only metal (Cd) may have originated from farming practices (Atafar et al. 2010; Xue et al., 2014), like commercial phosphate and inorganic fertilizers applications (Nziguheba and Smolders 2008).

The component ($PC_2$), with a variance of 13.9% was negatively loaded with sand and positively loaded with silt and clay respectively. The result is in tandem with the finding of Moss et al. (1975), and Lautridou and Ozouf (2016) who reported that soil fractions originated from a variety of physical processes; involving chemical weathering of rock and physical weathering processes.

The $PC_3$ with the variance of13.3% was positively loaded with exchangeable cation and percentage basic saturation. The positive loading between CEC and base saturation was observed by Gaspar (2019) who reported that Mg content in crops and plants increased as Mg saturation of the CEC increased. Meanwhile, Dassenakis et al. (2003), Yuan et al. (2004), Ubuoh et al. (2021) have used the concentrations of the exchangeable fraction as an indicator of anthropogenic impact on the environment. The $PC_4$ with a variance of 12.5% was positively loaded with Mn, Fe, and Zn. It has been reported that Zn can be associated with Fe and Mn oxides of the soil or sediments (Ramos et al., 1999), and Zn can originate from farming practices, which is in agreement with the finding of Shan et al. (2013). The $PC_5$ with a variance of 11.4% was positively loaded with Pb. The lead and zinc in soil may have originated from vehicles tire wear and solid wastes (Shan et al., 2013), signifying anthropogenic sources (Ghrefat and Nigem, 2006) while $PC_6$ with a variance of 9.9% was positively loaded with exchangeable acidity and cadmium, which indicate that positively loaded metals in soils may be influenced by terrestrial inputs (Benoit et al., 1994; De Souza Machado et al., 2016).

#### *4.5 Pollution assessment indices for the heavy metals in the soil*

**Table 13.** Geo-accumulation index ($I\text{-}_{geo}$) of heavy metals of soil in Nworie River watershed

| Stations | Cd | Cr | Cu | Fe | Pb | Zn |
|---|---|---|---|---|---|---|
| $SSP_1$ | 0.768 | 7.5 | 0.019 | 0.217 | 0.026 | 0.056 |
| $SSP_2$ | 0.444 | 3.7 | 0.011 | 0.182 | 0.041 | 0.050 |
| $SSP_3$ | 0.629 | 4.3 | 3.9 | 0.221 | 0.031 | 0.071 |
| Mean | 0.613 | 1.5 | 0.011 | 0.206 | 0.033 | 0.059 |
| Remark | UM: $0 \le I_{-geo} \le 1$. | Mc: $1 \le I_{geo} \le 2$ | Mc: $0 \le I_{-geo} \le 1$ | UM: $0 \le I_{-geo} \le 1$. | Mc: $0 \le I\text{-}_{geo} \le 1$ | Mc: $0 \le I\text{-}_{geo} \le 1$ |

*UM: Uncontaminated-moderate, MC: Moderately contaminated.*

#### *4.6 Geo-accumulation index ($I_{-geo}$)*

Soil quality was measured using the I-geo index of classification proposed by Muller (1981) (Table 13). The mean I-geo Index values of agricultural soil samples within Nworie River watershed are indicated and the calculated $I_{-geo}$ values of Cd ranged between approximately 0.4 to 0.8, with the mean value of 0.6 as uncontaminated to moderately contaminated ($0 \le I_{-geo} \le 1$ ), Cr (3.7 to 7.5), with the mean of 1.5 as moderately contaminated ($1 \le I_{-geo} \le 2$), Cu (0.011 to 3.9), with the mean value of 0.011, Fe (0.182 to 0.221) with the mean of 0.21, Pb (0.03 to 0.041), with the mean 0.033 and Zn (0.050 to 0.071), with the mean of 0.059, indicating uncontaminated to moderately contaminated ($0 \le I_{-geo} \le 1$ ) respectively. Thus, the $I_{-geo}$ results of the sampled heavy metals in soils classified as uncontaminated to moderately contaminated according to Müller (1969) classes, are suspected to be due to human activities like agricultural practices and mining. The heavy metals responsible for the geo-accumulation in the soils are in a decreased sequence of: Cr ≥ Cd ≥ Fe ≥ Zn ≥ Pb ≥ Cu, constituting 61.93%, 25.31%, and 8.51%, 2.44% 1.36%, and 0.45% with a percentage of Cr dominating. Chromium had been in the parent materials of soils with little temporal and spatial variation in worldwide rural soils (Wu et al., 2010). Chromium toxicity can induce alterations in growth, photosynthesis, gas exchange attributes, and yield formation in crops (Anjum et al., 2016) and adversely affect soil microorganisms (Adriano 2017). From an environmental pollution perspective, Zn is often considered a toxic element, but very insoluble and very rare (Alloway, 1990). On the other hand, Cd has no essential biological function and is a highly toxic metal to plants and animals (Chen et al., 2019).

**Table 14.** Contamination Factor, degree of contamination, and pollution load Index of heavy metals in the soil of Nworie River watershed

| Stations | Contamination factor (cf) | | | | | | C/degree | PL1 |
|---|---|---|---|---|---|---|---|---|
| | Cd | Cr | Cu | Fe | Pb | Zn | | |
| $SSP_1$ | 3.826 | 3.7 | 0.094 | 1.083 | 0.132 | 0.280 | 5.419 ( 39.21% ) | 0.225 |
| $SSP_2$ | 2.214 | 1.9 | 0.055 | 0.906 | 0.206 | 0.251 | 3.634 (26.31%) | 0.107 |
| $SSP^3$ | 3.133 | 2.1 | 0.019 | 1.101 | 0.153 | 0.356 | 4.764(34.47 %) | 0.117 |
| Mean | 3.058 | 2.6 | 0.056 | 1.030 | 0.164 | 0.296 | 4.606 | 0.150 |
| Remark | 3 <cf< 6 (CC) | 1<cf<3 (MC) | cf< 1 (LC) | 1<cf<3 (MC) | cf< 1 (LC) | cf< 1 (LC) | < 8 (LDC) | 0.150 ≤ 1 (NP) |
| Percentage (%) | 42.4 | 36.0 | 0.7 | 14.2 | 2.2 | 4.1 | 13.82 | 0.449 |
| CC: Considerably contaminated, LC: Low contamination, MC: Moderate contamination, LDC: Low degree of contamination, NP:No pollution | | | | | | | | |

#### *4.6 Contamination Factor (CF), Degree of Contamination (CD), and Pollution Load Index (PLI)*

Table 14 lists the contamination factor of heavy metals in soil is between CF<1 which indicates low contamination, 1<CF<3 indicating moderate contamination, and 3<CF<6 indicating considerably contaminated. The degree of contamination in the table is <8, which indicates a low degree of contamination. While the pollution load index (PLI) is ≤ 1 indicates no pollution. The contamination factor, degree of contaminant and the pollution load of the heavy metals from the soil of Nworie River at $SSP_1$- $SSP_3$ are in Table 14. The table showed that at the three stations, cadmium (Cd) and iron (Fe) had contamination factors that ranged from 2.214 – 3.826 and 0.906 – 1.101 which were ≥ one (1), as categorized by Hakason (1980). The result showed that the soil had considerable contamination of Cd, which agrees with the finding of Chai et al. (2014) who reported the highest Cd having anthropogenic origins in Bohai Bay, China. The Cr and Fe recorded moderate contamination, while Cu, Pb, and Zn were ≤ zero (0) at $SSP_3$, indicating that the soils of the Nworie River are low contaminated, with the percentage of contamination factors ranging between approximately 0.7-42.4% in decreasing order of Cd ≥ Cr ≥ Fe ≥ Zn ≥ Pb ≥ Cu. The degree of contaminant (CD) ranges from 3.634 - 5.419 with $SSP_1$ having the highest degree and $SSP_2$ having the lowest in the soil of Nworie which was ≤ 8 degrees of contaminant stipulated by (Hakanson, 1980). The percentage of contamination degree of sampling points was in a decreased sequence of $SSP_1 \geq SSP_3 \geq SSP_2$, constituting 39.21%, 34.47 %, and 26.31% respectively.

The table showed that pollution load ranged from 0.225 in $SSP_1$ to 0.107 in $SSP_3$, in a decrease sequence of $SSP_1 \geq SSP_3 \geq SSP_2$, with the overall mean PLI recording 0.150≤ 1 with approximately 0.45% indicating no pollution by Tomlinson et al. (1980). This implies that the soil at the different course streams was not polluted by the heavy metals (Ubuoh et al., 2016), with the source being geogenic.

### *4.7 Ecological risk assessment*

**Table 15.** Ecological Risk Factor and Risk Index of Heavy Metals in the soil of Nworie Riverwatershed

| Stations | Ecological Risk Factor (Er) | | | | | Risk Index (Ir) |
|---|---|---|---|---|---|---|
| | Cd | Cr | Cu | Pb | Zn | |
| Station 1: ($SSP_1$) | 97.80 | $7.4x10^{-3}$ | 0.470 | 0.660 | 0.280 | 99.217 |
| Station 2: ($SSP_2$) | 66.42 | $3.8x10^{-3}$ | 0.275 | 1.030 | 0.251 | 67.980 |
| Station 3: ($SSP_3$) | 93.99 | $4.2x10^{-3}$ | 0.095 | 0.765 | 0.356 | 95.210 |
| Mean | 86.07 | $5.1x10^{-3}$ | 0.280 | 0.818 | 0.296 | 87.47 |
| Remarks | CPER | LPER | LPER | LPER | LPER | Low ecological risk |

The following categories were used to describe the risk factor: Er*i* < 40 = low potential ecological risk (LPER) , 40 ≤ Er*i* ≤ 80 = moderate potential ecological risk; 80 ≤Er*i* ≤ 160 = considerable potential ecological risk (CPER), 160 ≤ Er*i* ≤ 320 = high potential ecological risk and Er*i* 320 > =very high ecological risk at hand for the substance in question (Tesleem et al., 2018). The ecological risks of Cd in soils at ($SSP_1$) (97.80) and $SSP_3$ (93.99) were ≥ 80 while in $SSP_2$ recorded the ecological risk of 66.42 ≥ 40 but, ≤ 80. The ecological risk values indicate that Cd has a considerable potential ecological risk to the soil in $SSP_1$ and $SSP_3$ while the moderate potential ecological risk to the soil at $SSP_2$, with Cd posed a high-risk factor (Table 15). The result is also in line with (Ke et al. 2017; Saravanan et al., 2018), who reported Cd as the metal with a potential risk factor. The values of Pb, Cu, Zn, and Cr were below 40, indicating low potential ecological risk. The ecological risk indices of the heavy metals were in decreasing order: Cd ≥ Pb ≥ Cu ≥ Zn ≥ Cr, with the Cd accounted most of the total risks. The overall potential ecological risk as risk index (Ir) of heavy metals ranged from 67.980 in $SSP_2$ to 99.21 in $SSP_1$ ≤ 150 indicating low potential ecological risk (Tesleem et al., 2018), with the overall mean risk index being approximately 87.5 ≤Ir<150 which signifying low ecological risk for the entire Nworie River agricultural soil. Ultimately, the results of the ecological risk factor are in agreement with Ghrefata and Nigem (2006) who reported that Zn posed a low environmental risk, whereas Cd posed a medium environmental risk in sediments in Wadi Al-Arab Dam, Jordan respectively.

### *4.8. Summary and Conclusion*

The results of this study revealed that agricultural soils were predominantly sandy and moderately acidic, with cadmium above the WHO/FAO critical limit for agricultural soil. Agricultural soils recorded low nitrogen, moderate available phosphorous, very low exchangeable K and low-moderate exchangeable Ca. A correlation existed between physicochemical characteristics and heavy metals in soils depicting the same sources. Positively loaded variables are associated with human activities while negatively loaded variables are associated with lithogenic factors. The results suggested that agricultural soils were uncontaminated to moderately contaminated. Contamination factors indicated considerably contaminated moderately contaminated, and low contaminated. The contamination degree recorded a low degree of contamination, with no pollution. The ecological risk indices were in decreasing order: Cd ≥ Pb ≥ Cu ≥ Zn ≥ Cr. The potential ecological risk index and risk assessment code determined indicated that of the heavy metals examined, Cd posed the most significant ecological risk in the Nworie River watershed in agricultural soils studied. Therefore, human activities such as indiscriminate application of inorganic fertilizer, and disposal of solid waste along the slopes of Nworie River valley should be avoided within the upper, middle, and lower areas of the watershed. This will help in eliminating the ecological risk associated with Cd pollution in the watershed.

## References

Abbas, H. and Ebrahim, P. (2011). Heavy metals assessment and identification of their sources in agricultural soils of Southern Tehran, Iran. Environmental Monitoring and Assessment. 176(1-4): 677-691.

Acholonu, A. D. W., Okorie, P. U., Fipps, M. N. and Davis, K. L. (2008). Chemical profile of Nworie River in Owerri Imo state. 93rd ESA annual meeting at the Midwest Airlines Center Milwaukee, Wisconsin USA.

Acosta, J. A., Faz, A., Martínez-Martínez, S. and Arocena, J. M. (2011). Enrichment of metals in soils subjected to different land uses in a typical Mediterranean environment (Murcia City, Southeast Spain). Appl Geochem, 26: 405–41.

Adamu, U. K., Muhammad, A. and Adam, I. A. (2014). Evaluation of soil reaction, exchangeable acidity, and cation exchange capacity of soils from kano university of science and technology wudil teaching, research, and commercial farm, Gaya. Bayero Journal of Pure and Applied Sciences, 7(1): 52 – 55.

Adeoye, G. O., and Agboola, A. A. (1984). Relationship between soil physical and chemical characteristics and ear-leaf concentration of P, K, Mg, Zn, Fe, Cu, Mn and relative yield of maize in soils derived from sedimentary rocks of South-Western Nigeria. Fertilizer Research 5: 109–119.

Adriano, D. C. (2017). Trace elements in terrestrial environments: biogeochemistry, bioavailability, and risks of metals. Springer, New York.

Ahukaemere, C. M., Akamigbo, F. O. R., Onweremadu, E. U., Ndukwu, B. N., and Osisi, F. A. (2015). Soil Carbon and Nitrogen Forms and Sequestration concerning Agricultural Land Use Types in a Humid Agro-ecosystem. Journal of Global Biosciences, 4(3): 1655-1665.

Aki, E., and Ediene, V. E. (2018).Characteristics and classification of soils derived from Awi sandstone formation in Awi, Akamkpa local government area of Cross River State, Nigeria. World Scientific News, 112: 135-145.

Allison, F. E. (1973). Soil organic matter and its role in crop production, Elsevier publishers, New York.

Alloway, B. J. (1990). Heavy metals in soils, 2nd ed. Blackie Academic and Professional, London.

Anache, J. A. A., Wendland, E. C., Oliveira, P. T. S., Flanagan, D. C., and Nearing, M. A. ( 2017). Runoff and soil erosion plot-scale studies under natural rainfall: a meta-analysis of the Brazilian experience. Catena, 152: 29–39

Anjum, S. A., Li, J. H., Lv, J., Zong, X. F., Wang, L., Yang, A. J., Yan, R., Zohaib, A., Song, J. X. and Wang, S. G. (2016) . Regulation mechanism of exogenous ALA on growth and physiology of Leymus chinensis (Trin.) under salt stress. Chilean Journal of Agricultural Research, 76(3): 314–320.

Atafar, Z, Mesdaghinia, A., Nouri, J., Homaee, M., Yunesian, M., Ahmadimoghaddam, M. and Mahvi, A. H. (2010). Effect of fertilizer application on soil heavy metal concentration. Environ Monit Assess, 160(1): 83–89.

Bai, J. H., Cui, B. S. and Chen, B. (2011). Spatial distribution and ecological risk assessment of heavy metals in surface sediments from a typical plateau lake wetland, China. Ecological Modeling, 222(2): 301-306.

Bartolomeo, A. D., Poletti, L., Sanchini, G., Sebastiani, B. and Morozzi, G. (2004). Relationship among parameters of lake polluted sediments evaluated by multivariate statistical analysis. Chemosphere, 55: 1323–1329.

Benlkhoubi, N., Saber, S., Lebkiri, A., Rifi, E. H., Elfahime, E. and Khadmaoui, A. (2015). Accumulation of heavy metals in irrigated agricultural soils by the waters of hydraulic basin of Sebou in city of Kenitra (Morocco). Int. J. Innov Appl Stud, 12(2): 334 - 351.

Benoit, G., Oktay-Marshall, S. D., Cantu, A., Hood, E. M., Coleman, C. H. and Corapcioglu, M. O. (1994). Partitioning of Cu, Pb, Ag, Zn, Fe, Al and Mn between filter-retained particles, colloids and solution in six Texas estuaries. Marine Chemistry, 45(4): 307-336.

Benton, J. (1999). Soil Analysis Handbook of Reference Methods by J. Benton Jones Jr. (Editor)

Bentum, J. K., Adotey, J. P. K., Koka, J., Koranteng-Addo, E. J., Yeboah, A. and Boamponsem, L. K. (2017). Assessment of lead, copper and zinc contamination of soil from

Bohn, H. L., NcNeal, B. L. and O'Connor, G. A. (1985) . Soil Chemistry, 2nd edn, John Wiley & Sons, New York.

Brady, N. C. and Weil, R. R. (2008) .The nature and properties of soil, 14 ed. Prentice-Hall, Upper Saddle River, New Jersey.

Bray, R. H. and Kurtz, L. T. (1945). Determination of Total Organic and Available Forms of Phosphorus in Soils. Soil Science, 59: 39-45.

Cai, L., Xu, Z., Ren, M., Guo, Q., Hu, X., Hu, G., Wan, H. and Peng, P. (2012). Source identification of eight hazardous heavy metals in agricultural soils of Huizhou, Guangdong Province China. Ecotoxicol Environ Saf, 78:

Canadian Council of Ministers of the Environment, CCME, (2007). Canadian soil quality guidelines for the protection of environmental and human health. Summary tables. Updated September, 2007.

Chai, M., Shi, F., Li, R. and Shen, X. (2014). Heavy metal contamination and ecological risk in Spartina alterniflora marsh in intertidal sediments of Bohai Bay, China. Mar. Pollut. Bull. 2: 84- 115

Chen, D., Wei, W. and Chen, L. (2017). Effects of terracing practices on water erosion control in China: a meta-analysis. Earth Sci. Rev.

Chen, L., Genmei, W., Shaohua, W. Z., Zhenang, C., Chunhui, W. and Shenglu, Z. (2019). Heavy Metals in Agricultural Soils of the Lihe RiverWatershed, East China: Spatial Distribution, Ecological Risk, and Pollution Source. Int. J. Environ. Res. Public Health, 16: 20 -94.

Chikwendu, M. U., Uchendu, U. and Ogbonna, A. N. (2019). Determining the physicochemical properties of soil in the selected erosion sites in the rainforest ecosystem in Abia State, Nigeria. Journal of Research in Forestry, Wildlife and Environment. 11(3): 215-233.

Christian, E. E. and Beniah, O. I. (2020): Characterisation of some soils from flood basin in Amakohia, Owerri, Nigeria, International Journal of Environmental Analytical Chemistry.

Dassenakis, M., Andrianos, H., Depiazi, G., Konstants, A., Karabela, M., Sakellari, A. and Scoullos, M. (2003). The use of various methods for the study of metal pollution in marine sediments. the case of Euvoikos Gulf, Greece. Geochemistry, 18: 781– 794.

Dawaki, U. M., Dikko, A. U., Noma, S. S. and Aliyu, U. (2013). Heavy Metals and Physicochemical Properties of Soils in Kano Urban Agricultural Lands .Nigerian Journal of Basic and Applied Science , 21(3): 239-246.

De–Souza, Machado, A. A., Zarfl, C., Rehse, S. and Kloas, W. (2016). Low-Dose Effects: Nonmonotonic Responses for the Toxicity of a Bacillus thuringiensis Biocide to Daphnia magna. Environ. Sci. Technol. 51(3): 1679– 1686.

Dhyan, S., Chhonkar, P. K. and Pandey, R. N. (1999). Soil, plant & water analysis-A method manual. IARI, New Delhi.

Dos Anjos, M. J., Lopes, R. T., de Jesus, E. F. O., Assis, J. T., Cesareo, R. and Barradas, C. A. A. (2000). Quantitative analysis of metals in soil using X-ray fluorescence. Spectrochim Acta B 55: 1189–1194.

Draft Report (2016). DRAFTEIA of the Proposed Calabar-Ikom-Katsina Ala Superhighway Project Submitted to Federal Ministry of Environment, Abuja. REPORT NO.: S-015.6.

Duru, M., and Nwanekwu, K., (2012). Physicochemical and microbial status of Nworie River, Owerri, Imo State, Nigeria. Asian Journal of Plant Science and Research, 2(4): 433-436.

Edosomwan, N. I., Nwachukwu, A. A. and Osemweta, L. O. (2001). A comparative study of selected soil properties of an alfisol in various land utilization types in central southern Nigeria. Journal of Agricultural Resources, 17: 3-12.

Emmanuel, A., Louis, H., Akakuru, O. U., Adeola, O. A., Timothy, F. T., Amos, P. I., Banu, H. D. and IIu, D. (2018). Assessment of Organic Carbon and Available Nitrogen in the Soil of Some Selected Farmlands Located at Modibbo Adama University of Technology, Adamawa State, Nigeria, J Environ Anal Chem. 5: 2

Enwezor, W. O., Ohiri, A. C., Opubaribo, E. E. and Udoh, E. J. (1988). A Review of Soil Fertility Investigators in South Eastern Nigeria, Vol. HFDA Lagos Nigeria.

Enwezor, W. O. , Udo, E. J., Usoroh, N. J. , Ayotade, K. A. , Adepetu, J. A. , Chude, V. O. , and Udegbe, C. I. (1989). Fertilizer Use and management practices for crop in Nigeria (Series No 2). Produced by the Fertilizer Procurement and

Distribution Division of the Federal Ministry of Agriculture Water Resources and Rural Development, Lagos, Nig.

Enyoh, C. E. and Isiuku, B. O. (2020). Characterization of some soils from flood basin in Amakohia, Owerri, Nigeria, International Journal of Environmental Analytical Chemistry,

Esu, I. E. (1991). Detailed soil survey of NIHORT farm at Bunkure Kano state, Nigeria. Institute for Agricultural Research Samaru, Zaria, Nigeria.

Eyong, M. O. and Akpa, E. A. (2019). Physicochemical Properties of Soils derived from Sandstone Parent Materials under Selected Land use types at Agoi-Ibami in Central Cross River State, Nigeria. World News of Natural Sciences, 23: 1-12

Food Agricultural Organization (FAO) (2006). Food and Agriculture Organization of the United Nations, Vialedelle Terme di Caracalla, 00153 Rome, Italy

Food Agricultural Organization (FAO) (2002). Food and Agricultural Organization of United Nations publications, Rome (2002).

Food Agricultural Organization (FAO) (2014). World reference base for soil resources 2014. World Soil Resources Report 106. Rome. 120

Food Agricultural Organization (FAO) (1995) .Programme for the World Census of Agriculture 2000. Statistical Development Series No. 5. Rome.

Federal Ministry of Environment (FMEnv) (1991). National Interim Guidelines and Standards for Industrial Effluents, Gaseous Emissions and Hazardous Waste Management in Nigeria. 91-110.

Fosu-Mensah, B. Y., Emmanuel, A., D., Yirenya, T. and Frank, N. (2017). Heavy metals concentration and distribution in soils and vegetation at Korle Lagoon area in Accra, Ghana. Cogent Environmental Science, 3: 1405 - 1488.

García-Ruiz, J. M., Beguería, S., Nadal-Romero, E., González-Hidalgo, J. C., Lana-Renault, N. and Sanjuán, Y. (2015). A meta-analysis of soil erosion rates across the world. Geomorphology 239: 160–173.

Gee, G. W. and Or, D. (2002). Particle Size Analysis. In: Dane, J.H. and Topp, G.C., Eds., Methods of Soil Analysis, Part 4, Physical Methods, Soils Science Society of America, Book Series No. 5, Madison, 255-293.

George, R. (2009). Land Evaluation for Rainfed Agriculture Food and Agricultural Organization of United Nations. Rome pp.237.

Ghrefat, H. and Nigem, Y. (2006). Assessing Mn, Fe, Cu, Zn, and Cd pollution in bottom sediments of Wadi Al-Arab Dam, Jordan. Chemosphere, 65: 2114–2121.

Gotelli, N. J. and Ellison, A. M. (2004). A primer of ecological statistics. Sinauer Associates, Sunderland, Massachusetts, USA.

Haskanson, L. (1980). An ecological risk index for aquatic pollution control a sedimentological approach. Water Research, 14(8): 975-1001.

Hazelton, P. and Murphy, B. (2007). Interpreting soil test results. What do all the numbers mean? csIRo Publishing, Victoria.

Hungarian Standard Institution (HIS) (1998). MSZ 21470-1. Environmental protection. Testing of soils. Sampling. Hungarian Standard Institution, Budapest.

Huang, S. S, Liao, Q. L., Hua, M., Wu, X. M., Bi, K. S., Yan, C. Y., Chen, B. and Zhang, X. Y. (2007). Survey of heavy metal pollution and assessment of agricultural soil in Yangzhong district, Jiangsu province, China. Chemosphere, 67: 2148–2155.

Ibe, F. C., Isiuku, B. O. and Enyoh, C. E. (2017). World News Nat. Sci. 13: 27

Isirimah, N. O., Igwe, C. and Iwegbue, C. M. A. (2003). Important Ions in Soils Environment In: Introductory Soil Chemistry and Biology for Agric and Biotech. OsiaIn'l Pub. Lt. PH. pp. 34-97.

Isiuku, B. O. and Enyoh, C. E. (2020). Environ. Anal. Health Toxicol. 35(1): 1

Juo, A. S. R. (1975). Selected Methods for Soil and Plant Analysis. International Institute of Tropical Agriculture (IITA), Ibadan, Nigeria.

Ke, X., Gui, S., Huang, H., Zhang, H., Wang, C. and Guo, W. (2017). Ecological risk assessment and source identification for heavy metals in surface sediment from the Liaohe River protected area, China. Chemosphere, 175: 473-

Khan, M. U., Malik, R. N. and Muhammad, S. (2015). Health risk assessment of consumption of heavy metals in market food crops from Sialkot and Gujranwala Districts, Pakistan. Hum Ecol Risk Assess, 21: 327- 237.

Kingsley, J., Akpan-Idiok, A. U., Ayito, E. O. and Penizek, V. (2020). Mineralogical properties of soils developed from colluvial deposits of Southern Nigeria. Bulg. J. Agric. Sci., 26(3): 605–611.

Lal, R. (2018). Digging deeper: A holistic perspective of factors affecting soil organic carbon sequestration in agroecosystems. Global Change Biology (Early View),

Landon, J. R. (1991). Booker tropical soil manual: A Handbook for soil survey and Agricultural land Evaluation in the tropics and subtropics, Longman Scientific and Technical, Essex, New York. 474p.

Lautridou, J. P. and Ozouf, J. (2016). "Experimental frost shattering". Progress in Physical Geography. 6 (2): 215–232.

Li, J., Lu, Y., Yin, W., Gan, H., Zhang, C., Deng, X. and Lian, J. (2009). Distribution of heavy metals in agricultural soils near a petrochemical complex in Guangzhou, China. Environ Monit Assess. 153: 365–375.

Li, Z. Y., Ma, Z. W., van der Kuijp, T. J., Yuan, Z. W. and Huang, L. (2011). A review of soil heavy metal pollution from mines in China: pollution and health risk assessment. Sci. Total Environ. 468–469, 843–853.

Lian, C., Genmei, W., Shaohua, W., Zhen, X., Zhenang, C., Chunhui, W. and Shenglu, Z. (2019). Heavy Metals in Agricultural Soils of the Lihe River Watershed, East China: Spatial Distribution, Ecological Risk, and Pollution Source. Int. J. Environ. Res. Public Health, 16: 20-94

Liao, M., Chen, C. L. and Huang, C. Y. (2005). Effect of heavy metals on soil microbial activity and diversity in a reclaimed mining wasteland of red soil area. J. Environ. Sci. (China), 17: 832-837.

Liu, J., Yin, P., Chen, B., Gao, F., Song, H. and Li, M. (2009). Distribution and contamination assessment of heavy metals in surface sediments of the Luanhe River Estuary, northwest of the Bohai Sea. Mar. Pollut. Bull., 109: 633–639.

Loganathan, P. (1987). Laboratory Manual of Soil and Plant Analysis. Rivers State University of Science and Technology, Port- Harcourt, Nigeria.

Loska, K., Wiechuła, D. and Korus, I. (2004).Metal contamination of farming soils affected by industry. Environ. Int. 30: 159–165.

Manno, E., Varrica, D. and Dongarra, G. (2006). Metal Distribution in Road Dust Samples Collected in anUrban Area Close to a Petrochemical Plant at Gela, Sicily, Italy. Atmospheric Environment, 40: 5929-5941.

Manoj, K., Kumer, B. and Padhy, P. K. (2012). Characterization of materials in water and sediments of Subarnarekha River along the projects sites in Lower Basin, India. Universal Journal of Environmental Research and Technology, 2(5): 402-410.

Mohmand, J., Eqani, S. A., Fasola, M. Alamdar, A., Mustafa, I., Ali, N., Liu, L., Peng, S. H. and Shen, H. (2015). Human exposure to toxic metals via contaminated dust: bio-accumulation trends and their potential risk estimation .Chemosphere, 132: 142-155.

Mohsen, N. and Alireza, P. (2014). Application of geoaccumulation index and enrichment factor for assessing metal contamination in the sediments of Hara Biosphere Reserve, Iran, Chemical Speciation and Bioavailability, 26(2): 99-105,

Muller, G. (1981): The heavy metal pollution of the sediments of Neckars and its tributary: An Inventory. Chem. Zeitung, 105: 157-164.

Nanos, N. R. and Martín, J. A. (2012). Multiscale analysis of heavy metal contents in soils: spatial variability in the Duero river basin (Spain) Geoderma, 189: 554–562.

Naveedullah, M. Z., Hashmi, C., Yu, H. S., Dechao, D., Chaofeng, S., Liping, L. and Yingxu, C. (2013). Risk Assessment of Heavy Metals Pollution in Agricultura Soils of Siling Reservoir Watershed in Zhejiang Province, China, Hindawi Publishing Corporation BioMed Research International, 1-10

Njoku, C. C. (2017). Assessment of fertility status of soils used for cassava production in Owerri, area of Imo State, Nigeria. Journal of Agriculture and Food Sciences, 15(2):

Norbert, N. F., Aaron, S. T., George, B. C., Kenneth, G. A. and Vivian, B. C. (2018). Selected physicochemical properties and quality of soils around some rivers of Cameroon. J. Soil Sci. Environ. Manage, 9(5): 68- 80,

Nziguheba, G. and Smolders, E. (2008) Inputs of trace elements in agricultural soils via phosphate fertilizers in European countries. Sci Total Environ, 390(1): 53–57.

Okereke, J. N., Nduka, J. N., Ukaoma, A. A. and Ogidi, I. O. (2019). Level of Heavy Metals in Soil Samples from Farmlands along Highways in Parts of Owerri, Nigeria. World Journal of Innovative Research, 7(1): 01-07.

Olayinka, B. U., Esan, O. O., Anwo, I. O. and Etejere, E. O. (2017). Comparative growth analysis and fruit quality of two varieties of tomato under hand weeding and pendimenthalin herbicide. J. Agric. Sci. 12(3): 149-161.

Omuto, C. C and Vargas, R. (2018). Soil nutrient loss assessment in Malawi Technical Report. the Food and Agriculture Organization of the United Nations and the UNDP-UNEP Poverty-Environment Initiative and the Ministry of Agriculture, Irrigation and Water Development, Malawi.

Onweremadu, E. U., Amaechi, J. U., and Ndukwu, B. N. (2011). Vertical Distribution of Cadmium and Lead on Soils Affected by Metropolitan Refuse Disposal in Owerri, Southeastern Nigeria. Iranica Journal of Energy and Environment, 2(1): 62-67.

Osakwe, S. A. and Okolie, L. P. (2015). Physicochemical characteristics and heavy metals contents in soils and cassava plants from farmlands along a major highway in Delta State, Nigeria. J. Appl. Sci. Environ. Manage, 19(4): 695-704.

Osujieke, D. N., Onweremadu, E. U., Ahukaemere, C. M. and Ndukwu, B. N. (2016). Classification of soils of a toposequence underlain by coastal plain sand in South-east Nigeria. Nig. J. Soil and Env. Res. 14: 256 – 263.

Oumenskou, H., Mohamed, E., Baghdadi, A. B., Mohamed, W. E., Lalla, A. K. and Mohamed, A. (2018). Assessment of the heavy metal contamination using GIS-basedapproach and pollution indices in agricultural soils from Beni Amirirrigated perimeter, Tadla plain, Morocco. Arabian Journal of Geosciences, 11: 692.

Owanda, A. P., Tri, and Pra, R. Z. (2018). Chemical characteristics of the surface sediment in the Java Sea. IOP Conf. Series: Earth and Environmental Science, 176: 012 – 015

Pinta. M. (1970). Agricultural Applications of Flame Photometry, 431-478.

Rahaman, A., Afroze, J. S., Bashar, K., Ali, Md. F. and Hosen, Md. R. (2016). A Comparative Study of Heavy Metal Concentration in DifferentLayers of Tannery Vicinity Soil and Near Agricultural Soil. American Journal of Analytical Chemistry, 7: 880 - 889

Ramos, L. , Fernaudez, M. A. , Gonzalez, M. J. , and Hernande, . L. M. (1999). Heavy metal pollution in water, sediments and earthworms from the Ebro River, Spain. Bull. Environ. Contam. Toxicol. 63: 305-311.

Rodríguez, M. J. A., Ramos-Miras, J. J., Boluda, R. and Gil, C. (2013) .Spatial relations of heavy metals in arable and greenhouse soils of a Mediterranean environment region (Spain). Geoderma, 200: 180–188

Rooney, C. P., Fang-Jie, Z. and Steve, P. M. (2007). Phytotoxicity of nickel in a range of European soils: Influence of soil properties, Ni solubility and speciation. Environmental Pollution, 145(2): 596-605

Saravanan, P., Krishnakumar, S., Pradhap, D., Silva, J. D., Arumugam, K., Magesh, N. S. and Srinivasalu, S. (2018). Elemental concentration based potential ecological risk (PER) status of the surface sediments, Pulicat lagoon, and Southeast coast of India. Mar. Pollut. Bull., 133: 107–116.

Shan, Y., Wang, J., Li, Y., Zhang, K., Chen, Z., Liang, K., Zhang, J., Liu, J. J., Xi, J. L. and Qiu, L. (2013). Targeted genome modification of crop plants using a CRISPR-Cas system Nat. Biotechnol, 31: 686 - 688

Shao, D., Zhan, Y., Zhou, W. and Zhu, L. (2018). Current status and temporal trend of heavy metals in farmland soil of the Yangtze River Delta region: field survey and meta-analysis. Environ Pollut. 219: 329–336.

Sun, C., Liu, J., Wang, Y., Sun, L. and Yu, H. (2013). Multivariate and geostatistical analyses of the spatial distribution and sources of heavy metals in agricultural soil in Dehui, Northeast China. Chemosphere, 92: 517– 523

Sutherland, R. A. and Dejong, E. (1990). Estimation of sediment redistribution within agricultural field using Caesium-137, Crystal springs, Saskatchwan, Canada. Applied Geography, 10: 205-221

Tanimu, J., Uyovbisere, E. O., Lyocks, S. W. J. and Tanimu, Y. (2013). Cow dung management on the calcium and magnesium content and total microbial population in the northern guinea savanna of Nigeria. G.J B.A.H.S., 2(2): 7-11

Taylor, S. R. and McLennan, S. M. (1995). The geochemical evolution of the continental crust," Reviews of Geophysics, 33(2): 241–265

Tening, A. S., Chuyong, G. B., Asongwe, G. A., Fonge, B. A., Lifongo, L. L., Mvondo-Ze A. D., Che, V. B. and Suh, C. E. (2013). Contribution of some water bodies and the role of soils in the physicochemical enrichment of the Douala-Edea mangrove ecosystem. Afr. J. Environ. Sci. Technol. 7(5): 336-349

Tesleem, O. K., Akinade, S. O., Mustapha, T., Jimoh, O. and Fajemila, T. (2018). Heavy Metal Contamination and Ecological Risk Assessment in Soils and Sediments of an Industrial Area in Southwestern Nigeria . J Health Pollut. 8(19): 1809-1826.

Tomgouani, K. A. O., El Mejahed, K. and Bouzidi, A. (2007). Evaluation de la pollution métallique dans les sols agricolesirrigués par les eauxusées de la ville de Settat (Maroc). Bulletin de l'InstitutScientifique Rabat, 29: 89–92

Tomlinson, D. C., Wilson, J. G., Harris, C. R. and Jeffrey, D. W. (1980). Problems in the assessment of heavy metal levels in estuaries and the formation of a pollution index. Helgol. Wiss. Meeresunters, 33: 566-575

Ubuoh, E. A., Akhionbare, W. N., Oweremadu, E. and Onifade, O. A. (2010). Characterization of Soil Quality in Erosion Prone Environment of Ukpor, Nnewi-South L.G.A. of Anambra State, Nigeria. International Journal of Advances in Applied Sciences, 2(1): 1 - 8

Ubuoh, E. A., Onwughara, I. J. and Odey, E. (2020a). Susceptibility of Agricultural Land to Soil Degradation by Rainfall Using Aggregates' Stability Indices in Parts of Abia State, South Eastern Nigeria. Jordan Journal of Earth and

Environmental Sciences, 11(3): 211-221

Ubuoh, E. A., Ofoegbu . C., Chinwendu, C., Precious, C, Ota, H. O. and Zhifeng, Y. (2021). Evaluating the spatial distribution of soil physicochemical characteristics and heavy metal toxicity potential in sediments of Nworie river micro-watershed Imo state, southeastern Nigeria. Environmental Chemistry and Ecotoxicology, 3: 261–268

Ubuoh, E. A., Onwughara, I. J. and Ogbonna, P. C. (2020b). Soil physicochemical characteristics along gully gradients in the selected humid tropical agro-ecological environments in Abia, Southeastern Nigeria . Jr. of Erosion and Environmental Degradation Journal of Erosion and Environmental Degradation (JEED) FUTO, June 2020.ISSN 115-1943

Ubuoh, E. A and Ogbonna, P. C. (2018). Effects of some anthropogenically induced environmental hazards on soil fertility indices, germination and growth of maize and soybeans in Imo State, Nigeria. African Journal of Agriculture Technology and Environment, 7(2): 30-43.

Ubuoh, E. A., Ufot U. O. and Ezenwa, L. (2016) :Influence of Temperature Dynamics on Phosphorus Availability in Humid Tropical Soils of Southeastern Nigeria. Journal of Basic and Environmental Sciences, 3: 140-147.

Ubuoh, E. A., Onwughara, I. J. and Odey, E. (2020c). Effects of land use and land cover dynamics on soil erosion potentials in an agricultural land of Abia, Southeastern Nigeria. Journal of Erosion and Environmental Degradation June 2020.ISSN 115-1943

Ubuoh, E. A., Umezuruike, S. O., Nworuh, B. O. and Emeka. C. C. (2019). Assessment of Soil pH and Heavy Metal Concentrations in Agricultural Land Impacted with Medical Waste Incinerator (MWI) Flue Gas (FA) in Abia State, Nigeria. J. Appl Sci. Environ. Manage, 23(2): 275-282.

Ubuoh, E. A, Akhionbare, W. N., Onweremadu, E. and Onifade, O. A. (2013), Characterization of Soil Quality in erosion prone environment of Ukpor, Nnewi-South L.G.A of Anambra State, Nigeria. International Journal of Advances in Applied Sciences, 2(1): 1-8.

Ubuoh, E. A., Nwawuike, N. and. Obeta, M. C. (2014). Environmental Risk Assessment of Heavy Metal Concentrations in Road Runoff with Absorption Atomic Spectrophotomete, Imo State, Nigeria. Journal of Environment and Earth Science, 4(5):

Veličković, Z. N., Ivanković, V. S., Radovan, K., Dalibor, J., Zoran, B. and Jovica, B. (2016). Investigation of soil properties influence on the heavy metals sorption by plants and possibilities for prediction of their bioaccumulation by response surface methodology. J. Serb. Chem. Soc. 81 (8): 947–958

Verla, E. N., Verla, A. W. and Enyoh, C. E. (2020). Pollution assessment models of soils in Portharcourt city, rivers state, Nigeria. World News of Natural Sciences, 12: 1-23.

Verla, E. N., Verla, A. W. and Enyoh C. E. (2017). Pollution assessment models of soils in Portharcourt city, rivers state, Nigeria. World News of Natural Sciences, 12: 1-23.

Walkley, A. and Black, I. A. (1965). An Examination of the Degtjareff Method for Determining Soil Organic Matter and a Proposed Modification of the Chromic Acid Titration Method. Soil Science, 37: 29-38.

Wang, Y. Y., Wen, A. B., Guo, J., Shi, Z. L. and Yan, D. C. (2017). Spatial distribution, sources and ecological risk assessment of heavy metals in Shenjia River watershed of the Three Gorges Reservoir Area. Journal of Mountain Science, 14(2): 325-335.

WHO/FAO. (2001). Codex alimentarius commission. Foodadditives and contaminants. JointFAO/WHO Food Standards Programme, ALINORM 10/12A. Retrieved fromwww.transpaktrading.com/static/pdf/research/achemistry/introTofertilizers.pd

Wu, S., Xia, X., Lin, C., Chen, X. and Zhou, C. (2010). Levels of arsenic and heavy metals in the rural soils of Beijing and their changes over the last two decades (1985–2008). J Hazard Mater. 179(1): 860–868.

Xue, Y., Tristan, E., Jibin, H., Chun-Qin, Z., Steve, P., McGrath, Peter, R. S. and Fang-Jie, Z. ( 2014). Effects of nitrogen on the distribution and chemical speciation of iron and zinc in pearling fractions of wheat grain. Journal of Agriculture and Food Chemistry. 62: 4738– 4746.

Yap, C. K., Ismail, A. and Tan, S. G. (2003) Cd and Zn concentrations in the straits of Malacca and intertidal sediments of the west coast of Peninsular Malaysia. Mar Pollut Bull, 46(10): 1349–1353

Yaylali-Abanuz, G. (2011). Heavy metal contamination of surface soil around Gebze industrial area, Turkey. Microchem. J., 99: 82–92.

Yi, Y. J., Yang, Z. F. and Zhang, S. H. (2011). Ecological risk assessment of heavy metals in sediment and human health risk assessment of heavy metals in fishes in the middle and lower reaches of the Yangtze River basin. Environment Pollution, 159(10): 2575-2585.

Yu, B., Wang, Y. and Zhou, Q. (2014). Human health risk assessment based on toxicity characteristic leaching procedure and simple bioaccessibility extraction test of toxic metals in urban street dust of Tianjin, China

Yuan, C., Shi, J., He, B., Liu, J., Liang, L. and Jiang, G. (2004). Speciation of heavy metals in marine sediments from the East China Sea by ICP-MS with sequential extraction. Environ. Int., 30: 769– 783.

Yushu, S. M., Tysklind, F. H., Wei, O. S. and Chen, C. L. (2013). Identification of sources of heavy metals in agricultural soils using multivariate analysis and GIS. J Soils Sediments, 13: 720–729

Zawadzka, M., and Łukowski, M. I. (2010). The content of Zn, Cu, Cr in podzolic soils of Roztocze National Park at the line of metallurgical and sulphur and the highway, Acta Agrophysica, 16(2): 459 – 470

Zhang, L., Guo, S. and Wu, B. (2015). The Source, spatial distribution and risk assessment of heavy metals in soil from the pearl river delta based on the national multi-purpose regional geochemical survey. PLoS One, 10(7): 2732-2740..

Zhang, X., Yang, F., Luo, C., Wen, S., Zhang, X. and Xu, Y. (2009). Bioaccumulative characteristics of hexabromocyclododecanes in freshwater species from an electronic waste recycling area in China. Chemosphere, 76(11): 1572– 1578.

Zhao, Y., Shi, X., Huang, B., Yu, D., Wang, H., Sun, W., Oboern, I. and Blomback, K. (2007). Spatial distribution of heavy metals in agricultural soils of an industry-based peri-urban area in Wuxi, China. Pedosphere, 17: 44– 51.

المملكة الأردنية الهاشمية

صندوق دعم البحث العلمي

الجامعة الهاشمية

# المجلة الأردنية
# لعلوم الأرض والبيئة

# JJEES

مجلة علمية عالمية محكمة

المجلد (١٣) العدد (٢)

http:// jjees.hu.edu.jo/

ISSN 1995-6681

# المجلة الأردنية لعلوم الأرض والبيئة

## مجلة علمية عالمية محكمة

**المجلة الأردنية لعلوم الأرض والبيئة : مجلة علمية عالمية محكمة ومفهرسة ومصنفة، تصدر عن عمادة البحث العلمي في الجامعة الهاشمية وبدعم من صندوق البحث العلمي - وزارة التعليم العالي والبحث العلمي، الأردن.**



### ترسل البحوث إلكترونيا إلى البريد الإلكتروني التالي:

**رئيس تحرير المجلة الأردنية لعلوم الأرض والبيئة**

**jjees@hu.edu.jo**

**لمزيد من المعلومات والأعداد السابقة يرجى زيارة موقع المجلة على شبكة الانترنت على الرابط التالي:**

**www.jjees.hu.edu.jo**

المملكة الأردنية الهاشمية    صندوق دعم البحث العلمي    الجامعة الهاشمية

# JJEES

# المجلة الأردنية لعلوم الأرض والبيئة

المجلد (13) العدد (2)

مجلة علمية عالمية محكمة تصدر بدعم من صندوق دعم البحث العلمي

ISSN 1995-6681    jjees.hu.edu.jo    حزيران 2022